เอโซ-ไดเอซาคราวน์อีเทอร์เพื่อเป็นเซ็นเซอร์สำหรับไอออนโลหะและแอนไอออน

นายณรงค์ศักดิ์ ขุนรักษา

วิทยานิพนธ์นี้เป็นส่วนหนึ่งของการศึกษาตามหลักสูตรปริญญาวิทยาศาสตรดุษฎีบัณฑิต
สาขาวิชาเคมี ภาควิชาเคมี
คณะวิทยาศาสตร์ จุฬาลงกรณ์มหาวิทยาลัย
ปีการศึกษา 2559

AZO-DIAZACROWN ETHERS AS METAL ION AND ANION SENSORS

Mr. Narongsak Koonrugsa

A Dissertation Submitted in Partial Fulfillment of the Requirements
for the Degree of Doctor of Philosophy Program in Chemistry
Department of Chemistry
Faculty of Science
Chulalongkorn University
Academic Year 2016

Thesis Title	AZO-DIAZACROWN ETHERS AS METAL ION AND ANION SENSORS
By	Mr. Narongsak Koonrugsa
Field of Study	Chemistry
Thesis Advisor	Assistant Professor Saowarux Fuangswasdi, Ph.D.

Accepted by the Faculty of Science, Chulalongkorn University in Partial Fulfillment of the Requirements for the Doctoral Degree

.....Dean of the Faculty of Science
(Associate Professor Polkit Sangvanich, Ph.D.)

THESIS COMMITTEE

.....Chairman
(Associate Professor Vudhichai Parasuk, Ph.D.)

.....Thesis Advisor
(Assistant Professor Saowarux Fuangswasdi, Ph.D.)

.....Examiner
(Professor Nongnuj Muangsin, Ph.D.)

.....Examiner
(Assistant Professor Fuangfa Unob, Ph.D.)

.....External Examiner
(Assistant Professor Boontana Wannalerse, Ph.D.)

ณรงค์ศักดิ์ ขุนรักษา : เอโซ-ไดเอซาคราวน์อีเทอร์เพื่อเป็นเซ็นเซอร์สำหรับไอออนโลหะและแอนไอออน (AZO-DIAZACROWN ETHERS AS METAL ION AND ANION SENSORS) อ.ที่ปรึกษาวิทยานิพนธ์หลัก: ผศ. ดร. เสาวรักษ์ เฟื่องสวัสดิ์, 85 หน้า.

งานวิจัยนี้ทำการสังเคราะห์อนุพันธ์ เอโซ-ไดเอซา-18-คราวน์-6 อีเทอร์ 6 และพิสูจน์เอกลักษณ์ด้วยเทคนิค ^{1}H ^{13}C-NMR และแมสสเปกโตรสโกปี ผลการศึกษาสมบัติการตรวจวัดพบว่าอนุพันธ์เอสเทอร์ทั้ง 3 ชนิด คือ E1 E2 และ EE2 ไม่แสดงสมบัติการตรวจวัดเป็นพิเศษไม่ว่ากับโลหะไอออนชนิดใด ส่วนอนุพันธ์กรดและอนุพันธ์ไนโตรแสดงการเปลี่ยนแปลงสีและสมบติการตรวจวัดที่ขึ้นตัวละลายชนิดต่างๆ โดยในภาวะที่มีไอออนโลหะแทรนซิชันและโลหะหนัก อนุพันธ์กรด A2 แสดงการเปลี่ยนสีจากสีส้มไปเป็นโทนเหลืองและเขียวที่ไม่สามารถแยกแยะได้ด้วยตาเปล่า ทำให้ไม่สามารถนำไปใช้เป็นตัวรับรู้ทางสีได้ ในทางตรงกันข้าม อนุพันธ์ไนโตร N1 และ N2 แสดงการเลือกจำเพาะกับ Cr^{3+} ใน MeCN โดยมีการเปลี่ยนแปลงจากสีชมพูเป็นไม่มีสี พร้อมกับมีการดูดกลืนแสงเปลี่ยนไปทางช่วงความยาวคลื่นน้อยลงหรือทางสีฟ้าเท่ากับ 125 และ 165 nm ตามลำดับ ทั้งยังเกิดสารประกอบเชิงซ้องสองรูปแบบคือ ML_2 และ ML นอกจากนี้ Hg^{2+} ยังทำให้สารละลาย N1 และ N2 ใน DMSO เกิดการเปลี่ยนแปลงการดูดกลืนแสงไปทางความยาวคลื่นน้อยลงได้มากถึง 160 nm พร้อมกับเปลี่ยนจากสีม่วงเป็นไม่มีสี การเกิดสารประกอบเชิงซ้อน ML ระหว่าง Hg^{2+} กับ N2 มีค่าคงที่ในหน่วยลอการิธึมเท่ากับ 5.97 ค่าต่ำสุดที่วัดได้ด้วยตาเปล่าต่อไอออนที่สนใจมีค่าดังนี้ กรณีของ Cr^{3+} ใน MeCN พบว่า N1 ตรวจวัดได้ 0.09 ppm และ N2 ตรวจวัดได้ 0.27 ppm ส่วนกรณีของ Hg^{2+} ใน DMSO N1 ตรวจวัดได้ 0.90 ppm และ N2 ตรวจวัดได้ 1.40 ppm ซึ่งค่าต่ำสุดที่วัดได้ของ Cr^{3+} นี้สามารถนำไปใช้ตรวจวัดปริมาณ Cr^{3+} ที่ทำให้เกิดพิษเฉียบพลันต่อสิ่งมีชีวิตในแหล่งน้ำได้ นอกจากนี้ N1 และ N2 ยังแสดงการเลือกจำเพาะกับไอออนลบ F^- และ ทั้งใน MeCN และ DMSO โดยการเติม F^- ทำให้ N1 เปลี่ยนจากสีชมพูเป็นสีม่วงใน MeCN และเปลี่ยนจากจากสีม่วงเป็นสีน้ำเงินใน DMSO อันเป็นผลมาจากการเปลี่ยนแปลงการดูดกลืนแสงไปในทิศทางความยาวคลื่นมากขึ้นหรือทางสีแดงประมาณ 50-60 nm สำหรับกรณีของ $H_2PO_4^-$ พบว่ามีการเปลี่ยนจากสีชมพูหรือม่วงเป็นไม่มีสี เนื่องจากมีการเปลี่ยนแปลงการดูดกลืนแสงไปทางความยาวคลื่นน้อยลงประมาณ 130-160 nm ผลทั้งหมดนี้แสดงให้เห็นถึงโอกาสในการนำ N1 และ N2 ไปใช้เป็นตัวรับรู้ทางสีเพื่อตรวจวัดไอออนโลหะ Cr^{3+} Hg^{2+} และไอออนลบ F^- $H_2PO_4^-$ ได้อย่างมีศักยภาพ

ภาควิชา เคมี ลายมือชื่อนิสิต .....

สาขาวิชา เคมี ลายมือชื่อ อ.ที่ปรึกษาหลัก .....

ปีการศึกษา 2559

5272296923 : MAJOR CHEMISTRY

KEYWORDS: DIAZA-18-CROWN-6 ETHER / AZOBENZENE / TAUTOMERIZATION / NAKED-EYE SENSER / CHROMIUM ION / FLUORIDE ION / DIHYDROGEN PHOSPHATE ION / MERCURY ION

NARONGSAK KOONRUGSA: AZO-DIAZACROWN ETHERS AS METAL ION AND ANION SENSORS. ADVISOR: ASST. PROF. SAOWARUX FUANGSWASDI, Ph.D., 85 pp.

Six azobenzene-diaza-18-crown-6 derivatives were synthesized and characterized by ^{1}H, ^{13}C-NMR, and mass spectroscopies. The three ester derivatives E1, E2 and EE2 did not show any special sensing property towards any metal ion. Acid and nitro derivatives showed solvatochromic effects and dependent sensing properties in various solvents. The acid derivative A2 displayed inseparable color yellow or green from orange upon addition of transition and heavy metal ions in DMSO which, unfortunately, could not be used as optical chemosensor. In contrast, the nitro derivatives N1 and N2 showed selectivity toward Cr^{3+} in MeCN by color changing from pink to colorless with a blue shift of 125 and 165 nm, respectively. Both sensors form complex ML_2 and ML with Cr^{3+} in MeCN. Hg^{2+} also induced a large blue shift around 160 nm in the UV-Visible spectra of N1 and N2 in DMSO with color change from purple to colorless. The value of log K for ML complex of N2 with Hg^{2+} is equal to 5.97. The naked eye detection limit towards target ions are 0.09 and 0.27 ppm for N1 and N2 for Cr^{3+} in MeCN, and 0.90 and 1.40 ppm for N1 and N2 for Hg^{2+} in DMSO. This low detection limit for Cr^{3+} could be used to monitor Cr^{3+} that bring acute toxic to aquatic life. Furthermore, N1 and N2 showed selectivity towards F^- and in both MeCN and DMSO: F^- could induce a color change of N1 from pink to purple in MeCN and from purple to blue in DMSO as a result of a red shift of 50-60 nm. $H_2PO_4^-$ also induced a color change from pink or purple to colorless with a 130-160 nm blue shift. Thus N1 and N2 could be potentially employed as chromogenic sensors for both metal ions such as Cr^{3+} and Hg^{2+} and anions like F^- and $H_2PO_4^-$.

Department: Chemistry Student's Signature .....

Field of Study: Chemistry Advisor's Signature .....

Academic Year: 2016

ACKNOWLEDGEMENTS

This thesis would have never been completed without the support from many people in many aspects.

First of all, I wish to express my deepest appreciation to my advisor Assistant Professor Dr. Saowarux Fuangswasdi for her kindnesses, suggestions and supports throughout my Ph. D. career. I would like to thank the committee (Assoc. Prof. Dr. Vudhichai Parasuk, Prof. Dr. Nongnuj Muangsin, Assist. Prof. Dr. Fuangfa Unob and Assist. Prof. Dr. Boontana Wannalerse) for their valuable comments and useful suggestions (which were a lot of helpful advices).

Furthermore, I am grateful to the partial financial support from Thailand Research Fund (RTA5380003), the 90th Aniniversary of Chulalongkorn University Fund (Ratchadaphiseksomphot Endowment Fund) and Teaching Assistant scholarship.

In addition, it is my privilege to thank Supramolecular Chemistry Research Unit (SCRU) for its encouragement and supports.

Finally, I cannot find the word to thank for the precious support from my beloved family who always cheer up and stand beside me when I feel down.

Narongsak Koonrugsa

CONTENTS

Page

Page

Page

LIST OF FIGURES

LIST OF SCHEMES

LIST OF TABLES

LIST OF ABBREVIATIONS AND SYMBOLS

g	gram
mg	milligram
mL	milliliter
cm	centimeter
nm	nanometer
mmol	millimole
M	molar
mM	millimolar
μM	micromolar
eq	equivalent
ppm	part per million
MHz	megahertz
°C	degree Celsius
δ	chemical shift
m/z	mass-to-charge ratio
λ_{max}	wavelength at maximum absorption
o-, p-	position of substituent on aryl group (*ortho*, *para*)
s, d, t, m	splitting patterns of ^{1}H-NMR (singlet, doublet, triplet, multiplet)
Ar	aryl moiety
Et	ethyl moiety
Me	methyl moiety
Ts	tosyl moiety
TsCl	tosylchloride
CCA	cinnamic acid
DMAP	4-dimethylaminopyridine
Et_3N	triethylamine
HCl	hydrochloric acid
NaOH	sodium hydroxide

$NaNO_2$	sodium nitrite
CH_2Cl_2	dichloromethane
DMSO	dimethylsulfoxide
EtOH	ethanol
EtOAc	ethyl acetate
MeOH	methanol
THF	tetrahydrofuran
TLC	thin-layer chromatography
MALDI-TOF	matrix-assisted laser desorption/ionization time-of-flight mass spectrometry
^{1}H-NMR	proton nuclear magnetic resonance spectrometry
^{13}C-NMR	carbon-13 nuclear magnetic resonance spectrometry
IR	infrared spectroscopy
UV-Vis	UV-Visible spectrometry
ICT	Intramolecular Charge Transfer
M:L	metal to ligand ratio
A:L	anion to ligand ratio
ML_2	metal ligands complex (M:L = 1:2)
ML	metal ligands complex (M:L = 1:1)

CHAPTER I

INTRODUCTION

1.1 Supramolecular chemistry and sensing applications

The supramolecular chemistry or host guest chemistry, introduced by Prof. Lehn in 1978 [1], is the chemistry of supramolecule which is an association of two or more chemical species held together by intermolecular force. This molecular interaction creates the basis of extremely specific processes already found in nature like recognition, transportation, regulation, for example, protein-protein assembling, enzymatic reaction, and cellular recognition [2,3]. Nowadays, supramolecular chemistry has been applied in many fields, one of which is the development of chemosensors.

Molecular sensors or chemosensors are molecules which recognize and give signal such as redox potential, optical or fluorescent response for specific analytes [4-11]. A chemosensor generally composes of two molecular units which are a binding unit for selective interaction with analytes like cation, anion or neutral molecule, and a signaling unit that gives out signal upon the mentioned interaction. The concept of chemosensor is shown in Figure 1.1

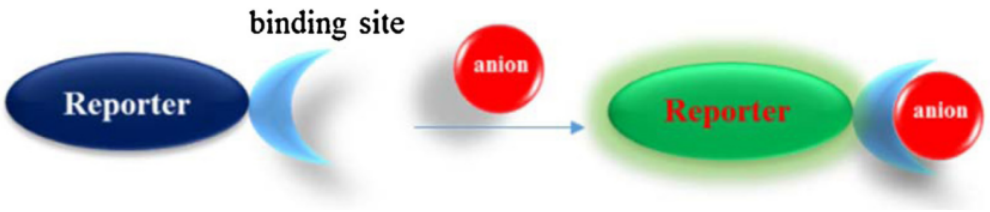

Figure 1.1 Schematic presentation of interaction of a chemosensor with a guest analyte [12]

1.2 Basic design of chromogenic sensors

Metal ions and anions play important role in a wide range of chemical, environmental, industrial and biological processes [13, 14]. However, some metal ions and some anions such as mercury, lead, chromium and fluoride can induce an illness when an excess amount of these ions get into an organism. One way of the

contamination of these toxic ions in the environment is through industrial wastes [13, 15]. The fabrication of effective sensors for these ions with high affinity is thus in high demand, in particular colorimetric sensors that can be seen by human eye as they are low cost and can provide immediate qualitative information without requiring any spectroscopic instrumentation [16-19].

There are many classes of binding units for metal ions, for example, acyclic, and macrocyclic ligands. The effective binding unit known as “polyethylene glycol” is a series of oxygen atoms alternate with ethylene moieties, i.e., $–OCH_2CH_2OCH_2CH_2-$. The term “podand” (Figure 1.2), given by Weber and Vögtle, refers to this class of acyclic polyethylene glycol binding units [20, 21]. This type of acyclic hosts usually shows less cation affinity than cyclic analogues because of their higher degree of flexibility, leading to lacking of preorganization. Like podand, the cyclic binding unit “crown ether”, discovered by Pedersen [1-3], possesses oxygen atoms that can act as binding sites for metal ions and its crown size is critical to selective binding behavior. Having only oxygen atom donors, the unmodified cyclic ether, e.g. 18-crown-6, has been known to be effective for binding of hard metal ions such as alkali and alkaline earth metal ions. In contrast, the modification of crown ether to diaza-crown, such as diaza-18-crown-6 in Figure 1.2, leads to a favorable affinity for soft metal ions like transition ones due to the presence of soft nitrogen donor atoms. The efficiency of diaza-crowns can be ameliorated by addition of two side arms at nitrogen atoms which can form encapsulated and lipophilic complexes with stabilities intermediate between crown ethers and cryptands, the bicyclic analogues [1]. Apart from the size of the crown cavity, the selectivity on the complexation is also determined by the position of flexible side arms and their donor group that can provide further coordination to the guest cation in the crown ring.

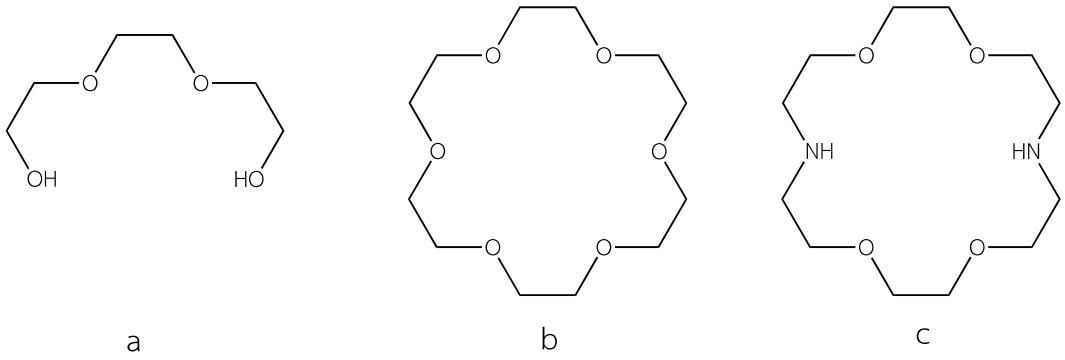

Figure 1.2 Example of (a) podand: triethylene glycol (b) crown ether: 18-crown-6 and (c) diaza-18-crown-6

One of the signaling units that has been used is the unit that gives color known as chromophores. Most chromophores are covalent unsaturated groups that usually absorb in the visible region, which corresponds to the energy for promoting π electrons from a lower energy ground state to a higher energy excited state. The chromogenic organic compounds usually compose of aromatic rings with conjugate double bond system such as azobenzene, rhodamine, pyrene, etc (Figure 1.3) [22-26]. The azophenol groups have been universally employed as signaling unit. Many derivatives of azophenol exhibit chemogenic behavior as a result of structural change induced by interactions [4, 7-9, 19, 27-30]. For example, calixarenes containing azobenzene show hypsochromic effect (blue shift) while their quinone-hydrazone analogues give bathochromic effect (red shift), a process known as tautomerization. Furthermore, the tautomerization of the molecule can be more intense by an addition of functional groups, such as ester or carboxyl groups at *ortho* position to azo group which can stabilize the quinone-hydrazone form. Nitrogen atoms in azobenzene also play important role to metal ion binding [25, 31].

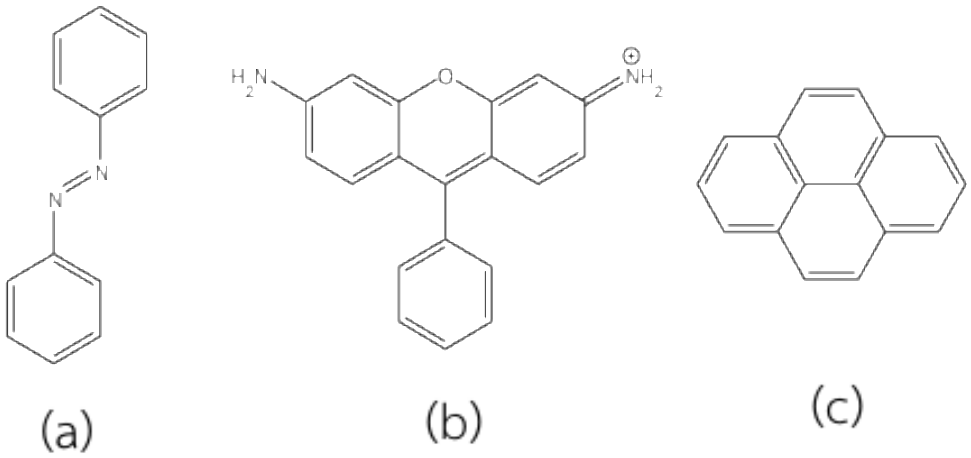

Figure 1.3 Examples of chromophores: (a) azobenzene, (b) rhodamine, (c) pyrene

1.3 Aza-crown and diaza-crown chemosensor

Aza-crown ethers and diaza-crown ethers (Figure 1.4) have been used as binding unit in many researches [32-38]. They possess binding ability toward transition metal ions that play various important roles in biochemistry and environmental science. Recently, many researchers have been interested in modifying and developing ion-selective sensor based on aza- and diaza-crown ethers by addition of signaling units to produce signal changes upon binding with metal ions.

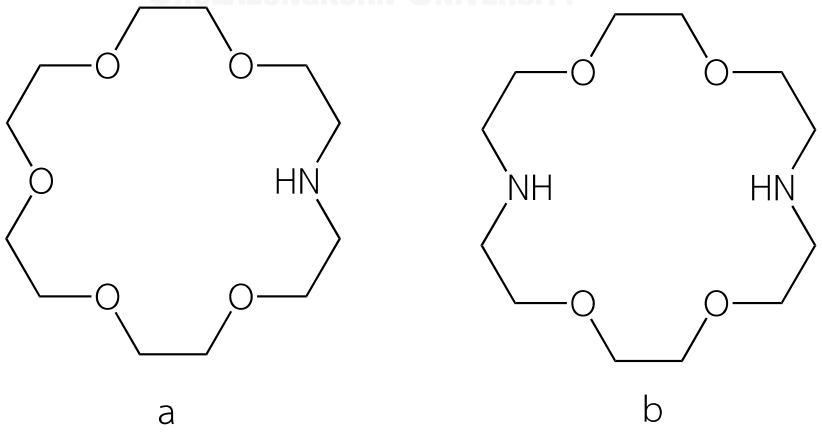

Figure 1.4 Examples of azacrown: (a) aza-18-crown-6 ether (b) diaza-18-crow-6 ether

The complexation of bis-(*p*-chlorophenol)-containing diaza-18-crown-6 (**L1**) with $Cu(NO_3)_2$, investigated by UV-Vis spectrophotometry, showed large bathochronic shifts from 287 nm to 316 nm [39]. The X-rays crystal structure analysis revealed that **L1** formed a stable 1:1 complex with Cu^{2+} using two nitrogen atoms and two oxygen atoms from diazacrown ether as donor atoms.

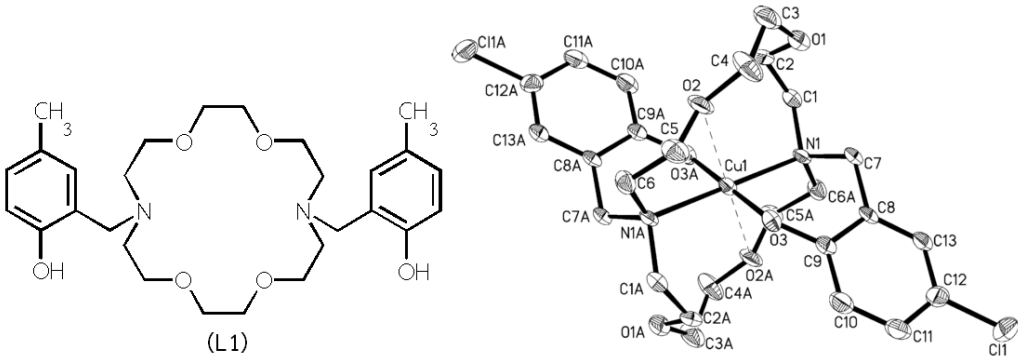

Figure 1.5 Bis-(*p*-chlorophenol)-containing diaza-18-crown-6 (**L1**) and the X-rays crystal structure of complex.

In 2013, the aryl-amine containing azacrown ether ring and bodipy (**L2**) were synthesized by the Schiff base condensation [40]. The spectroscopic-electrochemical properties of **L2** showed that addition of Hg^{2+} (20 eq) to the Schiff base ligand solution induced hypsochromically shifted around 30 nm in UV-Visible absorption due to an extended conjugation of the π-system of the bodipy groups with the nitrogen-oxygen atoms of the azacrown ether. Moreover, Hg^{2+} could induce a more intense emission which hypsochromically shifted to 485 nm of the emission spectra. These can be attributed to the chelation-induced enhanced fluorescence (CHEF) mechanism.

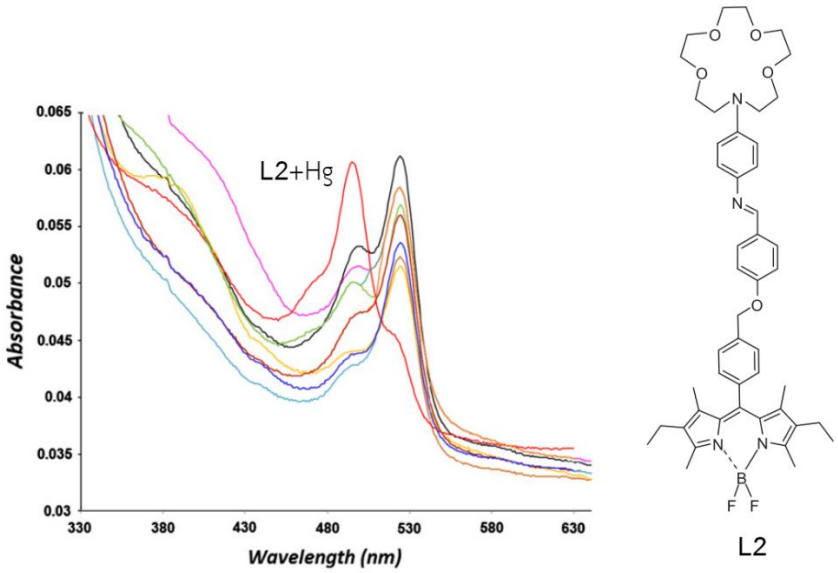

Figure 1.6 UV-Visible spectra of aryl-amine containing azacrown ether (**L2**) in the presence of metal ions and **L2** structure

Fluorescent chemosensor containing coumarins based on diaza-18-crown-6 ether (**L3**), reported by Li et al. [38], exhibited high selectivity for Fe^{3+} ion: addition of Fe^{3+} (100 eq) into **L3** induced fluorescence quenching due to a paramagnetic Fe^{3+} center and a coumarin ligand to Fe^{3+} charge transfer (LMCT). Because of this result, **L3** was selective for Fe^{3+} in aqueous in a wide pH range with a good discrimination of iron valence states.

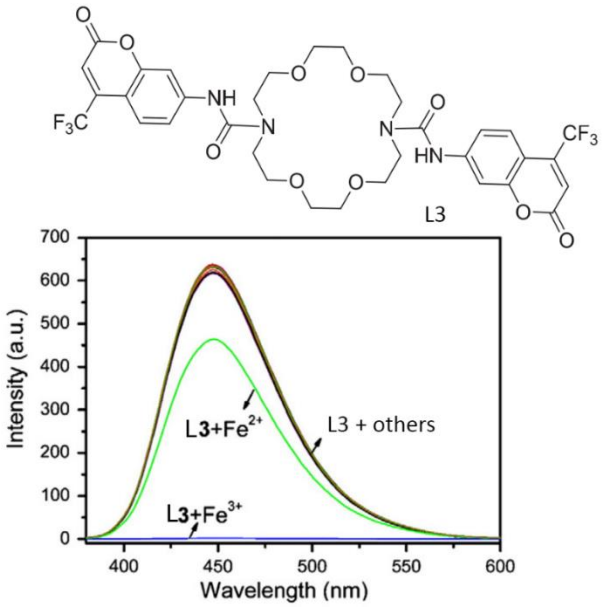

Figure 1.7 fluorescent chemosensor containing coumarins based on diaza-18-crown-6 ether (**L3**), and fluorescent spectra of **L3** in the metal ions

1.4 Azobenzene-quinone hydrazone tautomerism

There are many reports about tautomerization of azobenzene to quinone-hydrazone [25, 28, 31, 41-43]. Azobenzene compounds usually show two absorption bands, i.e., $\pi \rightarrow \pi^*$ transition band of the azo group (-N=N-) at 360-400 nm and $n \rightarrow \pi^*$transitions of the hydrazone group (-NH-N) at 500-576 nm. These bands correspond to the tautomerization of azobenzene and quinone-hydrazone as shown in Figure 1.8.

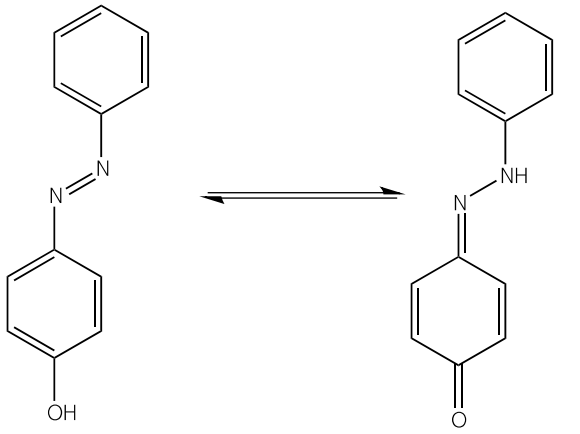

Azobenzene Quinone-hydrazone

Figure 1.8 tautomerization of azobenzene

The protonation on aminoazobenzene derivatives by UV-Visible and resonance Raman spectroscopies was investigate and compared with the result from quantum-chemical calculations by Matazo et al. [44]. The calculations revealed that the hydrazone form showed a maximum absorption with a difference longer wavelength around 120 nm from that of the azo form. This result could be explained by a large difference in electronic dipole moment between ground and excited due to the enhancement of the electron delocalization of the quinoid structure in hydrazine form.

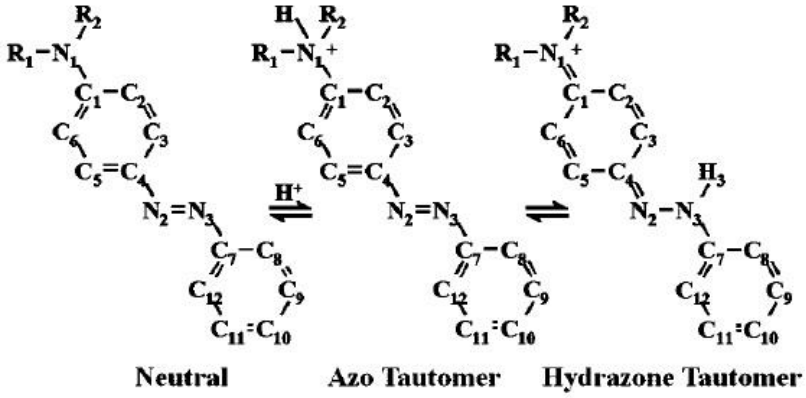

Figure 1.9 Structures of the neutral and protonated species of 4-amino (R = H) and 4-(dimethylamino)azobenzene (R =CH3) involving the azo-hydrazone tautomeric equilibrium.

The tautomerization of azobenzene depends on interaction between azobenzene with another guest such as cations, anions and solvents. In 1983, Mahmoud et al .[42]

found that protic media could block electrons at the azo group through an intermolecular hydrogen bonding, resulting in a difficult excitation of the n-electrons to the antibonding π^* orbital and exhibition of azobenzene absorption band at shorter wavelength. In contrast, aprotic media generated more absorption of quinone-hydrazone than that of azobenzene. From this property, azophenol has been universally employed as signaling units hoping in change conformation when they bind with analyte.

1.5 Chomogenic sensors based on azobenzene-dye

Azophenol has been universally employed as signaling units because of its pronounced chromogenic behavior towards many cations and anions. The azo dyes or phenols with N=N functional group exist in 2 forms, i.e. quinone-hydrazone and azo form. The N=N or azo group plays important role to binding with metal ions.

1.5.1 Chomogenic metal ions sensors based on azobenzene-dye

Kim et al. reported azo-coupled calix[4]arenes having signaling unit as *ortho*-acid diazophenyl (**L4**) and *ortho*-ester diazophenyl (**L5**) for metal ion sensors [25, 31]. The UV-vis abosorption of these chemosensors showed characteristic peaks of both azophenol and quinone-hydrazone forms (Figure 1.10). After addition of metal ion into the solution, they exhibited an increase in absorption intensity at wavelength at maximum absorption (λ_{max}) of quinone-hydrazone (480, 487 nm) and a decrease at λ_{max} of azophenol (355, 345 nm). While the chemosensor **L4** showed color changes in the presence of alkaline earth, transition and heavy metal ions; the chemosensor **L5** showed color changes only in the presence of transition and heavy metal ions but not with alkali and alkaline earth metal ions. The *ortho*-ester group was capable of stabilizing quinone-hydrazone form when chemosensors bound with metal ions as proposed in Figure 1.11.

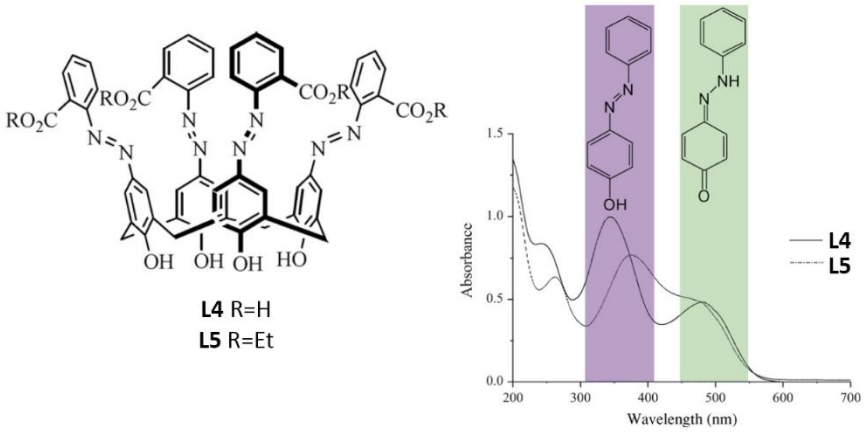

Figure 1.10 Structure and absorption spectra in MeCN of diazo-coupled calix[4]arene **L4** and **L5** [27]

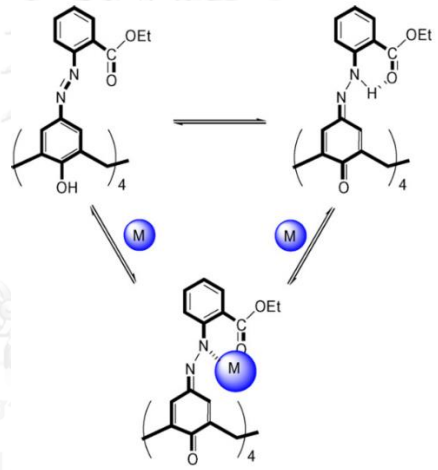

Figure 1.11 Plausible complexation mechanism of azo-coupled calix[4]arenes with transition metal ions [33]

Arylazo-coupled calix[4]arene derivatives were reported in 2005 [45] and 2007 [24]. These chemosensors (**L6**, **L7**) revealed Hg^{2+} ion selectivity over other metal ions due to a large bathochromic shift. These observations imply that there is a subtle balance between metal complexation-induced release of protons from the azobenzene to the quinone-hydrazone tautomer. It was reported that the structure for azocalix[4]arene-Hg^{2+} complexes were stabilized by two pairs of intramolecular hydrogen-bonding interaction between undissociated phenolic OH groups and

neighboring dissociated phenolate anion (Figure 1.12). The NMR experiment indicated that the nitrogen atoms of azo were donor atoms

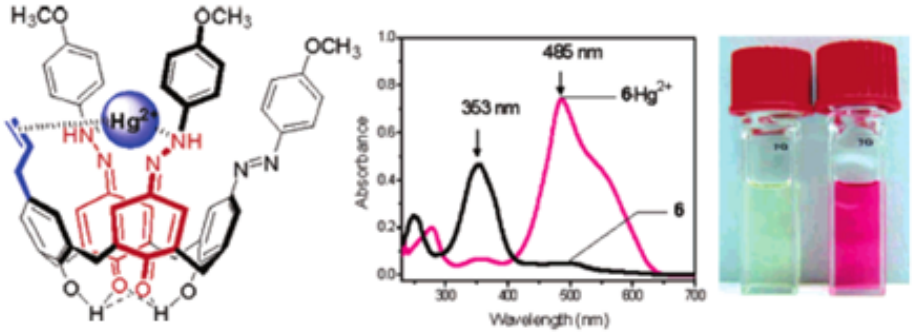

Figure 1.12 Possible binding mode, UV-Visible and color change of azocalix[4]arene **L7** with Hg^{2+}

The synthesized azo-azomethine receptor **L8**, shown in Figure 1.14, showed selectivity toward Cu^{2+} more than any other metal ion [46]. UV-Visible spectrum of the free ligand exhibited an intense band centered at 355 nm ascribed to $\pi \rightarrow \pi^*$ transition of the chromophores. Addition of Cu^{2+} ion to the receptor solution led to a decreasing in the absorbance at 335 nm and an increasing of a new band at 482 nm. This observation could be explained by internal charge transfer (ICT) process between copper ion and the receptor molecule.

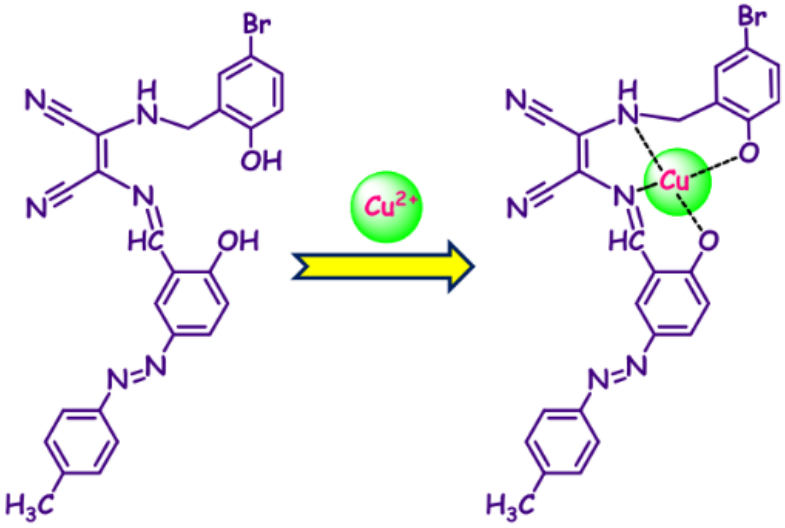

Figure 1.13 Plausible complexation of azo-azomethine receptor (**L8**) with Cu^{2+}

1.5.2 Chomogenic anions sensors based on azobenzene-dye

Not only azobenzene-dyes could be used as singnaling unit for metal ions sensors as mentioned in section 1.5.1, they could also sense anions via hydrogen bonding. For instance, *para*-nitro 4-hydroxy azobenzenes, reported by K. Rezaeian and H. Khanmohammadi in 2014 [19] and by S.-Y. Na, H.-J. Kim in 2015 [45], were used as signaling unit for anions. It was found that fluoride and acetate induced a conformation change from azobenzene to quione-hydrazone, leading to a bathochromic or red shift in UV-Visible spectra. This significant red shift was ascribed to the charge transfer interactions occurred between the electron-rich donor units (oxygen of azophenol) to the electron-deficient acceptor units (-NO_2). The ^{1}H-NMR confirmed that the color response was due to a hydrogen bond formation between phenolic OH groups and anion, followed by deprotonation.

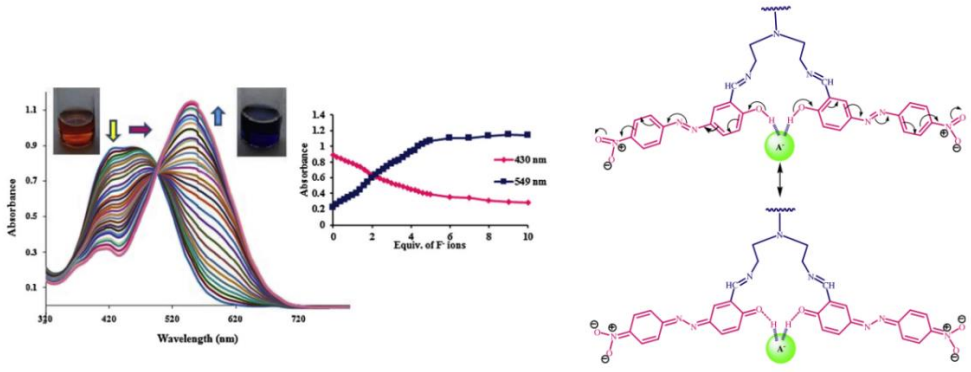

Figure 1.14 UV-Visible titration and plausible complexation of sensor base on nitro-azobenzene (**L9**) with anion (F^-)

In 2014, Radchatawedchakoon et al. synthesized a series of highly selective azo bye-thiosemicarbazones based annion sensors [47]. The sensing properties of these sensors were determined by naked-eyes and UV-Visible spectra. Only the addition of acetate anion led to an obvious change from light yellow to orange. The binding unit in the anion sensor was confirmed by ^{1}H-NMR: upon addition of 1.0 equiv of acetate, the signal of phenol –OH and –NH_2 shifted upfield from 11.51, 8.38 and 8.17 to 11.09, 7.79, and 7.61 ppm, respectively. The proton shift stopped after adding of 1 equiv. of AcO^-, indicating that –OH and –NH_2 did not act as a binding site but the interaction of

the anions with the sensor was mainly due to proton-transfer to the anions rather than hydrogen-bonding. The selectivity of sensor **L10** for AcO^- could be ascribed to the basicity of the anions in aqueous solution.

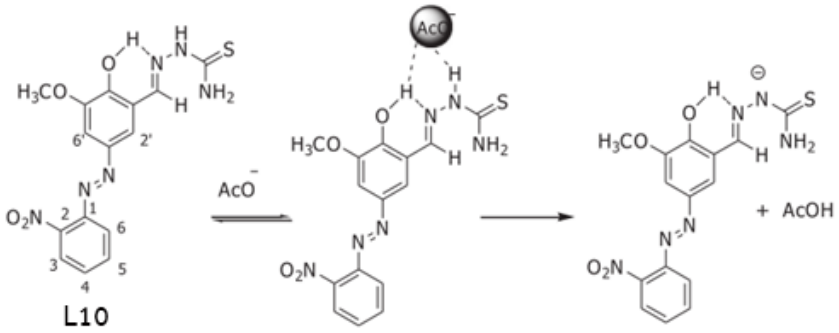

Figure 1.15 Proposed host-guest binding mode of L10 and AcO^-

The tautomerization of azobenzene also depends on anion coordination, i.e., Na Kaur et al. reported a study of azo dye coupling with benzimidazole (**L11**) in 2015 [48]. This receptor responded with a dramatic color change from colorless (λ_{max} at 315 nm) to dark yellow (λ_{max} at 470 nm) upon addition of 50 equivalents of CN^-, F^-, AcO^-, and $H_2PO_4^-$. The stability constant values revealed that AcO^- bound most strongly and interaction with various anions was in the order of $AcO^- > CN^- > F^- > H_2PO_4^-$. This result could be explained by intermolecular proton transfer from phenyl OH to the acetate ion rather than proton transfer to the benzimidazole nitrogen. Upon interaction with anions, deprotonation of the –OH group occurs, which can reinforce the formation of hydrazone via tautomerization. This will result in a band at longer wavelength at 470 nm allowing for visual naked-eye detection.

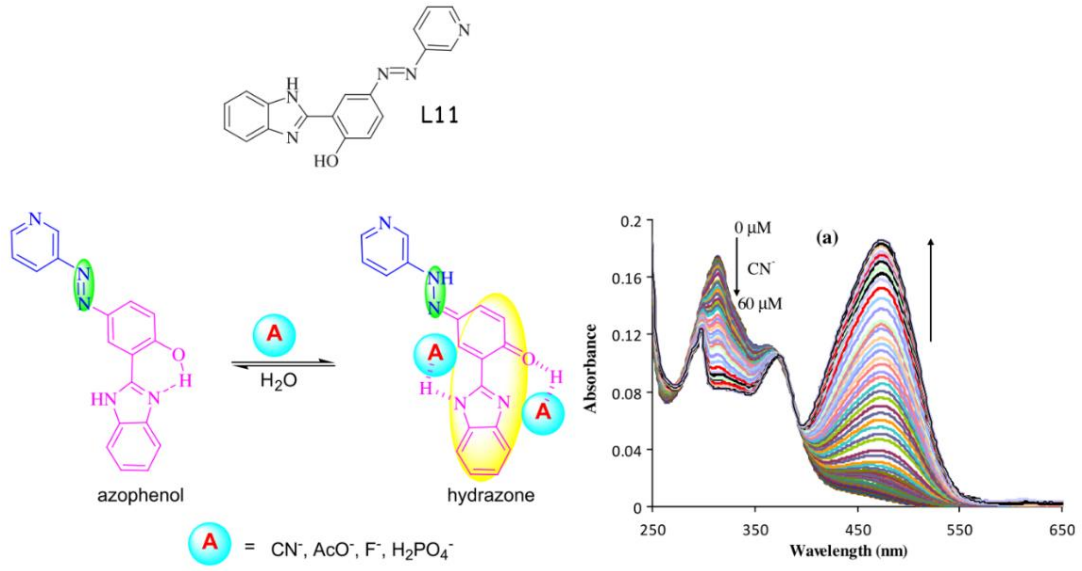

Figure 1.16 Structure of benzimidazole **L11**, plausible complex of azo dye coupling with **L11** and its UV-Visible titration with CN^-

In 2015, N-monosubstituted diaminomaleonitrile-based azo-azomethine dyes were synthesized. The sensor **HL**[1] modified with *para*-nitro substituent exhibited high affinity for F^-, AcO^- and $H_2PO_4^-$ This study showed that the electron-withdrawing group could decrease the electron density of nitrogen and oxygen atoms and increase the acidity of the hydrogen-bind donors, facilitating the deprotonation. The detailed ^1H NMR corroborated that anion recognition was based on the deprotonation of hydroxyl group [49].

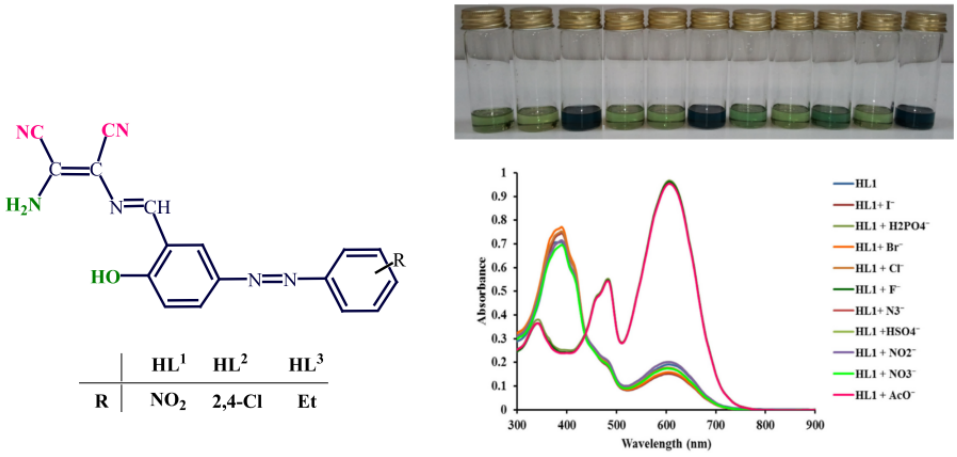

Figure 1.17 Structure of sensor **HL**^{n} (**n=1-3**), color changes and UV-Visible absorption spectra of sensor **HL**[1] in the presence of 5 eq of various anions

1.6 Concept of this research

There are many methods for metal ion detection such as cyclic voltammetry, atomic absorption, fluorescence spectroscopy, etc. However, these methods need expensive, complicated instruments, and an operating experts which add to a high cost. To reduce the cost of detecting metal ion in the environment, a visible sensor was designed. Chromogenic sensors are easy to use and low cost. They can also employ simple UV-Visible spectrophotometer for detailed analysis. The designed naked-eye sensors in this research consisted of diaza-18-crown-6 acting as a binding unit linked to π-conjugated azobenzene acting as both binding and signaling units. Ester and acid units were also added to assist the binding with metal ions at *ortho*-position of azobenzene. The *para*- nitro unit were added to enhance the delocalization of π-electron. The synthesized molecules were expected to change from a light to a visibly dark color upon interaction with guest ions. The proposed structures also offered advantages in a way that the required precursor such as polyethylene glycol and nitrite salt are common and inexpensive and the azo coupling reaction is rather simple.

The first set of the ligands in this research was *ortho*- ester derivatives. The expected donor units in this set were (a) diazacrown ring containing oxygen atoms and nitrogen atoms known to offer good interaction with transition metal ions, and (b) the ester moieties on azobenzene rings at *ortho*-position hoped to bind with transition metal ion and stabilize the quinone hydrazone via form six-membered ring with hydrogen atom of quinone hydrazine [19].

The second set of the ligand in this research was designed by expanding carbon linkage between diazacrown and azobenzene in hope for increasing ligand flexibility which should allow wrapping around the metal ions.

The third set of the ligand was designed by changing the functional group from ester to carboxylic acid group which was less steric than ester group. So, the metal ion should easily bind with this ligand.

The fourth set of the ligands in this work was obtained by varying the functional group on the azobenzene from *ortho*-position to *para*-nitro group. The idea behind

this series was based on the fact that good optical sensors depend on the electron distribution in π conjugation system. The presence of interaction between ligand and metal ion could affect the electron flow, resulting in an enhancement or a quenching of the charge transfer interactions between electron rich and electron poor substituents on azobenzene. This phenomenon could induce a large change of absorbed energy for excitation of π electron leading to an obvious change of UV-Visible absorption spectra and color. The good distribution π conjugation system consists of good election donor and good election acceptor on the opposite site. Since 4-hydroxy azobenzene has hydroxyl group which is a good electron donor group, the distribution of π electron thus could be enhanced by addition of a good electron accepting group at the *para*- position, moreover, the *para* position was less steric than *ortho*-position, leading to easy binding with metal ion.

1.7 Objective and scope of this research

1) To synthesize and characterize azo dye-based crown ethers containing ester, carboxylic acid and nitro groups
2) To study their optical sensing properties towards metal ions and anions by naked eye observation and UV-Visible spectrophotometry

CHAPTER II

EXPERIMENTAL

2.1 General procedure

2.1.1 Instrument

Nuclear Magnetic Resonance (NMR) spectra were recorded on a Varian Mercury Plus 400 NMR spectrometer and Bruker DRX 400 MHz spectrometers. All chemical shifts were reported in part per million (ppm) using the residual proton or carbon signal in deuterated solvent as internal references. MALDI-TOF mass spectra were carried out on Bruker Daltonics MALDI-TOF using 2-cyano-4-hydroxy cinnamic acid (CCA) or dithranol as a matrix. UV-Visible absorption spectra were recorded by a Varian Cary 50 Probe UV-Vis spectrophotometer at 25 °C with a Julabo F33 temperature controller.

2.1.2 Materials

All chemicals and solvents for synthesis, purchased form Alrich, Fluka, Merck and TCI, were of commercial grades and used without purification. Anhydrous acetonitrile, dichloromethane, toluene and tetrahydrofuran were dried over CaH_2 or Na and distilled under nitrogen atmosphere before use. Methanol, acetonitrile and dimethyl sulfoxide used in sensing study were of spectro grade form LAB-SCAN and Merck. Silica gel plates used in thin-layer chromatography (TLC) were Kieselgel 60 F_{254}, 1 mm thick from Merck. Column chromatography was performed on stationary phases of either silica gel (Kieselgel 60) or alumina gel (Aluminium oxide 90 standardized) of 0.063 – 0.200 mm thickness from Merck. All ligands and salts used in sensing studies, i.e. nitrates of Li^+, Na^+, K^+, Mg^{2+}, Ca^{2+}, Cr^{3+}, Co^{2+}, Ni^{2+}, Cu^{2+}, Zn^{2+}, Cd^{2+} and Pb^{2+}, $HgCl_2$, and tetrabuthylammonium salts of F^-, Cl^-, Br^-, I^-, OH^-, OCl^-, NO_3^-, $H_2PO_4^-$, AcO^- and BzO^-, were vacuum dried before use. Ionic strength in UV-Vis spectrophotometric titration was kept constant by tetrabuthylammonium hexafluorophosphate.

2.2 Syntheses

A series of six azo dye-based crown ethers containing ester, carboxylic acid and nitro group was synthesized by coupling of phenol methyl diaza-crown ether with ethyl-2-aminobenzoate or 4-nitroaniline as shown in Scheme 2.1. Their characterizations were done by ^{1}H, ^{13}C-NMR, and mass spectroscopies. The synthetic details for each step were described in the following sections.

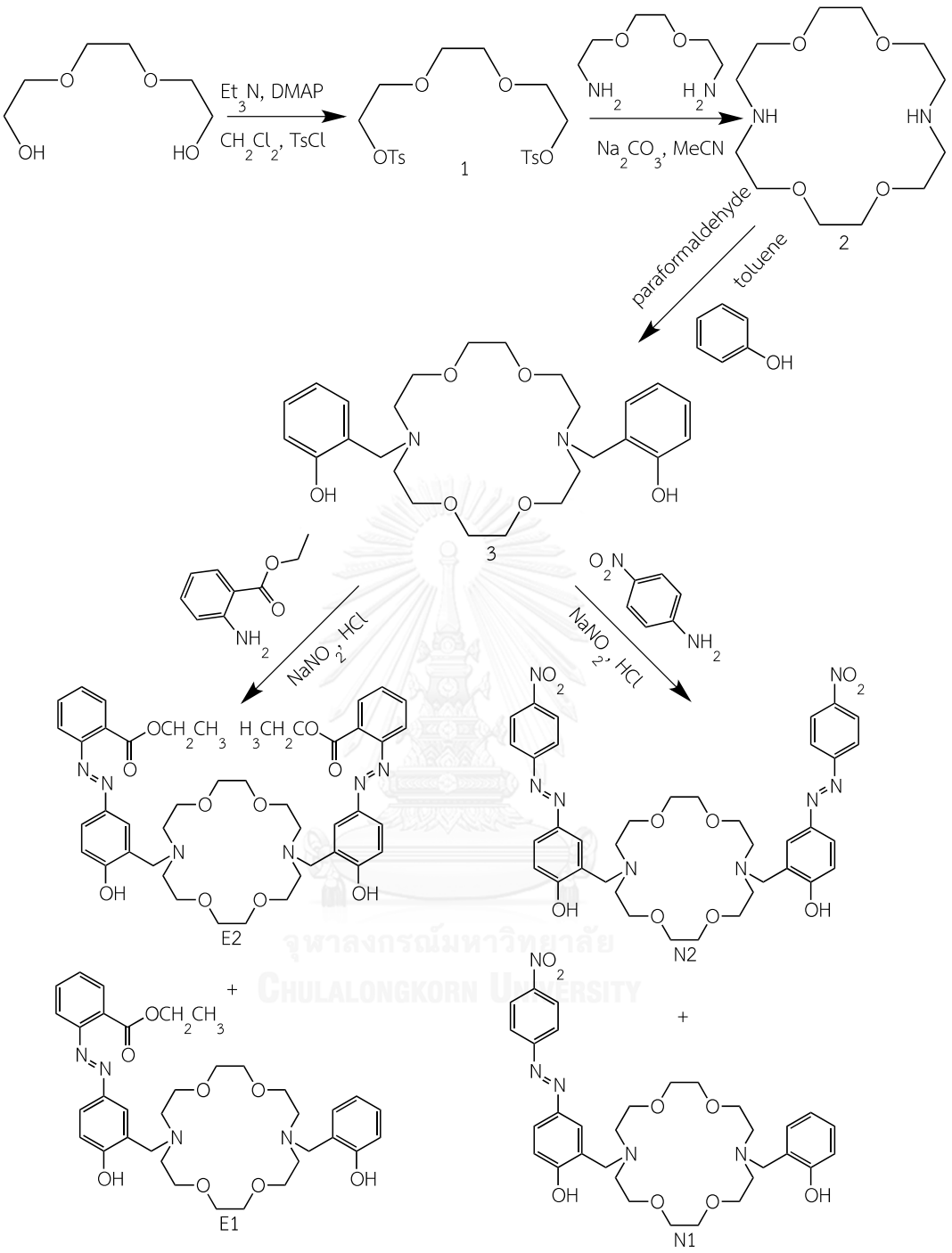

Scheme 2.1 Synthesis pathway of azo-diaza-18-crown-6 derivatives

2.2.1 Synthesis of receptors ester azo-diaza-18-crown-6 derivatives E2 and E1

2.2.1.1 Synthesis of triethyleneditosylate 1

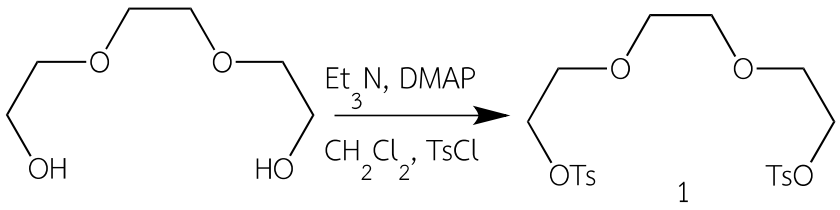

In a 100-mL round bottom flask, a mixture (50 mL) of dichloromethane solutions of triethyleneglycol (3.904 g, 26 mmol), triethylamine (7.892 g, 78 mmol), and DMAP was stirred for 30 minutes. Anhydrous solution of tosyl chloride (9.914 g, 52 mmol) was then added, and stirred for another 12 hours. Elimination of reactant residue was done by adding 3 M HCl to adjust the pH of this mixture to 1. After that the mixture was extracted with water three times and the organic phase was collected and removed by rotary evaporator. The crude product was recrystallized in methanol and the resulting solid was filtered and dried with 64.1 %yield (7.643 g). ^{1}H-NMR ($CDCl_3$, TMS): δ 2.44 (s, 6H, C*H*$_3$-Ar), δ 3.53 (s, 4H, CH_2-C*H*$_2$-OTs), δ 3.65 (t, 4H, CH_2-C*H*$_2$-O), δ 4.13(t, 4H, CH_2-C*H*$_2$-O), δ 7.34 (d, 4H, *Ar*), δ 7.79 (d, 4H, *Ar*) ppm.

2.2.1.2 Synthesis of diaza-crown ether 2

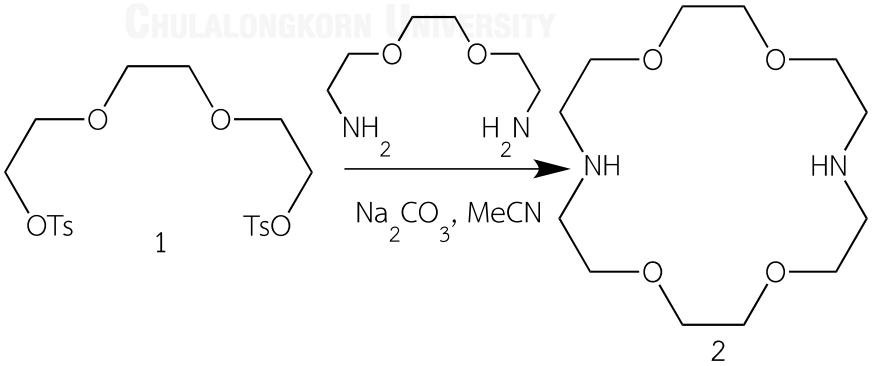

In a 100-mL two-neck round bottom flask equipped with a magnetic bar, anhydrous acetonitrile (50 mL) was used to dissolve trietyleneditosylate (4.425 g, 9.65 mmol), ethylenedioxy amine (1.430 g, 9.65 mmol), and Na_2CO_3 (10.175 g, 96 mmol). The reaction mixture was filtered after refluxing for 3 days and the solvent was evaporated with rotary evaporator. The crude product was purified by chromatography

on alumina using 1:9 ethanol:THF as eluent which was subsequently evaporated. The white solid was obtained with 26 %yield (0.658 g). ^{1}H-NMR ($CDCl_3$, TMS): δ 1.42 (s,H_2O), δ 2.20 (s, 2H, N*H*), δ 2.79 (m, 8H,NH-CH_2-CH_2), δ 3.59 (m, 16H,-OCH_2-) ppm.

2.2.1.3 Synthesis of phenol methyl diaza-crown ether 3

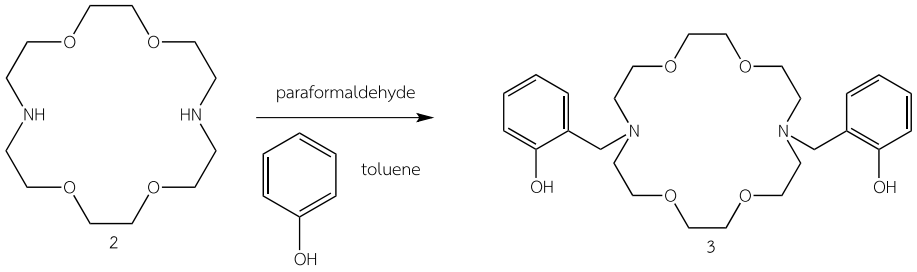

Phenol methyl diaza-crown ether 3 was synthesized according to a published method [50]. In a 50-mL two-neck round bottom flask equipped with a magnetic bar, a mixture of toluene solutions of diaza-crown (0.5249 g, 2 mmol), phenol (0.4517 g, 4.80 mmol), and paraformaldehyde (0.1472 g, 4.90 mmol) was refluxed for 12 hours. After that the solvent was evaporated under vacuum. A small amount of methanol was then added to help the crystallisation. After sonication for 30 minutes, the solid product was filtered and dried with 14 %yield (0.135 g). ^{1}H-NMR ($CDCl_3$, TMS):δ 2.86 (m, 8H, NC$H_2$$CH_2$), δ 3.61 (m, 8H, -CH_2CH_2O-), δ 3.67 (m, 8H, -OC$H_2$$CH_2$-), δ 3.81 (m, 4H, NCH_2Ar), δ 6.60-7.16 (m, 8H, *Ar*) ppm.

2.2.1.4 Synthesis of ester azo-diaza-18-crown-6 derivatives E2 and E1

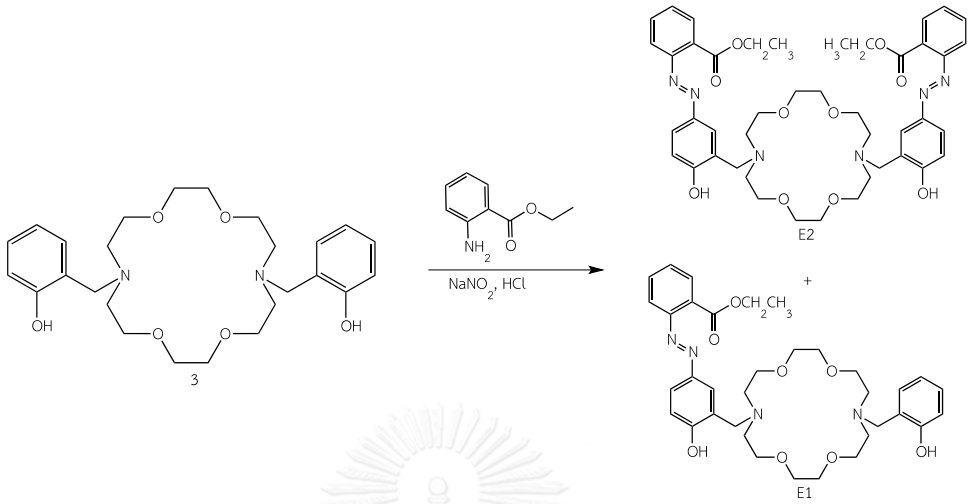

In a 50-mL two–neck round bottom flask, an aqueous solution (5 mL) of ethyl-2-aminobenzoate (0.3304 g, 2 mmol), $NaNO_2$ (0.1446 g, 2.1 mmol), and HCl (2.5 mL) was stirred at 0 °C for 15 minutes. Phenol methyl diaza-crown ether (0.4980 g, 1.05 mmol) in 25 ml of THF:pyridine (5:2) was then added and the stirring continued for 24 hours at the same temperature. After neutralization by 3 M HCl, the mixture was extracted by CH_2Cl_2 which was subsequently removed by rotary evaporator. The crude products were separated by chromatography on silica gel using 10% of methanol in dichloromethane as eluent. Both products appeared as orange oil: **E2** came out first with 24 %yield (0.154 g), followed by **E1** with 20 %yield (0.196 g).

Characterization of **E2**

^{1}H-NMR ($CDCl_3$, TMS): δ 1.30 (t, 6H, OCH_2CH_3), δ 2.86 (m, 8H, NCH_2CH_2), δ 3.62 (m, 8H, $-CH_2CH_2O-$), δ 3.69 (m, 8H, $-OCH_2CH_2-$), δ 3.90 (m, 4H, NCH_2Ar), δ 4.36 (m, 4H, OCH_2-), δ 6.75-7.30 (m, 6H, *Ar*-OH), δ 7.50-7.85 (m, 6H, *Ar*-CO-) ppm.

^{13}C NMR ($CDCl_3$, TMS): δ 164.8, 159.4, 152.8, 140.3, 131.4, 126.6, 126.4, 125.8, 123.7, 123.5, 122.6, 115.4, 113.0, 69.4, 68.7, 62.8, 59.6, 56.2, 16.2 ppm.

MALDI-MS $C_{44}H_{54}N_6O_{10}$ found m/z $[M]^+$ 827.579, calcd 826.93

Characterization of **E1**

^{1}H-NMR ($CDCl_3$, TMS):δ 1.31 (t, 3H, OCH_2CH_3), δ 2.57 (m, 2H, NCH_2CH_2), δ 2.63 (m, 2H, NCH_2CH_2), δ 3.67 (m, 8H, $-CH_2CH_2O-$), δ 3.69 (m, 8H, $-OCH_2CH_2-$), δ 3.90 (m, 4H,

NCH_2Ar), δ 4.36 (m, 4H, OCH_2-), δ 6.75-7.30 (m, 6H, *Ar*-OH), δ 7.50-7.85 (m, 6H, *Ar*-CO-) ppm.

^{13}C NMR ($CDCl_3$, TMS): δ 165.9, 160.2, 157.6, 153.7, 144.6, 133.4, 131.3, 129.9, 128.8, 127.8, 125.6, 125.1, 123.2, 122.9, 122.7, 121.0, 116.7, 115.8, 114.7, 70.5, 70.2, 69.0, 68.5, 60.9, 58.5, 57.9, 56.4, 56.2, 16.4 ppm.

MALDI-MS $C_{35}H_{46}N_4O_8$ found m/z $[M]^+$ 651.247, calcd 650.33

2.2.2. Synthesis of receptors ester azo-ethylene-diaza-18-crown-6 derivative EE2

Azo-ethyleny-diaza-18-crown-6 ester derivative was synthesized by coupling phenol ethylene diaza-crown ether with ethyl-2-aminobenzoate as shown in Scheme 2.2 and characterized by ^{1}H, ^{13}C-NMR, and mass spectroscopies. The synthetic details for each step were described in the following sections.

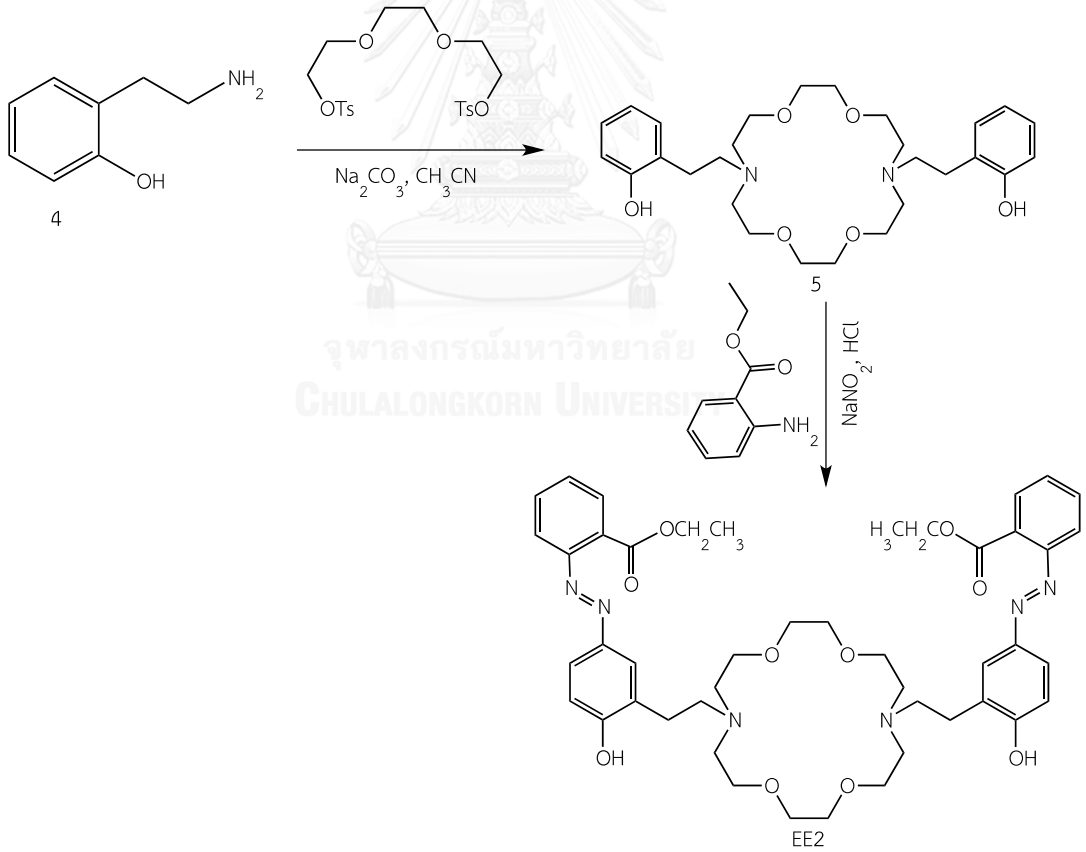

Scheme 2.2 Synthesis pathway of azo-ethylene-diaza-18-crown-6 ester derivatives **EE2**

2.2.2.1 Synthesis of phenol ethylene diaza-crown ether 5

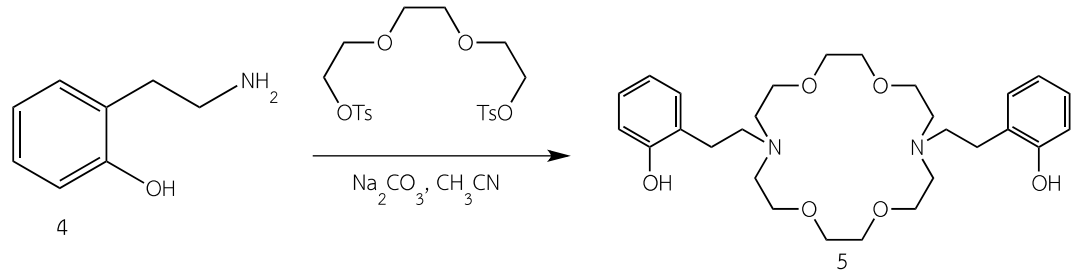

The starting 2-hydroxybenzylamine hydrochride **4** was prepared according to method which was reported by Wood et al. [51]. In a 50-mL two-neck round bottom flask equipped with a magnetic bar, trietyleneditosylate (0.458 g, 1.00 mmol), 2-hydroxybenzylamie hydochride (0.137 g, 1.00 mmol), and Na_2CO_3 (1.06 g, 20 mmol) were dissolved in anhydrous acetonitrile (20 mL) and refluxed for 3 days. After that the reaction mixture was filtered and acetonitrile was removed by rotary evaporator. The crude product was purified by chromatography on alumina using 1:9 ethanol:THF as eluent.After evaporation of the eluent,the yellow oil was obtained with 48% yield (0.223 g). ^{1}H-NMR ($CDCl_3$, TMS): δ 2.48 (s, 2H, N-C*H*$_2$-CH$_2$), δ 3.55 (s, 4H, CH$_2$-C*H*$_2$-O), δ 3.65 (t, 4H, CH$_2$-C*H*$_2$-O), δ 3.84 (t, 4H, CH$_2$-C*H*$_2$-O), δ 4.18 (t, 4H, CH$_2$-C*H*$_2$-Ar), δ 7.31 (d, 4H, *-Ar*), δ 7.84 (d, 4H, *-Ar*) ppm

2.2.2.2 Synthesis of ester azo-ethylene-diaza-18-crown-6 derivative EE2

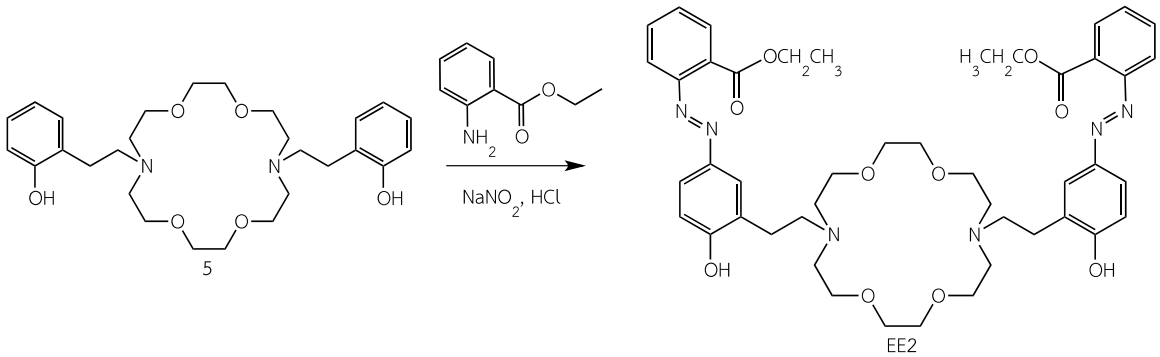

In a 50-mL two–neck round bottom flask, an aqueous solution (5 mL) of ethyl-2-aminobenzoate (0.1652 g, 1.0 mmol), $NaNO_2$ (0.6885 g, 10 mmol), and HCl (2.5mL) was stirred at 0 °C for 15 minutes. Phenol ethylene diaza-crown ether (0.488 g, 1.0 mmol) in 25 ml of THF:pyridine (5:2) was then added And thestirring continued at the

same temperature for 24 hours. 3 M HCl was then added to neutralize the mixture before extraction by CH_2Cl_2. After solvent evaporation, the crude product was purified and separated by chromatography on silica gel using 20% of methanol in dichloromethane as eluent. An orange oil **EE2** was obtained with 48% yield (0.406 g).

Characterization of **EE2**

^{1}H-NMR ($CDCl_3$, TMS): δ 1.31 (t, 3H, C*H*$_3$-CH$_2$), δ 1.39 (t, 2H, CH$_2$-C*H*$_2$-N), δ 2.38 (s, 2H, -C*H*$_2$-O), δ 3.61 (t, 2H, CH$_2$-C*H*$_2$-O), δ 4.10 (t, 2H, CH$_2$-C*H*$_2$-O), δ 4.30 (t, 2H, CH$_2$-C*H*$_2$-Ar), δ 4.35 (m, 2H, CH$_3$-C*H*$_2$), δ 7.31 (m, 4H, -*Ar*), δ 8.04 (m, 3H, -*Ar*) ppm

^{13}C NMR ($CDCl_3$, TMS): δ 164.8, 159.4, 152.8, 140.3, 131.4, 126.6, 126.4, 125.8, 123.7, 123.5, 122.6, 115.4, 113.0, 69.4, 68.7, 62.8, 59.6, 56.2, 16.2 ppm.

MALDI-MS $C_{44}H_{54}N_6O_{10}$ found m/z $[M+H]^+$ 855.864, calcd 854.42

2.2.3 Synthesis of receptors acid azo-diaza-18-crown-6 derivative A2

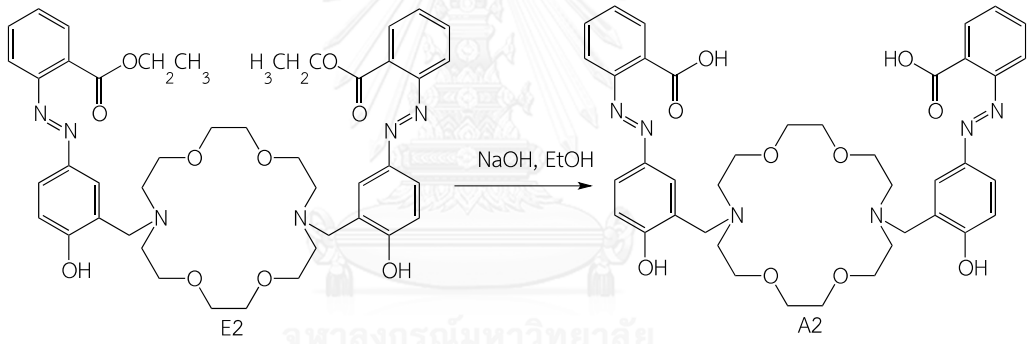

Scheme 2.3 Synthesis pathway of azo-diaza-18-crown-6 acid derivative **A2**

In a 50-mL two-neck round botton flask quipped with a magnetic bar, the mixture of **E2** (0.1654 g, 0.2 mmol) and NaOH (0.0160 g, 0.4 mmol) was dissolved in EtOH in water (1:1), After refluxed for 3 hours, 3 M HCl was added to neutralize the mixture pH. The extraction was performed using 20 ml CH_2Cl_2 3 times and the organic solvent was then removed by rotary evaporator. The crude product was purified by chromatography on silica gel using 20% of methanol in dichloromethane as eluent. The orange solid **A2** was obtained with 60 %yield (0.092 g,).

Characterization for **A2**

^{1}H-NMR ($CDCl_3$, TMS): δ 2.86 (m, 8H, NCH_2CH$_2$), δ 3.62 (m, 8H, -CH$_2$CH_2O-), δ 3.69 (m, 8H, -OCH_2CH$_2$-), δ 3.81 (m, 4H, NCH_2Ar), δ 6.71-7.24 (m, 6H, *Ar*-OH), δ 7.41-7.77 (m, 6H, *Ar*-CO-) ppm.

^{13}C NMR ($CDCl_3$, TMS) spectrum was as follows: δ 163.7, 160.4, 153.8, 139.3, 134.5, 127.6, 127.4, 124.3, 123.8, 123.5, 122.6, 115.4, 114.6, 69.7, 69.1, 59.2, 57.2 ppm.

MALDI-MS $C_{40}H_{46}N_6O_{10}$ found m/z $[M]^+$ 771.586, calcd 770.33

2.2.4 Synthesis of receptors nitro azo-diaza-18-crown-6 derivatives N2 and N1

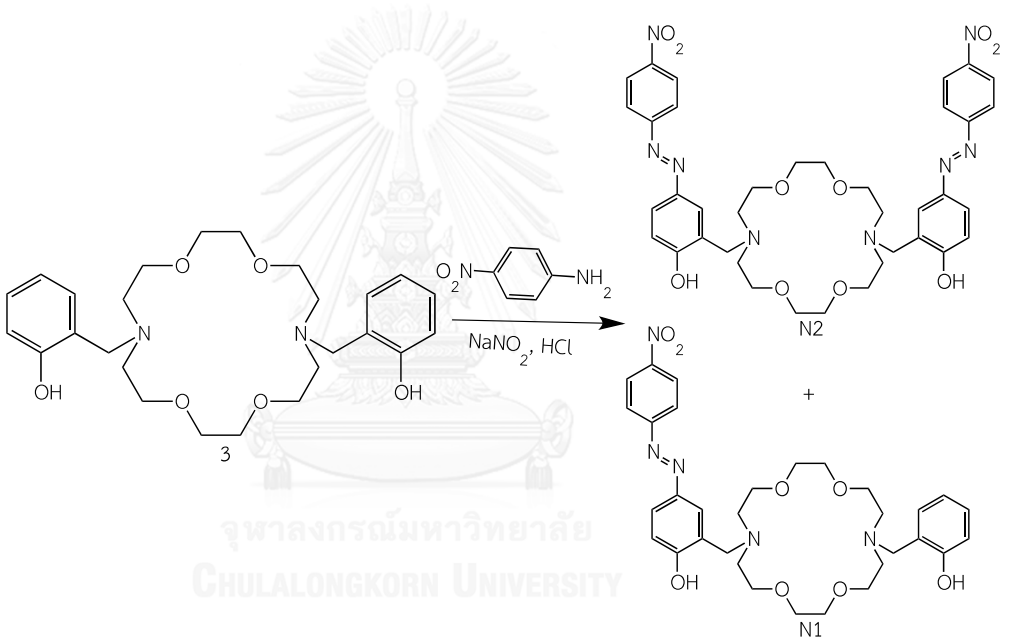

In a 50-mL two–neck round bottom flask, aqueous solution of *p*-nitroaniline (0.2762 g, 2 mmol), $NaNO_2$ (0.1446 g, 2.1mmol) and HCl 0.8 mL was stirred at 0 °C for 15 minutes. Phenol methyl diazacrown ether (0.4350 g, 1.05 mmol) in 20 ml of Na_2CO_3 solution (0.318 g in 5 mL of water) was then added and the stirring continued at 0 °C for 24 hours. After neutralization using 3 M HCl, it was then extracted by CH_2Cl_2 3 times andthe organic solvent was removed by rotary evaporator. The crude product was purified and separated by chromatography on silica gel using 20% of methanol in dichloromethane as eluent. The first product (**N2**) and second (**N1**) product appeared as black solid, yielded 0.132 g (17 %yield) and 0.182 g, (29 %yield), respectively.

Characterization for **N2**

^{1}H-NMR ($CDCl_3$, TMS): δ 3.51 (t, 8H, -CH_2CH_2O-), δ 3.62 (m, 8H, -CH_2CH_2O-), δ 3.78 (m, 8H, -CH_2CH_2O-), δ 3.91 (m, 4H, NCH_2Ar), δ 7.79 (m, 4H, *Ar*-NO_2), δ 7.82 (m, *Ar*-OH), δ 8.25 (m, 6H, *Ar*-OH) ppm.

^{13}C NMR ($CDCl_3$, TMS): 165.3, 157.1, 153.2, 144.5, 126.7, 124.0, 122.9, 122.7, 119.3, 113.8, 70.3, 69.1, 57.9, 55.5 ppm.

MALDI-MS $C_{38}H_{44}N_8O_{10}$ found m/z $[M]^+$ 772.432, calcd 772.32

Characterization for **N1**

^{1}H-NMR ($CDCl_3$, TMS): δ 2.81 (t, 4H, -OCH_2CH_2-), δ 3.07 (dt, 4H, OCH_2CH_2), δ 3.41 (d, 4H, -CH_2CH_2O-), δ 3.44 (m, 4H, -OCH_2CH_2-), δ 3.60 (m, 4H, -NCH_2CH_2-), δ 3.68 (m, 4H, NCH_2CH_2-), δ 3.75 (m, 2H, NCH_2Ar), δ 3.98 (m, 2H, NCH_2Ar), δ 6.34-7.01 (m, 4H, *Ar*-OH), δ 7.78, 8.35 (m, 4H, *Ar*-NO_2), δ 7.83 (m, 3H, *Ar*-OH) ppm. The ^{13}C NMR ($CDCl_3$, TMS): δ 164.3, 156.2, 153.4, 152.3, 145.4, 130.2, 128.7, 125.8, 125.4, 124.9, 123.0, 122.9, 122.8, 119.3, 115.6, 113.8, 71.6, 71.5, 68.9, 68.3, 59.1, 58.3, 56.7, 56.3 ppm.

MALDI-MS $C_{32}H_{41}N_5O_{10}$ found m/z $[M]^+$ 623.245, calcd 623.70

2.3 Study of sensing properties

The sensing properties of receptor **E1**, **E2, EE2**, **A1**, **N1,** and **N2** towards different cations and anions were investigated using UV-Vis absorption spectrophotometry and color observation. The concentration of all ligand stock solutions was typically 1×10^{-3} M and the exact concentration of metal salt stock solutions of about 0.01 M was determined by complexometric titration with EDTA. Tetrabuthylammonium hexafluorophosphate was used to keep ionic strength of all solutions constant at 0.01 M. The spectral color changes after complexation were recorded after addition of 5 equivalents of metal ion or anion solution into 1×10^{-5} – 1×10^{-4} M of ligand solution. All spectra were recorded in a 1 cm path length cuvette.

2.4 Competitive assay

A mixture of 2×10^{-5} M of **N1** or **N2** and one cation other than target ion in MeCN or DMSO was added 5 equivalents of Cr^{3+} or Hg^{2+}. UV-Vis spectra before and after competition were recorded and the absorbances at the wavelength of maximum absorption were then compared.

2.5 Detection limit study

Photographs of mixtures of sensor solution with various equivalents (0-10 eq) of target ion were taken. The sensors concentrations were 1×10^{-6} - 5×10^{-6} M.

2.6 Refinement of stability constants by program Sirko

In this research, program Sirko, developed and written in 1944 by Vetrogon and co-workers [52], was used for refining stability constants. To obtain stability constant, a possible stoichiometric model together with approximate value of stability constant must be entered. Then, the corresponding molar absorptivity and apparent stability constant were refined until an acceptable fitting judged by R-factor was obtained. This R-factor or Hamilton's R-factor is a value used to confirm a convergence of mathematical model of the equilibrium chemical system. The value of stability constant of the proposed stoichiometric model of the experimental data is confirmed by a comparison of the R-factor value with R-limit value: if R-factor is less than R-limit, the result is considered a fitting model.

CHAPTER III

RESULTS AND DISCUSSONS

3.1 Design and synthesis of chemosensors

The optical sensing molecules in this study were designed to consist of diaza-18-crown-6 ether connecting to derivatives of azobenzene in expectant that the sensor would turn from light to dark color upon interaction with guest ion. The variation in the ligands, shown in Figure 3.1, would be the functional group on the azobezene and the number of azo side arms. Note that the notation of ligands usually consists of one alphabet and one number: first letter being **E**, **A** or **N** which represents the functional group of azobenzene, i.e., *ortho*-ester (**E**), *ortho*-acid (**A**) or *para*-nitro (**N**). The followed number **1** or **2** refers to the number of azo (N=N) group in synthesized molecules. The ester derivative bearing ethylene bridge uses an exception of three letter notation **EE2** in which the middle **E** refers to ethylene.

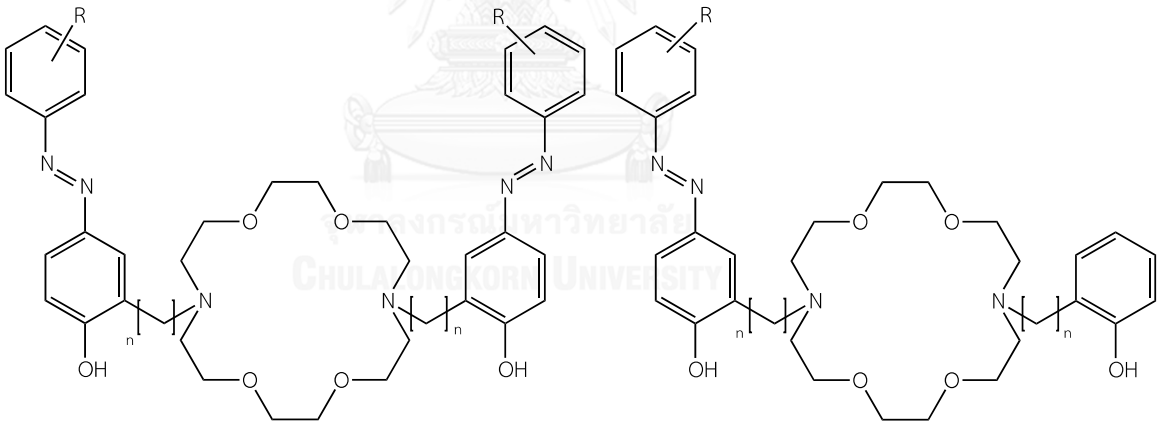

E2 n=1 R = *o*-$COOCH_2CH_3$

EE2 n=2 R = *o*-$COOCH_2CH_3$

A2 n=1 R = *o*-COOH

N2 n=1 R = *p*-NO_2

E1 n=1 R = *o*-$COOCH_2CH_3$

N1 n=1 R = *p*-NO_2

Figure 3.1 The target optical chemosensors

3.1.1 Ester azo-diaza-18-crown-6 derivatives E2 and E1

The first group of synthesized molecules is *ortho*-ethyl ester azobenzene diaza-18-crown-6, **E2** and **E1**. Derivatives of diphenyl diaza-18-crown-6 have been known to show selectivity toward metal ions [32-36]. To enhance the color perception from the molecule, the azobenzene is added into diphenyl diaza-18-crown-6. To stabilize the quinone-hydrazone, the *ortho*-ester group was added into the azobenzene because the oxygen atoms in *ortho*-ester group can form six membered ring with hydrogen atom in quinone-hydrazone. Moreover, this ester group can interact with metal ion.

Synthetic pathway of **E2** and **E1** was illustrated in Scheme 2.1 (page 19). They could be synthesized by coupling phenolic methyl diazocrown ether with ethyl- 2-aminobenzoate in the presence of in situ nitrous acid generation. The crude products were purified and separated by chromatography on silica gel using 10% of methanol in dichloromethane as eluent. Both separated products appeared as orange oil and were characterized by ^{1}H-NMR and mass spectroscopies. The first separated product was characterized as **E1** (24% yield) and the second one as **E2** (20% yield). The appearance of proton of methylene bridge signal is a multiplet peak at 3.90 ppm for **E2** and in the case of **E1**, the signal of proton of methylene bridges are two multiplet peak at 3.82 and 3.90 ppm. MALDI-MS mass spectra showed intense peak of m/z at 827.58 for **E2** and 651.25 for **E1** corresponding to $[M]^{+}$. It should be noted that only azo coupling products at *para* position to the hydroxy group in polar medium were separated and characterized, very likely because the unformed *ortho* coupling products would have been larger in size and less polar which would be unstable in polar medium used.

3.1.2 Ester azo-ethylene-diaza-18-crown-6 derivative EE2

To enhance the flexibilty of the ligand, the methylene bridge connecting diaza-crown ether to phenyl moieties was replaced by an ethylene bridge to obtain **EE2** which could be obtained by coupling phenol ethyl diaza-crown ether with ethyl-2-aminobenzoate in the presence of in situ nitrous acid generation. The synthesis pathway for chemosensor **EE2** is shown in Scheme 2.2 (page 23).

3.1.3 Acid azo-diaza-18-crown-6 derivative A2

The third group of synthetic molecule is *ortho*-acid azobenzene diaza-18-crown-6 **A2**. Carboxylic group was used instead of ester because it was less steric which should allow binding with metal ion. Similar to the *ortho*-ester group, the oxygen atoms of carboxylic group can stabilize the quinone-hydrazone via forming six membered ring with hydrogen atom of quinone-hydrazone.

The synthesis of **A2,** illustrated in Scheme 2.3 (page 25) could be accomplished by hydrolysis of ester azo-diaza-crown ether (**E2**) with NaOH. The resulting product **A2** appeared as orange solid after evaporation with 60 %yield. Its structure was confirmed by the signal of protons of ethyl ester in **E2** at 1.31 and 4.36 ppm, disappeared in ^{1}H-NMR spectrum of **A2**. MALDI-MS mass spectra supported the structures of the compound with intense peak of m/z at 771.59 for **A2** corresponding to $[M]^{+}$.

3.1.4 Nitro azo-diaza-18-crown-6 derivatives N2 and N1

The fourth group of synthesized compounds is *para*-nitro azobenzene diaza-18-crown-6, **N2** and **N1**. Being more electron withdrawing group than ester and acid group, nitro group can enhance the delocalization of **π**-conjugated system and induce the azo-quinone-hydrazone tautomerism by the rotation of proton from hydroxyl group to itself, promoting a red shift.

Synthetic pathway of **N2** and **N1** was illustrated in Scheme 2.1 (page 19) which was similar to that of ester derivatives. **N2** appeared first after evaporation as black solid (17 %yield) and **N1** appeared later as black solid (29 %yield). The structure of compounds **N2** and **N1** was confirmed by ^{1}H-NMR spectroscopy. The appearance of proton of methylene bridge signal was a multiplet peak at 3.91 ppm for **N2**. In the case of **N1**, the signal of proton in methylene bridge appeared as two multiplet peaks at 3.75 and 3.98 ppm. MALDI-MS mass spectra supported the structures of all the compounds with intense peak of m/z at 772.43 for **N2** and 623.25 for **N1** corresponding to $[M]^{+}$.

3.2 Optical properties of azo-diaza-18-crown-6 derivatives in various solvents

Azobenzene compounds usually show two absorption bands, i.e., $\pi \rightarrow \pi^*$ transition band of the azo group (-N=N-) at 360-400 nm and $n \rightarrow \pi^*$ transitions of the hydrazone group (-NH-N) at 500-576 nm. These bands correspond to the tautomerization of azobenzene and quinone-hydrazone as shown in Figure 3.2.

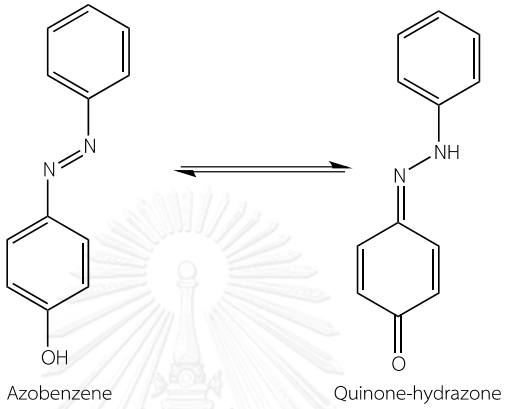

Figure 3.2 Tautomerization of azobenzene to quinone-hydrazone

Optical properties of six azo-diaza-18-crown-6 derivatives were studied by UV-Vis spectrophotometer. The absorption spectra of six ligands in MeOH at 1×10^{-4} M is shown in Figure 3.3. The three yellow ester derivatives namely **E1, E2**, **EE1** absorbed at λ_{max} of 350, 360 and 345 nm in MeOH, respectively. This band can be assigned to $\pi \rightarrow \pi^*$ transition of –N=N- in azobenzene form.

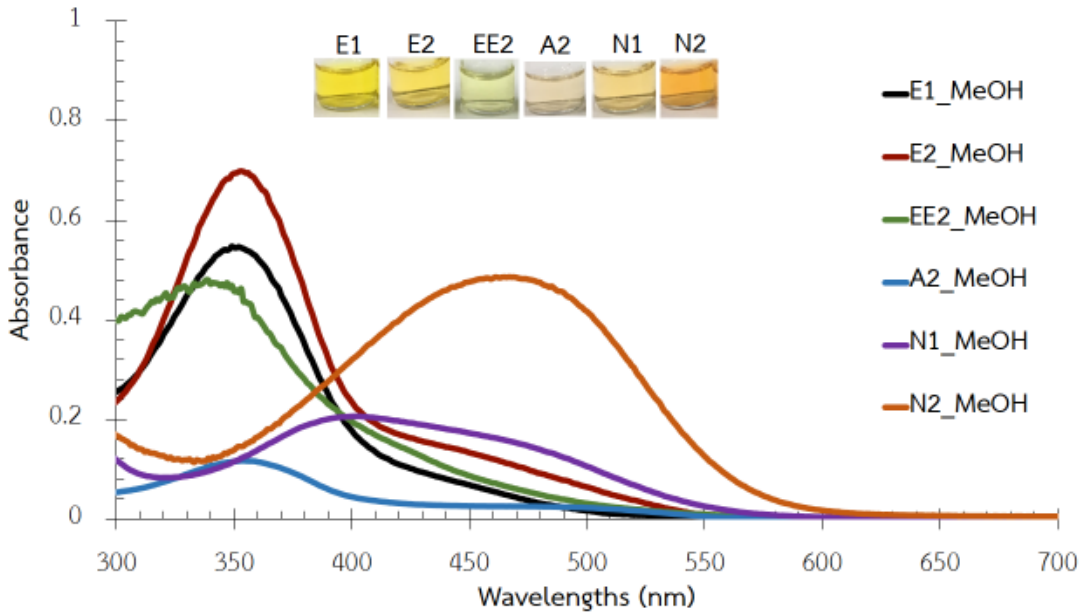

Figure 3.3 UV-Vis spectra and color of six ligands (1×10^{-5} M) in MeOH

The acid derivative **A2** showed solvatochromic effect in water, methanol, and DMSO yielding yellow, pale orange, and orange, respectively, with the maximum absorption at 380, 360 and 510 nm accordingly. In water, **A2** showed only one absorption band at 380 nm corresponding to $\pi\rightarrow\pi^*$ transition of azobenzene. However, in MeOH and MeCN, **A2** also displayed shoulder band at around 510 nm apart from λ_{max} at 360 nm. The characteristic absorption at 510 nm of quinone-hydrazone became a major band in DMSO. The major azobenzene band observed in water, MeOH and MeCN could be explained by an interaction of solvent with hydrogen atom in carboxylic group, adopting azo form. However, the major quinone-hydrazone band in DMSO might be the result of an intramolecular H-bonding between acid and nitrogen since because DMSO could not interact with proton of carboxylic acid group.

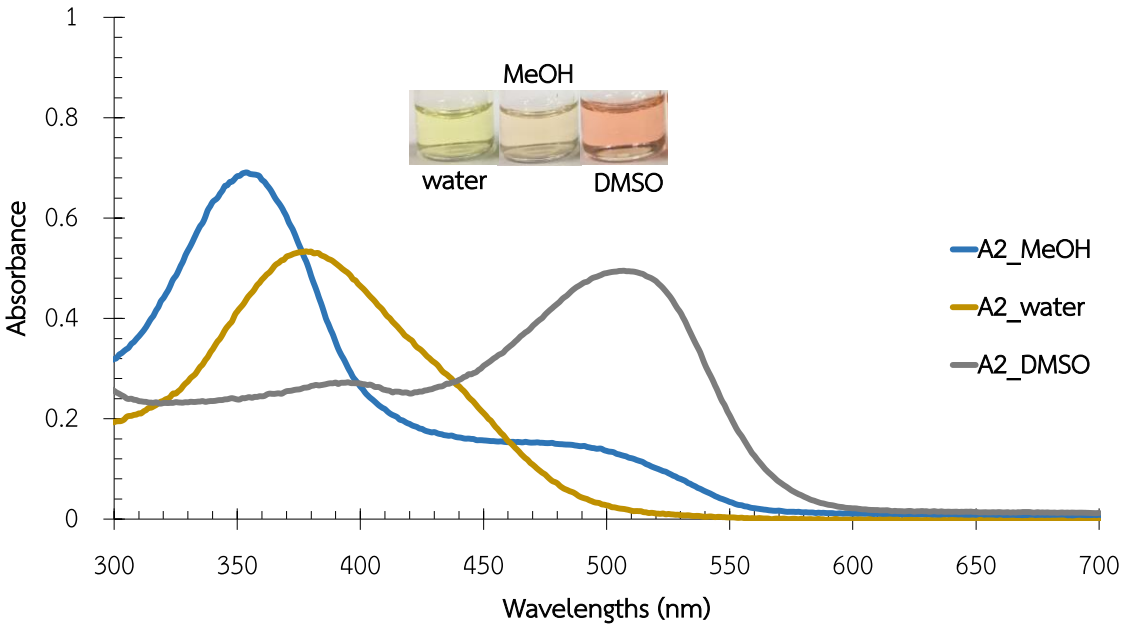

Figure 3. 4 UV-Vis spectra and color of A2 (1×10^{-4} M) in various solvents

The UV-Vis spectra of **N1** and **N2** in various solvents, such as toluene, EtOAc, MeOH, CH_2Cl_2, Acetone, MeCN, DMF, and DMSO are shown in Figure 3.5. **N1** and **N2** displayed visual color from yellow to purple. The λ_{max} that was shifted from 390-560 nm for **N1** and 390-560 nm for **N2** appeared to increase (from 390 to 555 nm) along with an increasing dielectric constant of solvent. Major quinone-hydrazone band and shoulder azobenzene band in aprotic solvents (DMSO, MeCN and DMF) were seen while only one strong band of azobenzene form was noticed in MeOH and EtOAc.

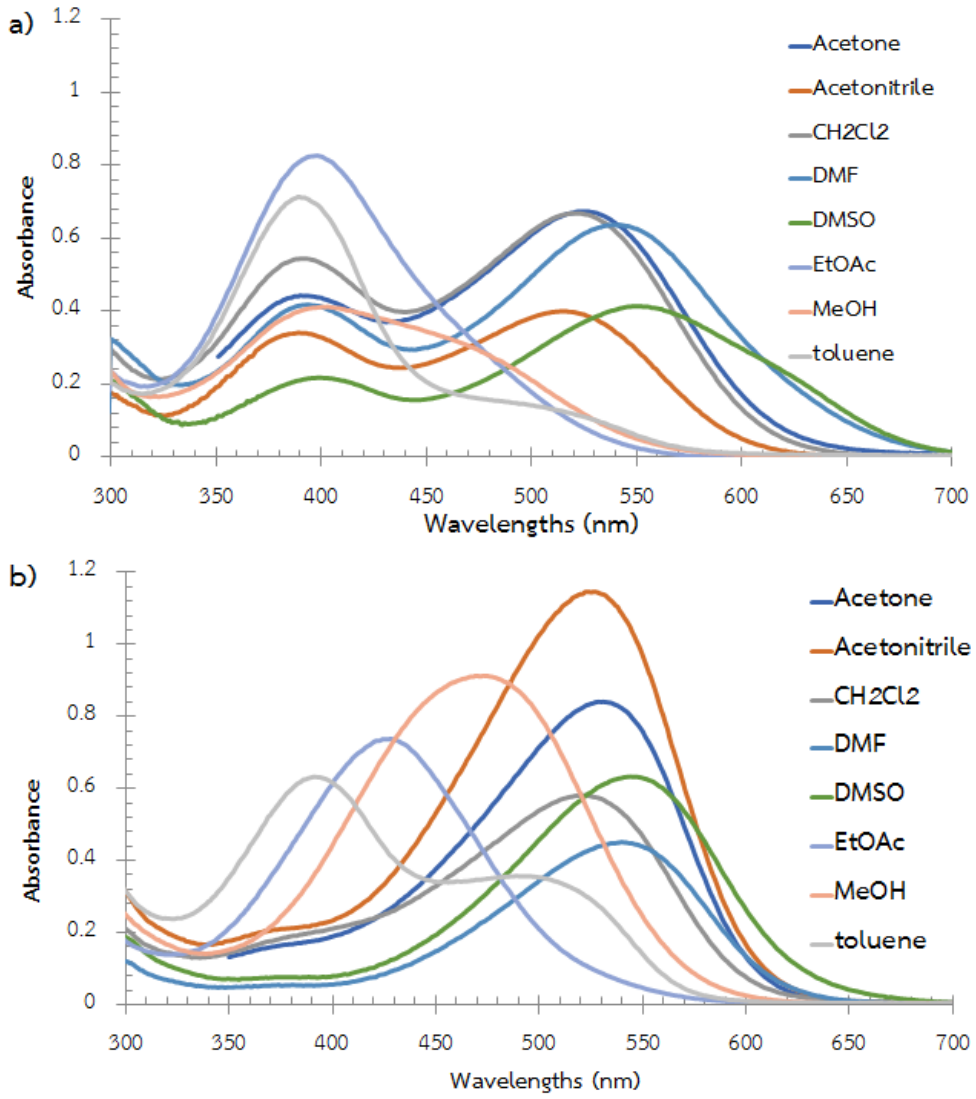

Figure 3.5 The UV-Vis spectra of **N1** and **N2** in various solvents

From the results of all synthesized compounds in various solvents, it could be summarized that the hydrogen bonding between protic solvent such as MeOH and lone pair electron of nitrogen atom in azobenzene prevents the quinone-hydrazone formation. The enhancement of tautomeriztion from azobenzene to quine-hydrazone relies on the elelectron withdrawing property of substituent groups which increases in order of *para*-nitro > *ortho*-acid > *ortho*-ethyl ester.

3.3 Sensing properties towards metal ions

The metal ions studied in the sensing property investigation could be divided into two groups: alkali and alkaline earth ions, e.g. Li^+, Na^+, K^+, Mg^{2+} and Ca^{2+}, and transition and heavy metal ions, e.g. Cr^{3+}, Co^{2+}, Ni^{2+}, Cu^{2+}, Zn^{2+}, Cd^{2+}, Hg^{2+} and Pb^{2+}. The UV-Visible spectra and color change were recorded after addition of 5 eq of metal ion into the ligand solution.

3.3.1 Sensing property towards metal ions

3.3.1.1 Ester derivatives E1, E2 and EE2

Adding 5 equivalents of alkali ions (Li^+, Na^+, K^+), alkaline earth ions (Mg^{2+}, Ca^{2+}) into **E1** solution did not change its color and UV-visible absorption pattern. As none of these metal ions could make any obvious change, addition of base was performed to deprotonate H atom of hydroxyl phenyl groups in expect that O^- might interact with metal ions more easily. It appeared that hydroxide ion induced increasing of absorbance of shoulder band at 425 nm and decreasing of absorbance at 350 nm. This result suggests that OH^- could deprotonate H atom of hydroxyl phenyl groups promoting $n \rightarrow \pi^*$ transition in quinone-hydrazone. Unfortunately, this spectral change was not enough to be noticed by human eye. Addition of all metal ions to basic **E1** solution did not show any obvious results as the color remained yellow.

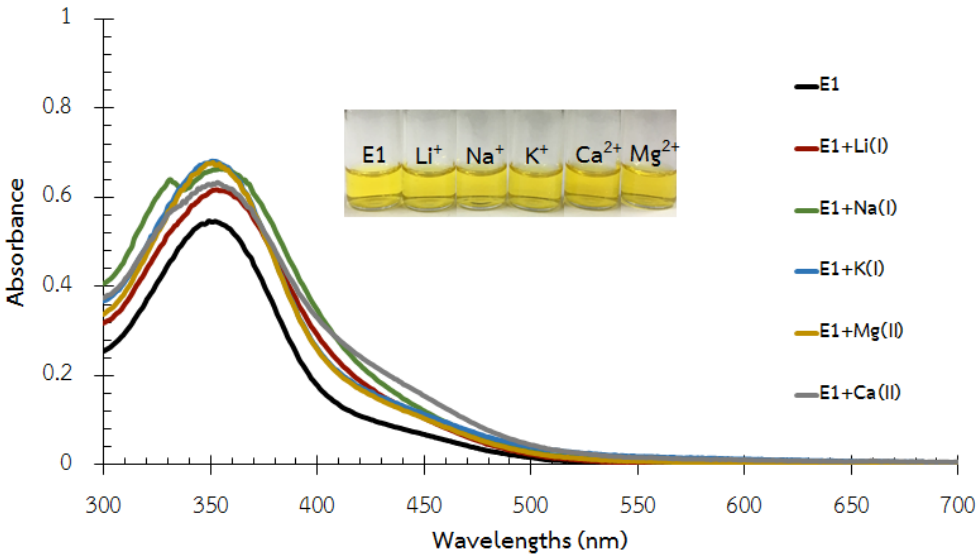

Figure 3.6 UV-Vis spectra and color changes of **E1** (1×10^{-5} M) in the presence of alkali and alkaline earth metal ions (5 eq) in MeOH

Alkali and alkaline earth metal ions in the **E2** solution were in the same yellow tone. The tautomerization from azobenzene to quinone-hydrazone did not occur as the value of λ_{max} upon metal addition was still around 340-405 nm. However, the color in the case of Ca^{2+} was a little more intense, which agreed with a small bathochromic shift of 45 nm seen in UV-visible spectrum (Figure 3.7). Some changes in chemical shift of ester protons in ^{1}H-NMR study of **E2** and Ca^{2+} in CD_3Cl were observed. The signal of hydrogen atom of ester group at 1.30 ppm and 4.36 ppm respectively appeared downfield to 1.41 and 4.45 ppm. This result suggests that Ca^{2+} binds with oxygen atom in ester group (Figure 3.8). The absorption spectra of **E2** in the presence of 5 equivalent of hydroxide ions did not show new distinct absorption band but an absorbance of small shoulder around 440 nm was enhanced, which are discussed in the result of **E1**., i.e, the deprotonation of hydroxyl phenyl groups occurs, resulting in enhancement of $n\rightarrow\pi^*$ transition in quinone-hydrazone. Similar to **E1**, the mixtures of metal ions and basic **E2** solution were in the same yellow tone.

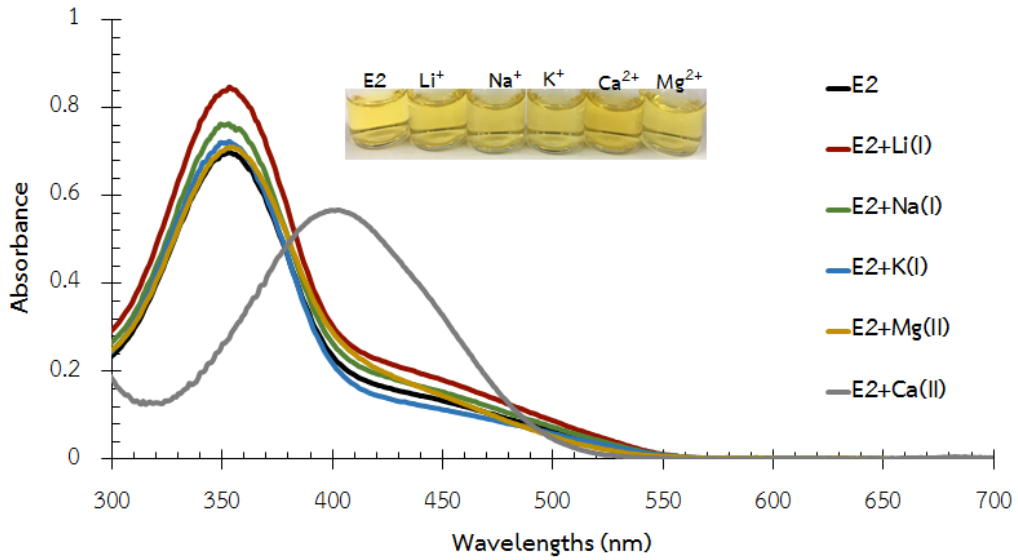

Figure 3.7 UV-Vis spectra and color changes of **E2** (1×10^{-5} M) in the presence of alkali and alkaline earth metal ions (5 eq) in MeOH

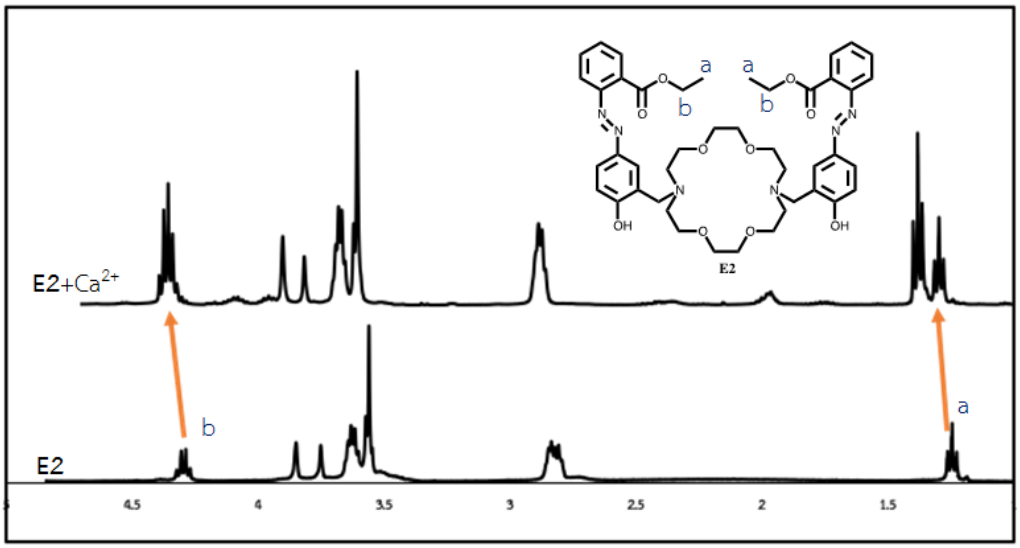

Figure 3.8 ^{1}H-NMR spectra of **E2** without and with Ca^{2+}

For **EE2**, addition of alkali and alkaline earth ions could not result in any change in color and UV-visible spectra which was similar to what described previously. The absence of optical changing toward the addition of metal ions implied that none of the interaction between this ligand and metal ions was strong enough to disturb the electrons in **π**-conjugated system. In other words, adding more carbon to increase flexibility somehow was not enough for the interaction to occur.

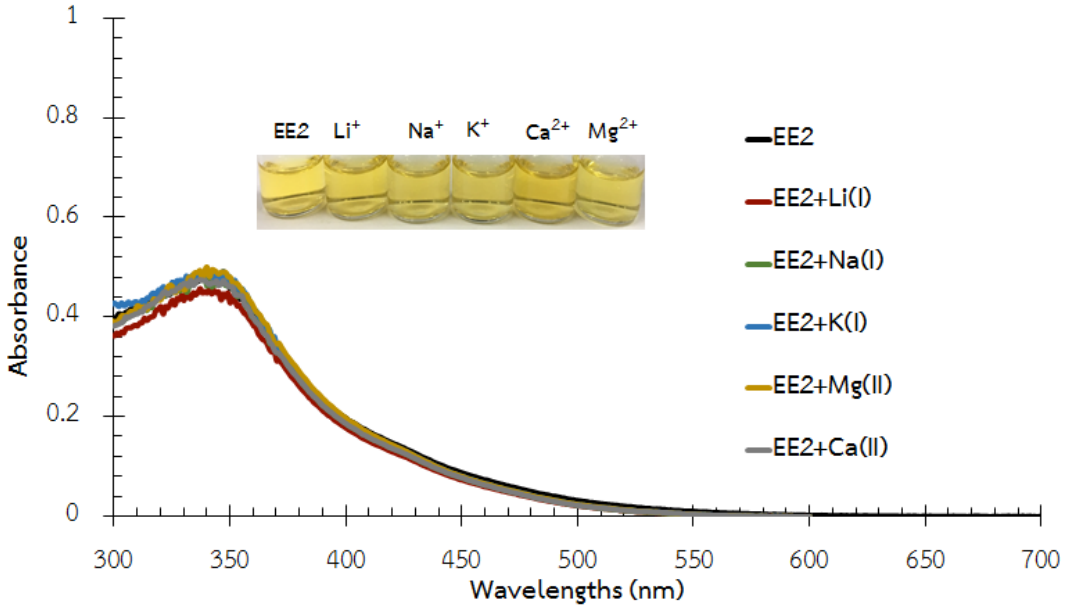

Figure 3.9 UV-Vis spectra and color changes of **EE2** (1×10^{-5} M) in the presence of various metal ions (5 eq) in MeOH

Similar to alkali and alkaline earth ions, addition of transition and heavy metal ions to the ester ligand solutions in MeOH did not induce any color change as can be seen in Table 3.1. However, the mixture of Cu^{2+} and Co^{2+} with **E2** were a little more intense in color and a small bathochromic shift of 25 nm, similar to the addition of Ca^{2+}, was observed (Figure 3.10). It should be mentioned that Ca^{2+} induced a larger shift than Cu^{2+} and Co^{2+}. This could be explained by its larger size and harder ion which is known to prefer oxygen atoms than Cu^{2+} and Co^{2+}, leading to a strong interaction between Ca^{2+} and ligand.

Table 3.1 Wavelengths at maximum absorption (λ_{max}) of **E1**, **E2** and **EE2** without and with transition and heavy metal ions in MeOH

Ions	Dye in MeOH		
	E1	**E2**	**EE2**
no ion	350	360	345
Cr^{3+}	345	360	345
Co^{2+}	350	360	345
Ni^{2+}	350	360	345
Cu^{2+}	365	405	345
Zn^{2+}	360	360	345
Cd^{2+}	360	350	345
Hg^{2+}	340	385	345
Pb^{2+}	360	360	345

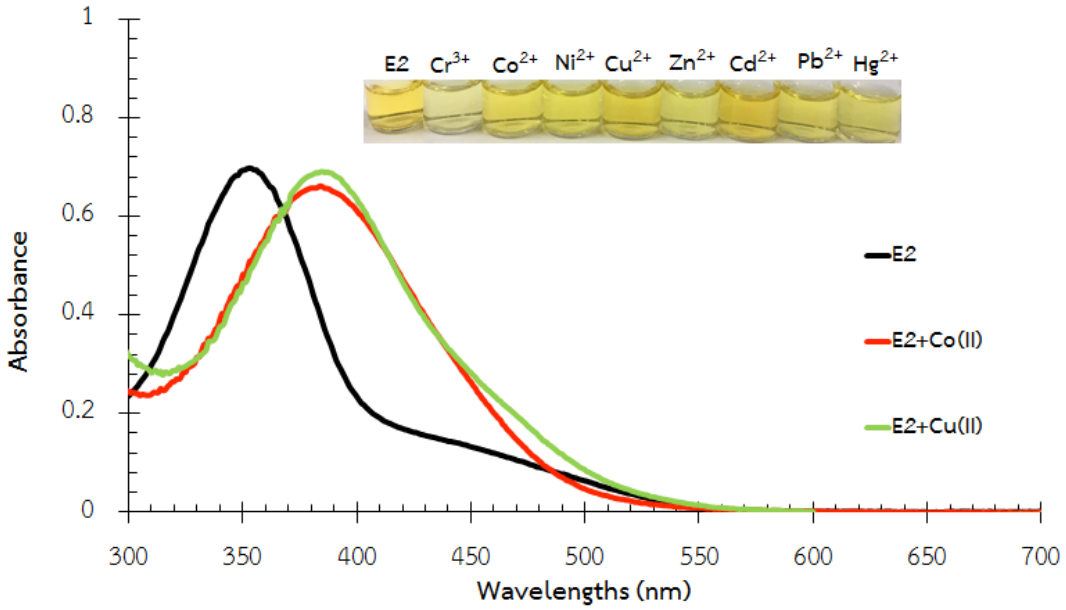

Figure 3.10 Selected UV-Vis spectra and color changes of **E2** (1×10^{-5} M) in the presence of metal ion (5 eq) in MeOH

As mentioned earlier, **E1**, **E2** and **EE2** solutions could not display any selective changes in color and absorption spectra upon addition of any metal ion, which

indicated a lack of interaction between metal ions and donor atoms close to the signal units, i.e., oxygen atoms in the *ortho*-ester electron donating groups and nitrogen atoms in azobenzene moieties. This suggests that *ortho*-ester group is too steric, very likely from the ethyl group in ester. Thus changing from ethyl in ester to hydrogen in acid would be interesting.

3.3.1.2 Acid derivative A2

The mixture of metal ions and **A2** in various solvents were resembling to that of ester derivatives. An interesting case was addition of Ca^{2+} in MeOH produced two absorption bands which were a small red shift of azobenzene band (50 nm) and an increasing of absorption intensity of quinone-hydrazone band (Table 3.2 and Figure 3.11). This result suggests that calcium ion induced tautomerization equilibrium. The azobenzene band changing to quinone-hydrazone band has been reported earlier [25]: metal ion could induce proton release from the azobenzene form of *ortho*-ester diazophynylcalix[4]arene forming quione-hydrazone tautomer. To explain a cause of the small red shift of azobenzene band, UV-Vis titration of **A2** with NaOH was performed. The absorption after addition of 5 eq of base to deprotonate acidic group showed peak at 400 nm with a small red shift of 40 nm and decreased intensity of shoulder band at 510 nm. This small red shift was similar to a small red shift of azobenzene band upon addition Ca^{2+}. Using this observation together with ^{1}H-NMR, it is likely that complexation of **A2** with Ca^{2+}not only induces some quinone-hydrazone formation but also azobenzene deprotonation.

Table 3.2 Wavelengths at maximum absorption (λ_{max}) of **A2** without and with metal ions

Ions	A2		
	H_2O	MeOH	DMSO
no ion	380	360, 500	380, 510
Li^+	380	360, 500	380, 510
Na^+	380	360, 500	380, 510
K^+	380	360, 500	380, 510
Ca^{2+}	380	400, 500	380, 510
Mg^{2+}	380	360, 500	380, 510

Major band is presented as underline number

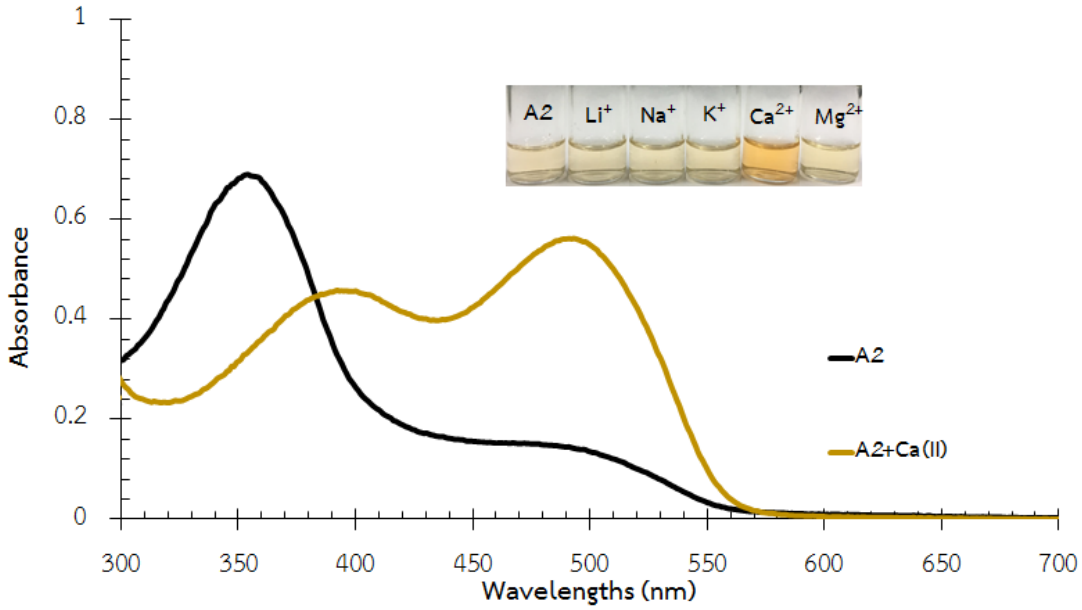

Figure 3.11 Selected UV-Vis spectra and color changes of **EE2** (1×10^{-5} M) in the presence of alkali and alkaline earth metal ions (5 eq) in MeOH

Color change of **A2** solutions in the presence of transition and heavy metal ion also depended on solvent types. The valves of λ_{max} after addition of 5 equivalents of metal ions into **A2** solution were shown in Table 3.3 together with large λ_{max} of $>$ 100 nm in parentheses. Note that a negative value means hypsochromic or blue shift. Addition of Cr^{3+} and Hg^{2+} to aqueous **A2** solution can turn its yellow color to colorless

which corresponding to a small blue shift (35 nm). The selectivity of **A2** toward Cr^{3+} and Hg^{2+} in water was inseparable with the naked eye, so it is not suitable as a sensor even if this ligand is soluble in water. For **A2** in MeOH, $Cu^{2+}$and Cd^{2+} induced the equilibrium of two tautomers, similar to Ca^{2+} addition. Large ions like Ca^{2+} and Cd^{2+} should be able to bind with both crown ether and oxygen atoms in carboxylic group. But a small ion like Cu^{2+} which is known to prefer nitrogen atom might bind with lower N of azo group.

Table 3.3 Wavelengths at maximum absorption (λ_{max}) of **A2** in various solvent without and with transition metal ions

Ions	A2		
	H_2O	MeOH	DMSO
no ion	380	360, 500	380, 510
Cr^{3+}	345	345	345 (–165)
Co^{2+}	380	365	370 (–140)
Ni^{2+}	380	365	385 (–125)
Cu^{2+}	380	410, 460	410
Zn^{2+}	380	375	360 (–150)
Cd^{2+}	390	400, 485	495
Hg^{2+}	345	360, 500	400 (–110)
Pb^{2+}	380	365, 500	360 (–150)

Major band is presented as underline number.

Interestingly, addition of transition and heavy metal ions to **A2** in DMSO in many cases induced a large blue shift of more than 100 nm accompanying a color change from orange to yellowish or greenish (Figure 3.12). The displacement of λ_{max} observed in this case is much larger than that in any other solvent. Regrettably, this color change was too weak to be precisely separated by human eye and it could not be used as selective ion sensor.

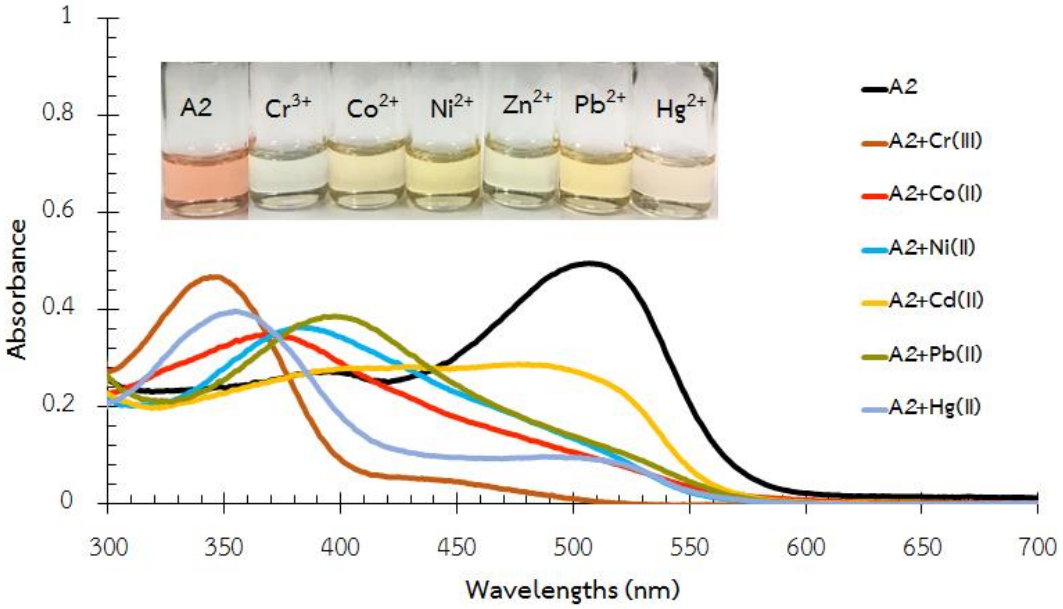

Figure 3.12 Selected UV-Vis spectra and color changes of **A2** (1×10^{-4} M) in the presence of various metal ions (5 eq) in DMSO

3.3.1.3 Nitro derivatives N1 and N2

Since the nitro derivatives showed solvatochromic effect in several solvents, it should be mentioned that only some solvents were chosen as representative for sensing property study. The first solvent was MeOH as both **N1** and **N2** showed only one azobenzene band in this solvent which was close to water and available in all laboratory. MeCN was also chosen not because of its availability but also because **N2** showed more intensity in this solvent. Lastly DMSO was studied because of its single and major band in the quinine-hydrazone region for both **N1** and **N2**.

Alkali and alkaline earth ions did not induce any significant change in all three solvents except in the case of **N1** in MeCN with Ca^{2+} and Mg^{2+} as can be seen in Table 3.4 and Figure 3.13. Although the addition of Ca^{2+} to **N1** in MeCN induced outstanding color change from pinkish red to orange but, due to time restriction, this system is not investigated further because of the metal's nontoxic behavior. The similarity of yellow color observed in the case of **N1** in MeCN with Mg^{2+} and other transition and heavy metal ions, described in the following paragraphs, makes it unsuitable to be employed as a naked eye sensor.

Table 3.4 Wavelengths at maximum absorption (λ_{max}) of **N1** and **N2** without and with metal ions

Ions	N1			N2		
	MeOH	MeCN	DMSO	MeOH	MeCN	DMSO
no ion	400	390, 520	410, 560	460	525	555
Li^+	400	390, 515	410, 560	480	525	555
Na^+	400	390, 517	410, 560	470	520	547
K^+	400	390, 515	410, 560	470	520	555
Ca^{2+}	440	490	410, 560	460	525	555
Mg^{2+}	407	400	410, 560	445	525	545

Major band is presented as underline number

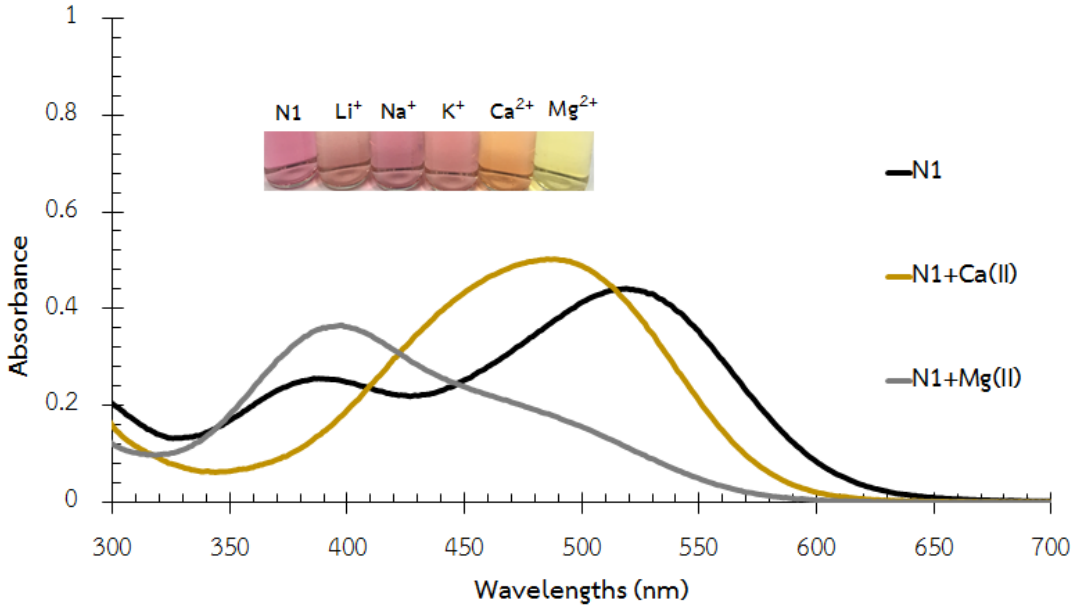

Figure 3.13 Selected UV-Vis spectra and color changes of **N1** (2×10^{-5} M) in the presence alkali and alkaline earth metal ions (5 eq) in MeCN

The values of λ_{max} after addition of 5 equivalents of transition and heavy metal ions into **N1** and **N2** solution, along with λ_{max} shift of larger than 100 nm in parentheses, were given in Table 3.5.

Table 3.5 Wavelengths at maximum absorption (λ_{max}) of **N1** and **N2** in various solvent without and with transition metal ions

Ions	N1			N2		
	MeOH	MeCN	DMSO	MeOH	MeCN	DMSO
no ion	400	390, <u>520</u>	410, <u>560</u>	460	525	555
Cr^{3+}	435	365 (–155)	510	440	370 (–155)	505
Co^{2+}	420	454	510	465	468	505
Ni^{2+}	430	460	498	430	468	490
Cu^{2+}	415	375 (–145)	500	460	435	540
Zn^{2+}	410	445	485	425	450	490
Cd^{2+}	450	437	522	455	435	520
Hg^{2+}	407	430	390 (–170)	455	400 (–125)	390 (–165)
Pb^{2+}	390	435	485	400	435	495

Major band is presented as underline number

The complexation of nitro derivatives with transition and heavy metal ions does depend on solvent type. A small shift of less than 50 nm was observed and the color change was not apparent when treating **N2** solution with transition metal ions and heavy metal ions. However, large blue shifts were seen in MeCN when some metal ions were added. Cr^{3+} induced the largest blue shifts for both **N1** and **N2** in MeCN. Their absorption spectra showed one characteristic peak of azobenzene with λ_{max} of around 365 nm for **N1** and 370 nm for **N2**. The blue shift of 155 nm in the case of Cr^{3+} in MeCN led to an obvious color change form pink to colorless. As Cr^{3+} is the smallest ion studied in this group, it is likely that It interacts with oxygen atom of hydroxyl group, preventing $n \rightarrow \pi^*$ transition in quinone-hydrazone and adopting azobenzene tautomer. To prove that Cr^{3+} interact with hydroxyl group in azobenzene, a UV-Vis titration of NaOH into a mixture of Cr^{3+} (5 eq) and **N1** or **N2** nitro derivatives was performed. It was found that 20 eq of base could turn azobenzene in a mixture of Cr^{3+} and ligands to quinone-hydrazone. This suggested that Cr^{3+} did not bind with O^- in the deprotonated ligand but rather OH group. Some electron density from hydroxyl group

would then be diverted to Cr^{3+} instead of **π** conjugated system resulting in a wider band gap or hypsochromic shift similar to what what reported in the complex of ortho-methoxy azobenzene derivative with Cu^{2+} where the metal bound with nitrogen atom in the ligand [53].

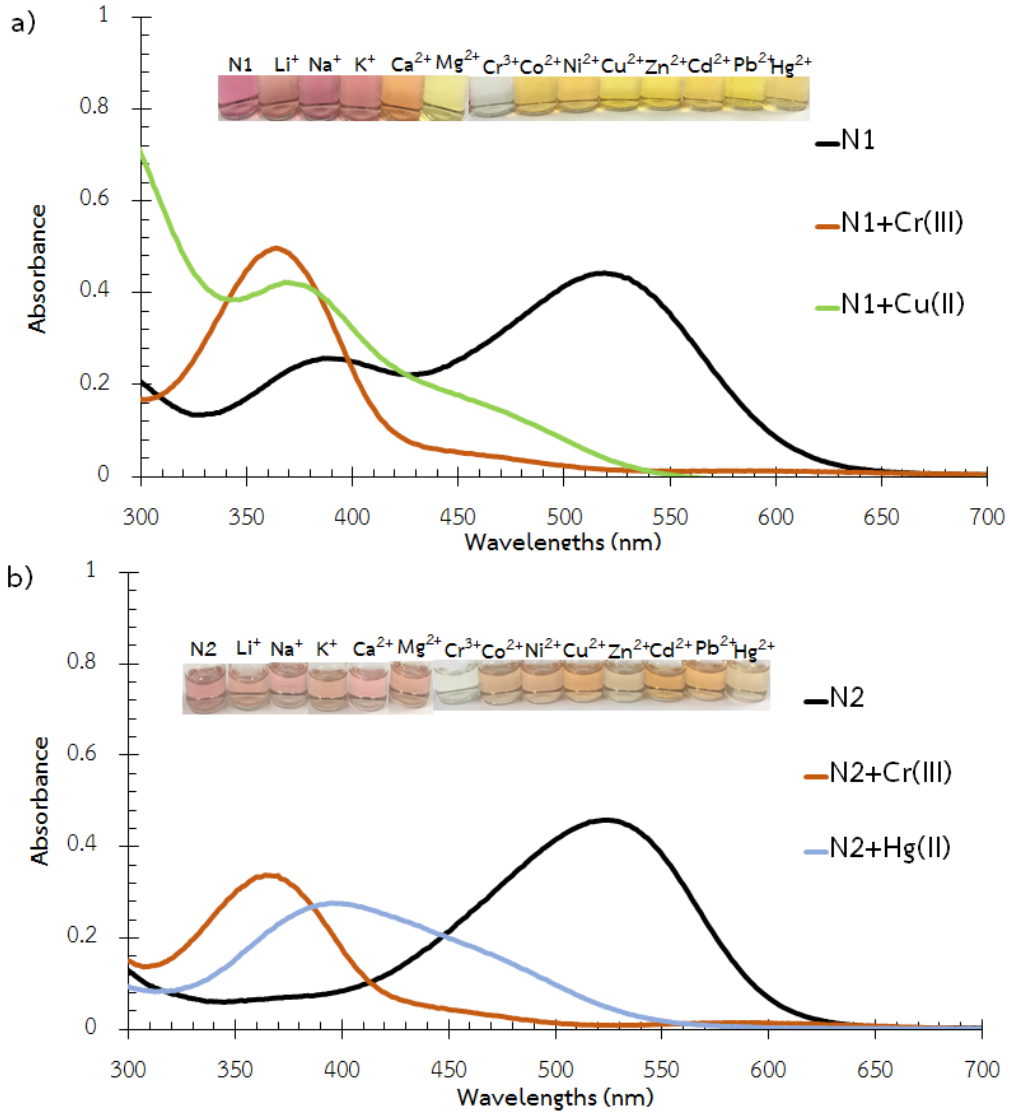

Figure 3.14 Selected UV-Vis spectra and color changes of sensors **N1** or **N2** (2×10^{-5} M) without and with metal ions (5 eq) in MeCN (a) **N1**, (b) **N2**

The addition of Hg^{2+} to **N1** and **N2** in DMSO induced a large blue shift around 165 nm (λ_{max} =390 nm) and turned purple solution to yellow. The ratio of absorbances at 390 nm after and before Hg^{2+} addition are 3.0 and 5.1 for **N1** and **N2**, respectively,

which suggests that Hg^{2+} interacts with **N1** and **N2** differently: Hg^{2+} could interact with nitrogen atoms in both azo groups in **N2**, leading to more azobenzene. Note that this increment is not seen in the case of Cr^{3+} in MeCN, which agrees well to the assumption that this smaller ion interacts with hydroxyl groups.

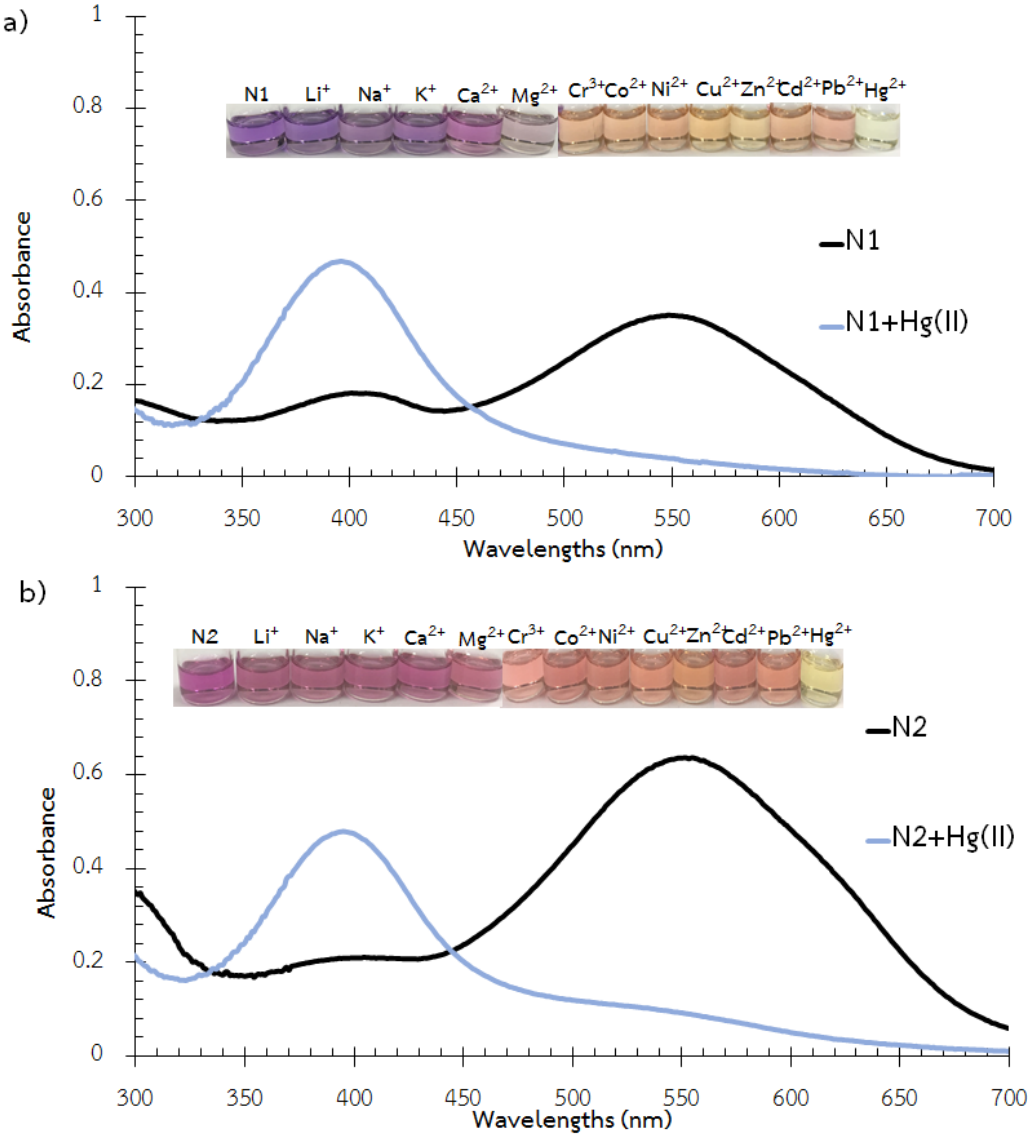

Figure 3.15 Selected UV-Vis spectra and color changes of sensors **N1** or **N2** (2×10^{-5} M) without and with metal ions (5 eq) in DMSO (a) **N1**, (b) **N2**

3.3.2 Competitive assay and detection limit

Since **N1** and **N2** bound selectively with Cr^{3+} in MeCN, a selectivity study was thus investigated. A competitive essay by addition of Cr^{3+} to a mixture of sensor and

another metal ion was performed and comparison of the absorbances at λ_{max} of Cr^{3+} complex before and after competition at 365 for **N1** and 370 nm for **N2** was realized (Figure 3.16). The absorbance of mixture of metal ions solution were as same as the absorbance of only chromium ion. Moreover, the addition of Cr^{3+} change the color of the mixture to colorless. It means that Cr^{3+} complex was stronger than another metal ion complexes

The detection limit of these optical chromosensor **N1** and **N2** towards Cr^{3+} was also explored by addition of various concentration of Cr^{3+} (0-1 eq for **N1** and 0-10 eq for **N2**) to 2.5×10^{-6} M sensor solution in MeCN. Photographs of this experiment, shown in Figure 3.17, indicate that the detection limits of **N1** and **N2** for Cr^{3+} that can be visibly distinguished by human eye are 1.75×10^{-6} M (0.09 ppm) for **N1** and 5.0×10^{-6} M (0.27 ppm) for **N2**. These values are lower than 0.57 ppm which is a value recommended by United States Environmental Protection Agency (EPA) for freshwater criterion maximum acute concentration for aquatic life. This means that **N1** and **N2** could be used to monitor Cr^{3+} in environment. To confirm that both **N1** and **N2** can be used as sensors in aquatic environment, addition of aqueuos solution to ligands in MeCN was carried out. It was found that both sensors were still effective when the water amount was less than 20% for **N1** and 50% for **N2**. This result attests that **N1** and **N2** are potential Cr^{3+} sensors.

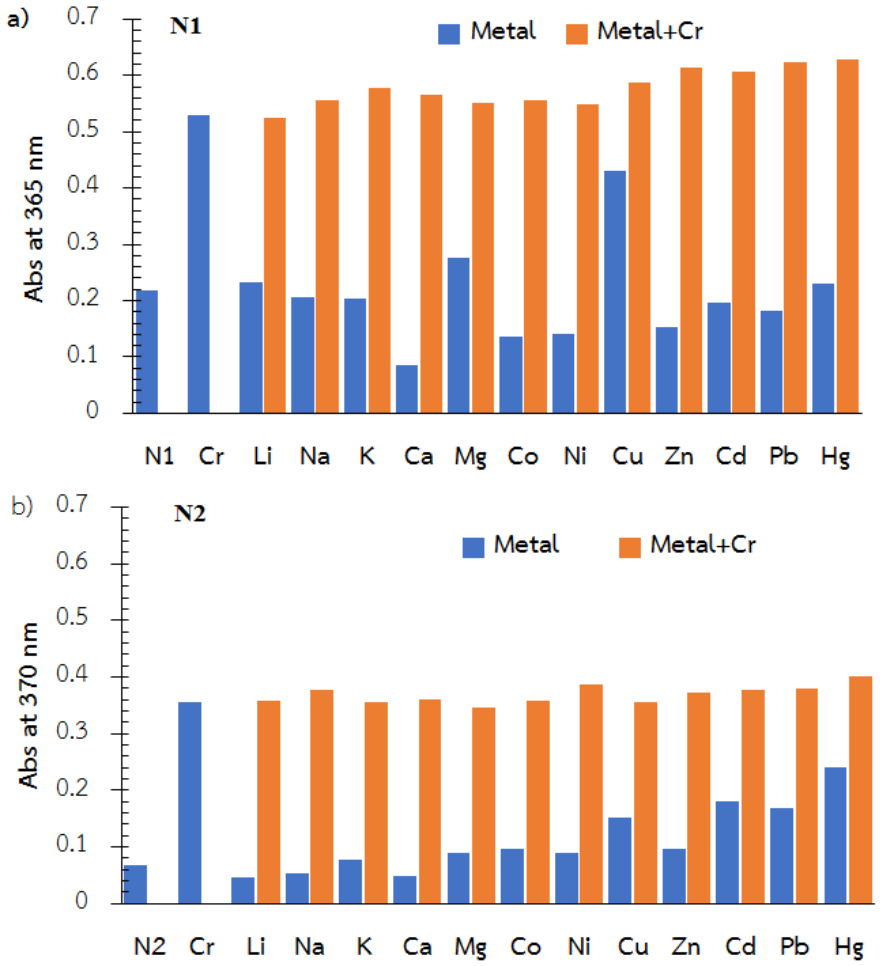

Figure 3.16 Competitive assay of sensor (2×10^{-5} M) towards Cr^{3+} (5 eq) in the presence of other metal ions (5 eq) in MeCN: (a) **N1**, (b) **N2**

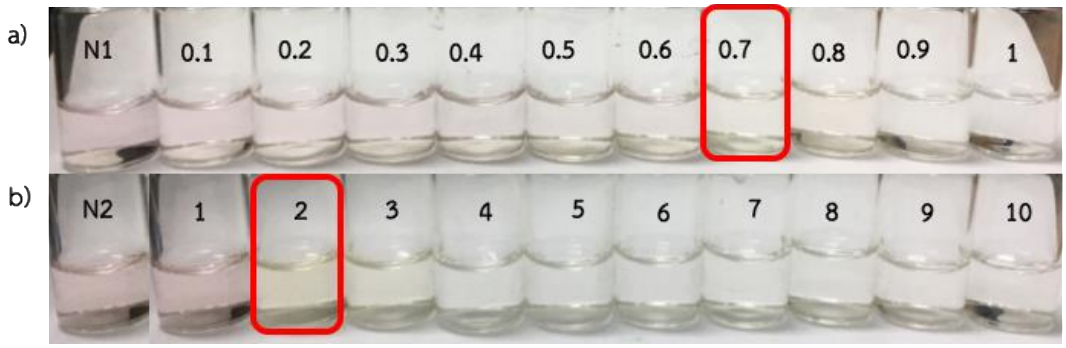

Figure 3.17 Visual changes of sensor with Cr^{3+} in MeCN: a) **N1** (2.5×10^{-6} M) with Cr^{3+} (0-1 eq), (b) **N2** (2.5×10^{-6} M) with Cr^{3+} (0-10)

A titration of Cr^{3+} into **N2** showed decreasing of absorbance at 525 nm increasing of absorbance at 370 nm with 2 isosbestic points. The first isosbestic point

at 451 nm was observed when ratio of metal to ligand was 0 to 0.5 eq. Moreover, when the ratio of metal to ligand is higher than 0.5 eq., the second isosbestic point at 386 nm appeared. These results suggest that Cr^{3+} formed not only ML_2 complex but also ML complex. However, the stability constants of these two complexes are too high to be refined accurately. It should be mentioned that titration of Cr^{3+} into **N1** also gave similar results, i.e. both ML_2 and ML complexes were observed.

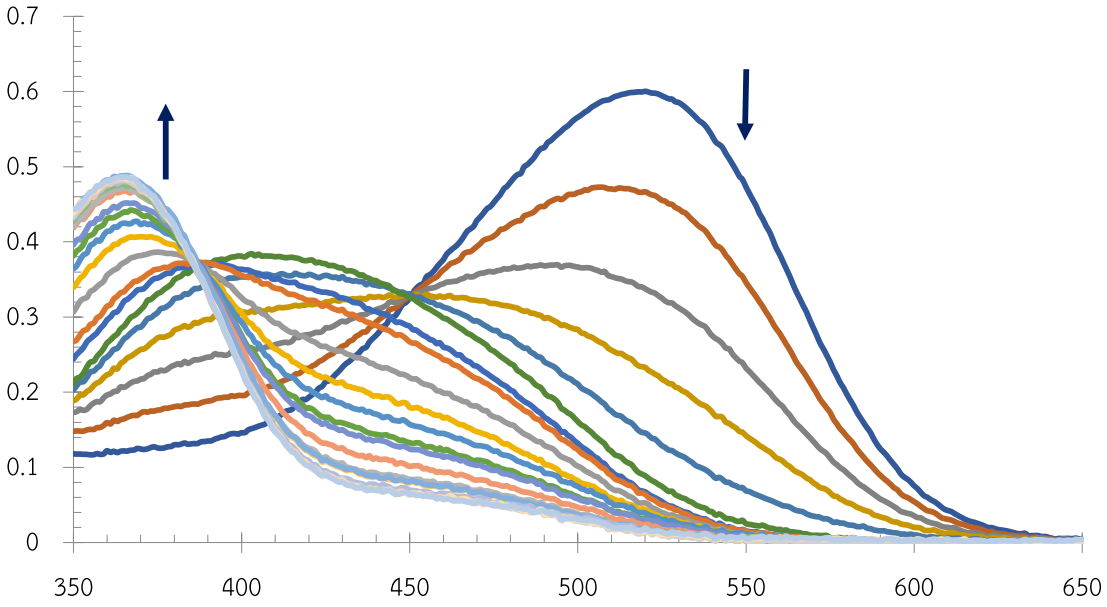

Figure 3.18 UV-Visible spectrophotometric titration UV-Visible of a) **N2** (1✕10–5 M) with 0-4 eq of Cr^{3+} in MeCN

A competitive essay by addition of Hg^{2+} in to a mixture of sensor and another metal ion was performed and comparison of the absorbances at λ_{max} of Hg^{2+} complex before and after competition at 390 for both **N1** and **N2** was realized (Figure 3.19). It was found that addition of Hg^{2+} to a mixture of ligand and another metal ion gave similar observation as a mixture of ligand and only Hg^{2+}, i.e. the color changed to colorless and the peak at 390 was observed. This result means that the interaction between Hg^{2+} and ligands are much stronger. In other words, **N1** and **N2** are selective towards Hg^{2+} in DMSO. Note that the higher absorbance recorded with Cu^{2+} was due to the absorption of Cu^{2+}.

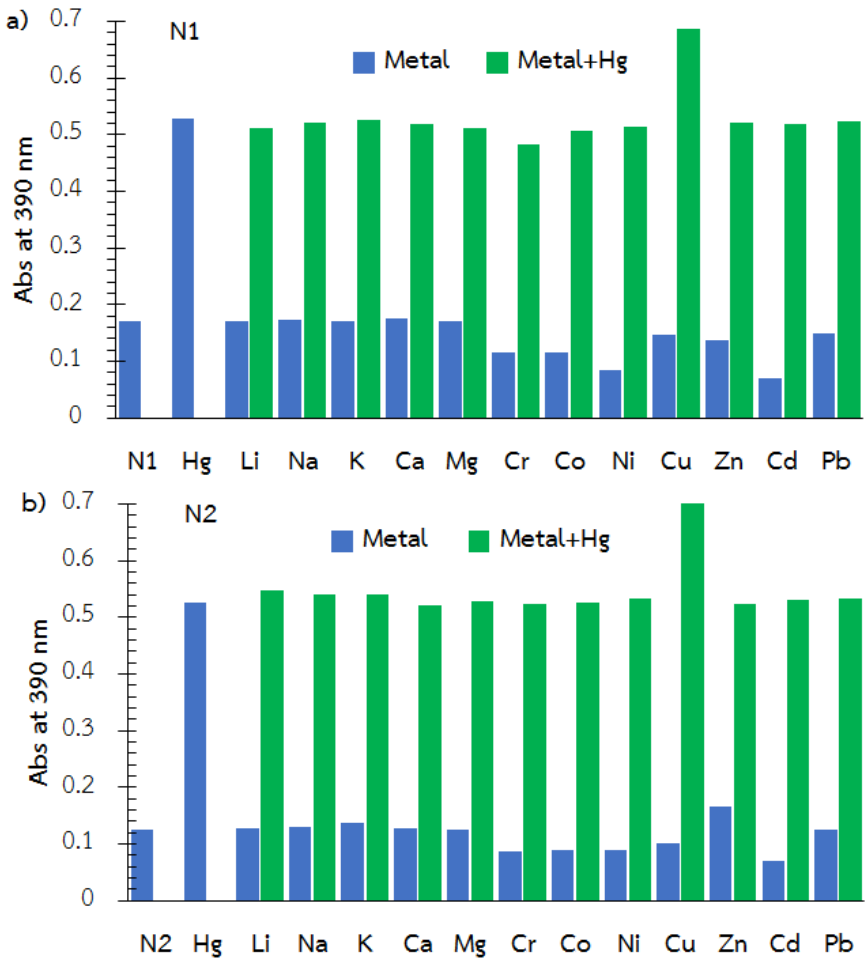

Figure 3.19 Competitive assay of sensor (2×10^{-5} M) towards Hg^{2+} (5 eq) in the presence of other metal ions (5 eq) in DMSO: (a) **N1**, (b) **N2**

The detection limit of these optical chemosensor **N1** and **N2** towards Hg^{2+} was also explored by addition of various concentration of Hg^{2+} (0-1 eq for **N1** and 0-10 eq for **N2**) to 5×10^{-6} M **N1** and 1×10^{-6} M **N2** in DMSO. Photographs of this experiment, shown in Figure 3.20, indicated that the detection limits of **N1** and **N2** for Hg^{2+} that can be distinguished with the naked eye are 4.5×10^{-6} M (0.90 ppm) and 7.0×10^{-6} M (1.40 ppm) for **N1** and **N2**, respectively.

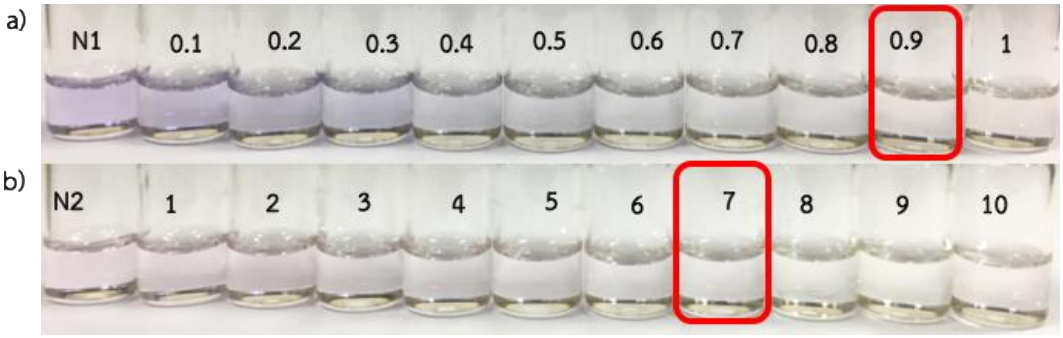

Figure 3.20 Visual changes of sensor with Hg^{2+} in DMSO: a) **N1** (2.5×10^{-6} M) with Hg^{2+} (0-1 eq), (b) **N2** (2.5×10^{-6} M) with Hg^{2+} (0-10)

The UV-Visible titration of Hg^{2+} into **N2** in the DMSO, shown in Figure 3.21, displayed only one isosbestic point at 444 nm when ratio of metal to ligand was less than 1 eq. This result suggested that Hg^{2+} induced a ML formation. This data was used to refined the stability constant via nonlinear least square algorithm in program Sirko [52]. The average stability constant in logarithmic units and the standard deviation from two independent experiments was 5.97 ± 0.01.

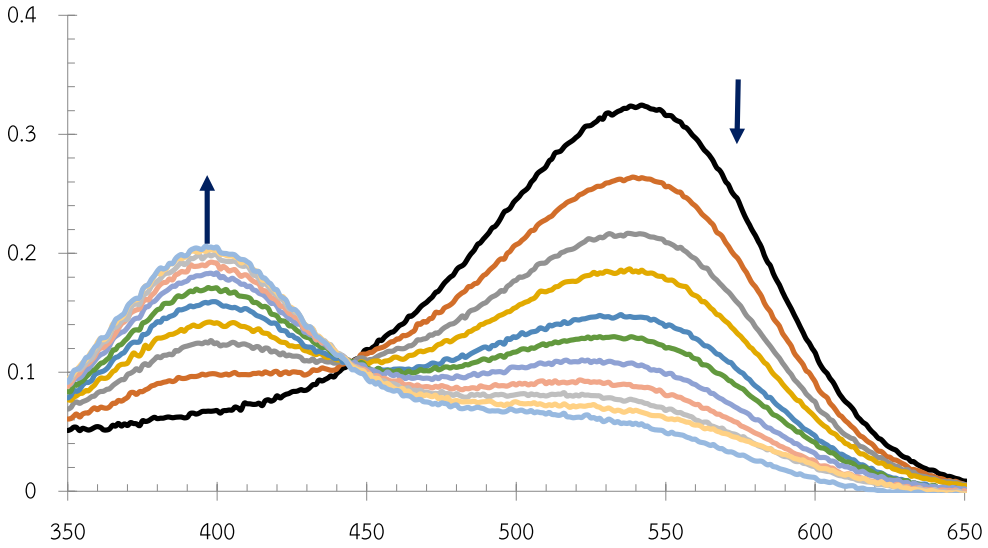

Figure 3.21 UV-Visible spectrophotometric titration UV-Visible of a) **N2** (1×10^{-5} M) with 0-1 eq of Hg^{2+} in DMSO

3.3.3 Sensing properties towards anions

Many publications stated that 4-hydroxy azobenzene can interact with many anions via hydrogen bonding and deprotonation. [19, 43, 47, 49]. Thus, the examination

of anion ion sensing was started from addition of hydroxide ion to deprotonation of ligands, in hope to increase the binding property. If addition of hydroxide ion could induce some color change, the sensing property for other anions would then be studied. To study anion ion sensing properties, 5 eq of anions (F^-, Cl^-, Br^-, I^-, OH^-, OCl^-, NO_3^-, $H_2PO_4^-$, AcO^- and BzO^-) was performed.

3.3.3.1 Ester derivatives E1, E2 and EE2

As mentioned in section 3.3.1.1. (page 35) that addition of hydroxide ion did not lead to any color change obvious to human eye UV-Visible spectra of **E1**, **E2** and **EE2** in the presence of OH^-, shown in Figure 3.21, are similar. This result could be explained by the electron withdrawing properties of *ortho*-ester groups in azobenzene being too weak to decrease electron density of oxygen atom in hydroxyl group of 4-hydroxy azobenzene leading to less acidic proton.

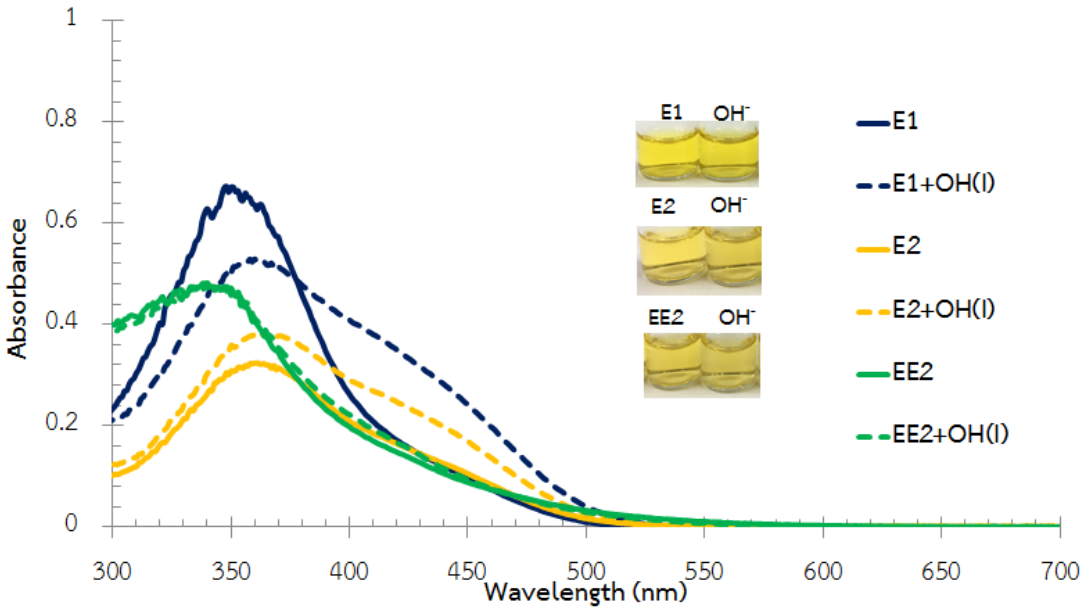

Figure 3.22 UV-Vis spectra and color change of sensors **E1**, **E2** and **EE2** (1×10^{-5} M) without and with OH^- (5 eq) in MeOH

3.3.3.2 Acid derivative A2

Unlike the results from ester derivatives, addition of hydroxide ion induced a change in UV-Visible spectra. Figure 3.23 showed that **A2** in MeOH and DMSO absorbed

with two absorption bands (bold lines) which explained in the section 3.3., i.e, in DMSO, **A2** displayed major absorption band at 510 nm and shoulder band at 360 nm, but major absorption band at 360 nm and shoulder band at 510 nm in MeOH. The mixture between ligand and base, shown by dash lines, absorbed only one peak at 390 nm 410 nm and 430 nm for MeOH, water, and DMSO, respectively, which correspond with $n \rightarrow \pi^*$ of azobenzene form. This result suggests that the deprotonated **A2** absorbs around 390-430 nm and the leaving proton should be that of carboxylic group as the negative charge of carboxylate ion could prevent electron transfer from hydroxyl group to π system molecule, resulting in tautomerization from quinone-hydrazone to azobenzene.

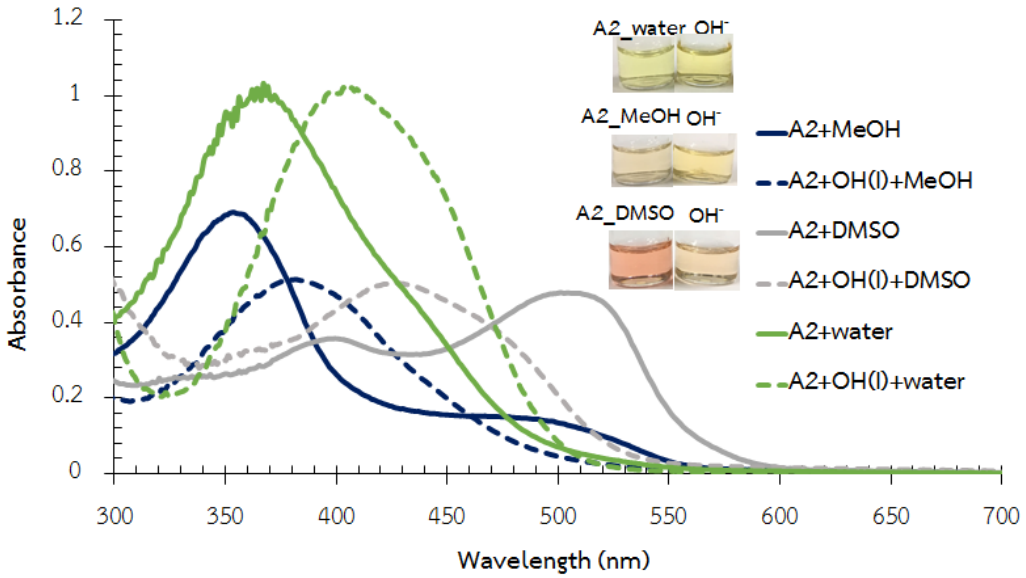

Figure 3.23 UV-Vis spectra and color change of sensors **A2** (1×10^{-4} M) without and with OH^- (5 eq) in various solvent

A UV-Visible titration of $(Bu)_4NOH$ into **N2** in MeOH was performed and the spectra were presented in Figure 3.24. The first isosbestic point at 450 nm appeared when the ratio of anion to ligand was 0-2 eq. The decrease of quinone-hydrazone band in this case suggests a tautomerization to azobenzene. When the ratio was higher, the second isosbestic point at 372 nm was observed which suggests a protonation at hydroxyl group in azobenzene.

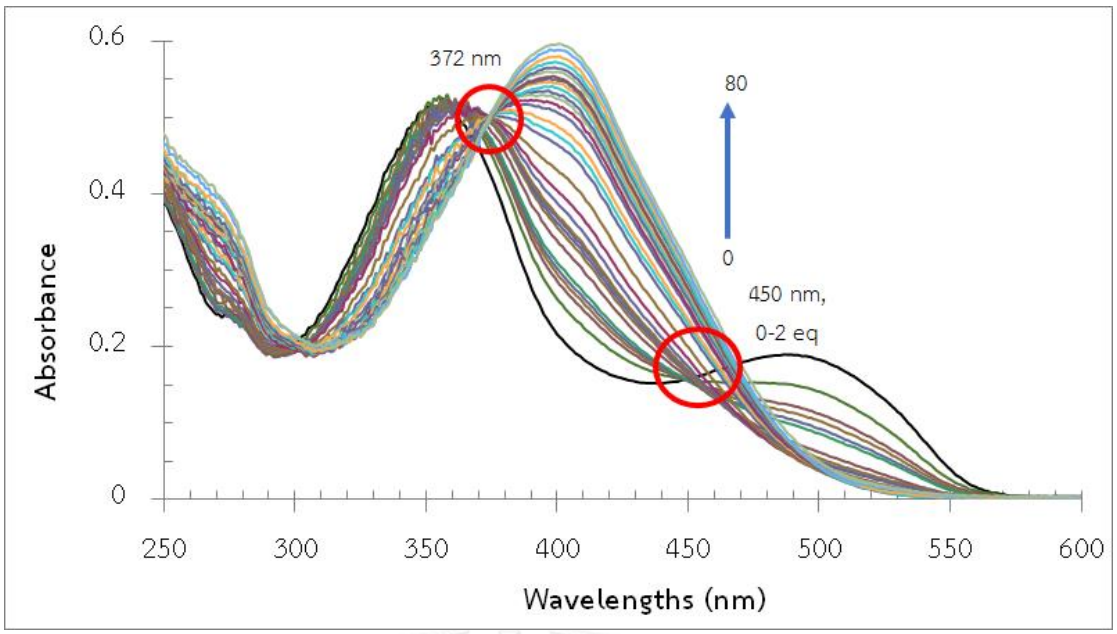

Figure 3.24 UV-Visible spectrophotometric titration UV-Visible of A2 (1×10^{-4} M) with OH^-

3.3.3.3 Nitro derivatives N1 and N2

It should be noted that addition 5 eq of hydroxide ion to nitro receptors in DMSO and MeCN induced more color intense. Because of this, sensing property towards other anions was also investigated in these solvents which will be discussed accordingly. However, in MeOH solution, hydroxide did not induce color change and UV-Visible absorption spectral change. This result suggests that hydroxide ion did not induce the conformation change in MeOH solution.

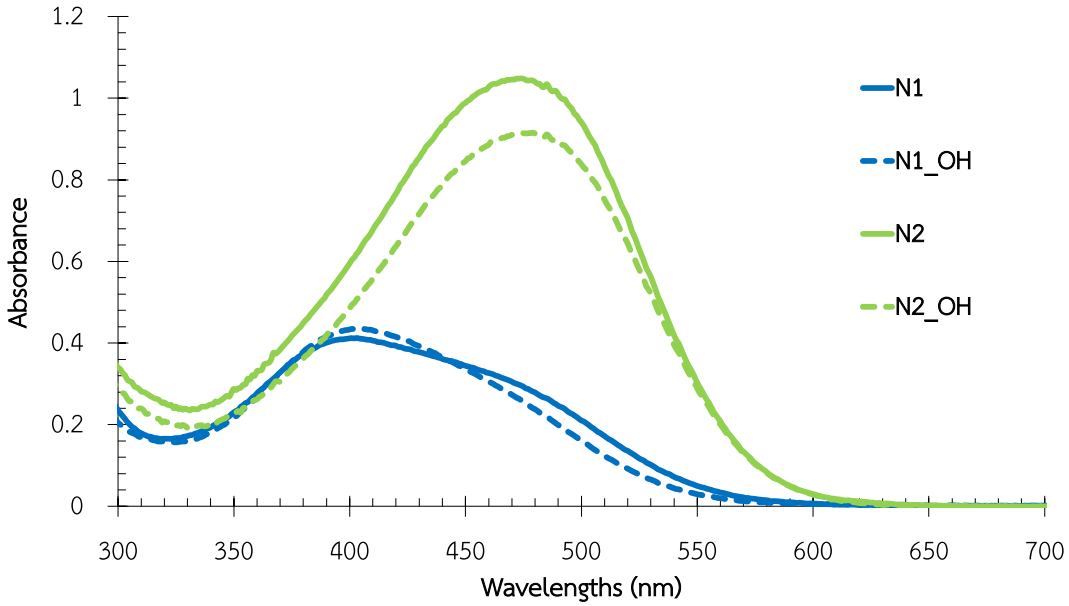

Figure 3.25 UV-Vis spectra of sensors **N1** and **N2** (2×10^{-5} M) without and with OH^- (5 eq) in MeOH

The study of sensing property towards anions in basic anions like AcO^-, BzO^-, and OH^- induced enhancement of absorbance at quinone-hydrazone form and reducing of absorbance at azobenzene form (Figure 3.26 and Figure 3.27). This result suggests that these anions induce tautomerization from azobenzene to quinone-hydrazone by depronation at hydroxyl group, resulting in a negative charge on oxygen atom. This negative charge could delocalize into π system and change to quinone hydrazone. Fluoride ions, however, gave a totally different observation, i.e., it induced a red shift of around 65 nm and 25 nm for **N1** and **N2**, respectively. This result could be explained by hydrogen bonding of hydrogen atom in NH of hydrazone with F^-. The interaction with fluoride anion increases the electron in the π system, leading to a decreasing of energy band gab and absorption at longer wavelength. This similar bathochromic shift was also observed in azo linked Schiff base ligand with F^- [54].

Table 3.6 Wavelengths at maximum absorption (λ_{max}) of **N1** and **N2** in various solvent without and with anion

Ions	N1		N2	
	MeCN	DMSO	MeCN	DMSO
no ion	390, <u>520</u>	410, <u>560</u>	525	555
F^-	585	610	540	615
Cl^-	390, <u>520</u>	410, <u>560</u>	525	555
Br^-	390, <u>520</u>	410, <u>560</u>	525	555
I^-	390, <u>520</u>	410, <u>560</u>	525	555
OH^-	529	550	540	555
OCl^{-+}	390, <u>520</u>	410, <u>560</u>	525	555
NO_3^-	390, <u>520</u>	410, <u>560</u>	525	555
$H_2PO_4^-$	390	400	390	400
AcO^-	520	550	525	555
BzO^-	520	410, <u>560</u>	525	555

Major band is presented as underline number

Impressively, not only red shift was observed in MeCN but also blue shift as can be seen in the case of dihydrogen phosphate ion. The conformation changed from quione-hydrazone to azobenzene form, leading to the hypsochromic shift from 560 nm to 390 nm for **N1**, and 525 nm to 390 nm for **N2**. The significant blue shift is possibly due to a hydrogen bonding between $H_2PO_4^-$ and OH in hydroxyl group resulting in a prevention of $n \rightarrow \pi^*$ transition in quinone-hydrazone form and tautomerization to azobenzene is favorable. To proof this assumption, a UV-Vis titration of NaOH into a mixture of $H_2PO_4^-$ (5 eq) and **N1** or **N2** derivatives was performed. The characteristic peak of quinone-hydrazone observed after addition of base suggests the deprotonation of hydroxyl group interrupts the interaction of the ligand and $H_2PO_4^-$. In other words, $H_2PO_4^-$ did not interact with O^- but hydrogen bond should occur between hydrogen atom in OH and oxygen atom in $H_2PO_4^-$.

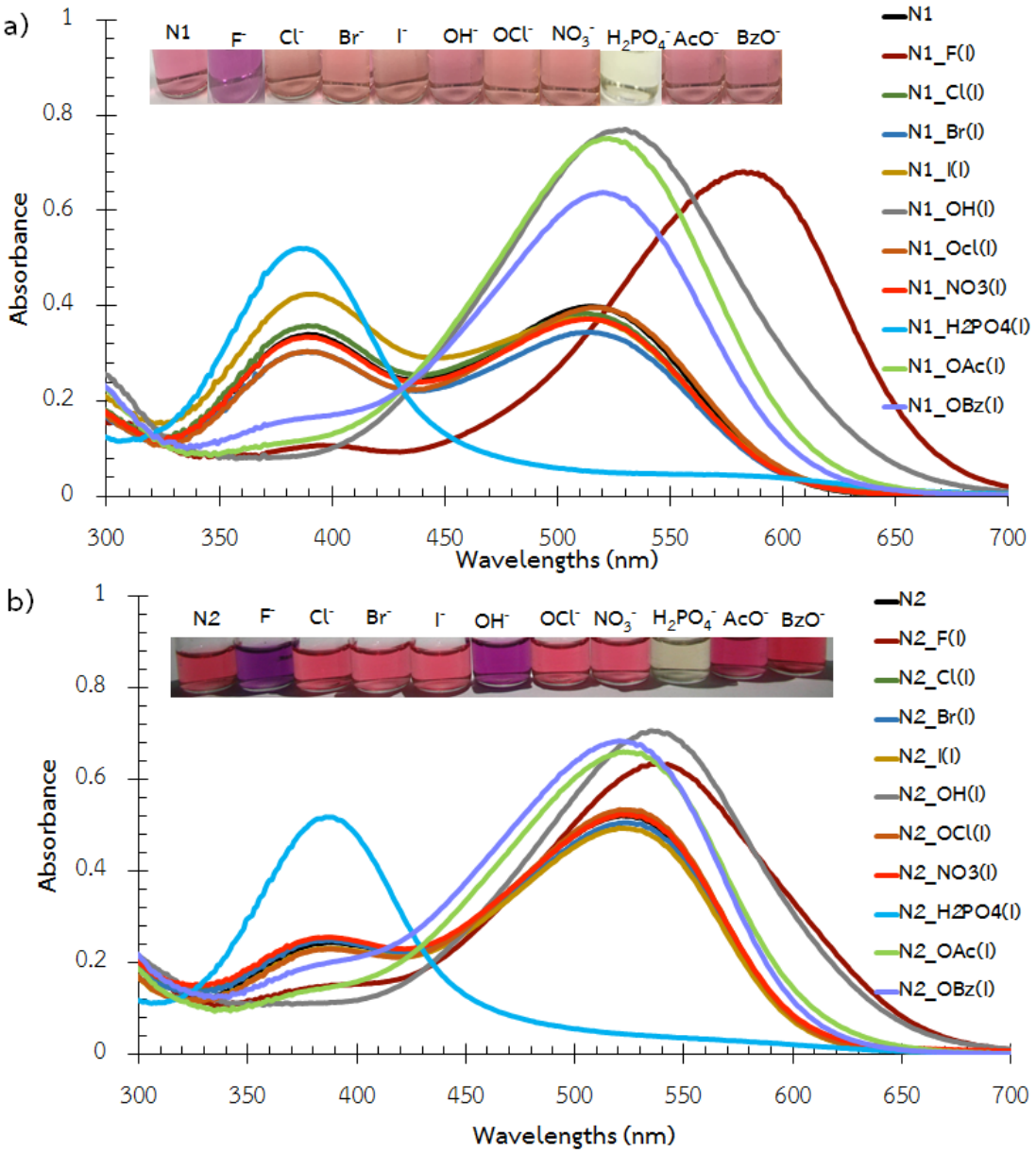

Figure 3.26 UV-Vis spectra and color change of sensors (a) **N1** and (b) **N2** (2×10^{-5} M) in the presence of various aions (5 eq) in MeCN

The sensing property towards anions in DMSO is similar to that in MeCN, i.e., absorbances increased when the basic anions such as AcO^-, BzO^-, and OH^- were added. Unluckily, the color change was not obvious to naked eye. Also, addition of F^- induced bathochromic shift of 50 and 65 nm, and $H_2PO_4^-$ hypsochromic shift of 120 and 155 nm in the cases of **N1** and **N2**, respectively.

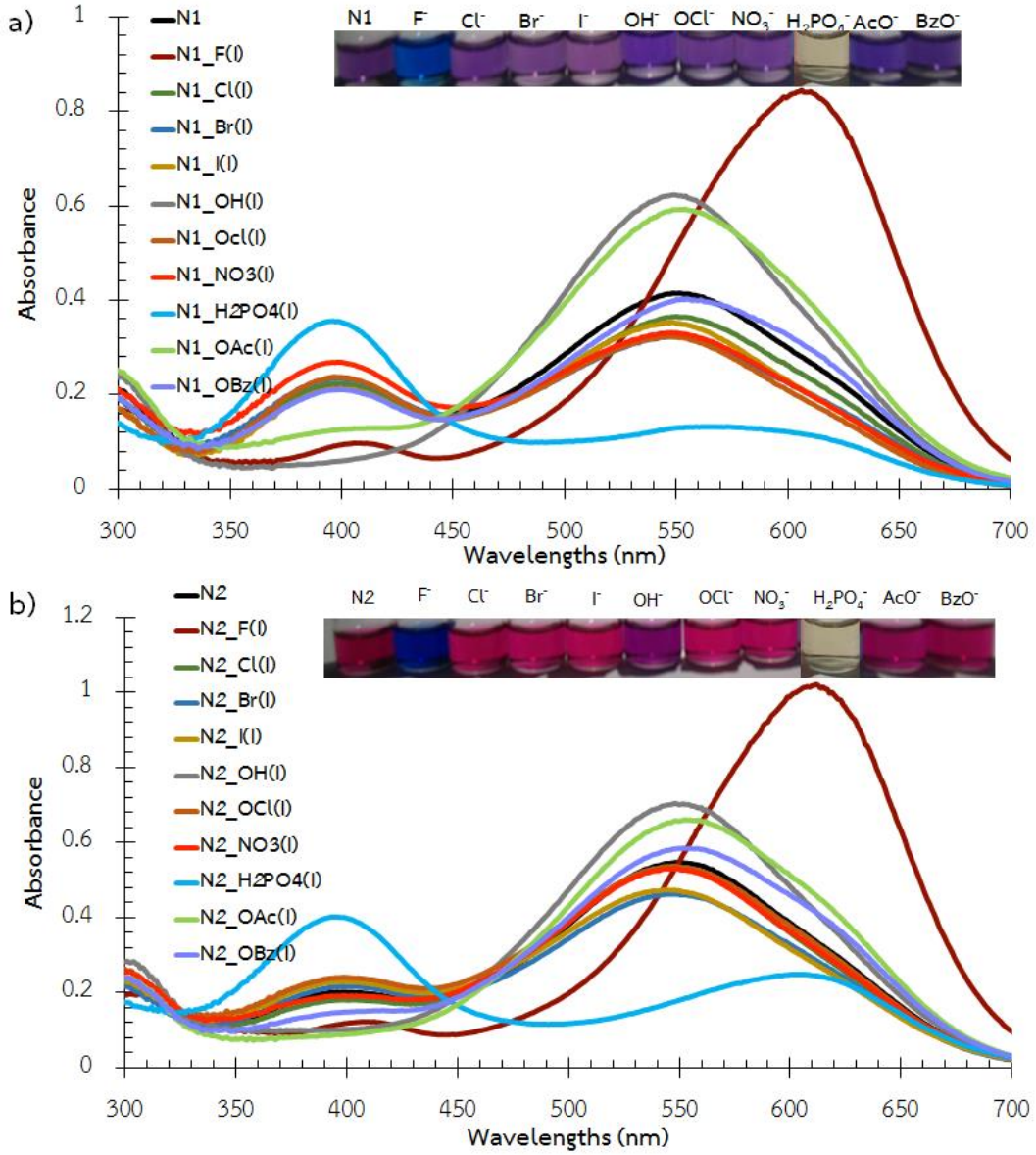

Figure 3.27 UV-Vis spectra and color change of sensors (a) **N1** and (b) **N2** (2×10^{-5} M) in the presence of various aions (5 eq) in DMSO

Since a notable color change was observed, spectrometric titrations of **N2** with fluoride ions in MeCN and DMSO were performed and the results are shown in Figure 3.28. The spectra showed one isosbestic point at 517 nm after A:L ratio of 1.5 in MeCN which suggested two complex formation. In DMSO, however, only one complex formation is evident because only one isosbestic point at 560 nm was observed throughout the titration.

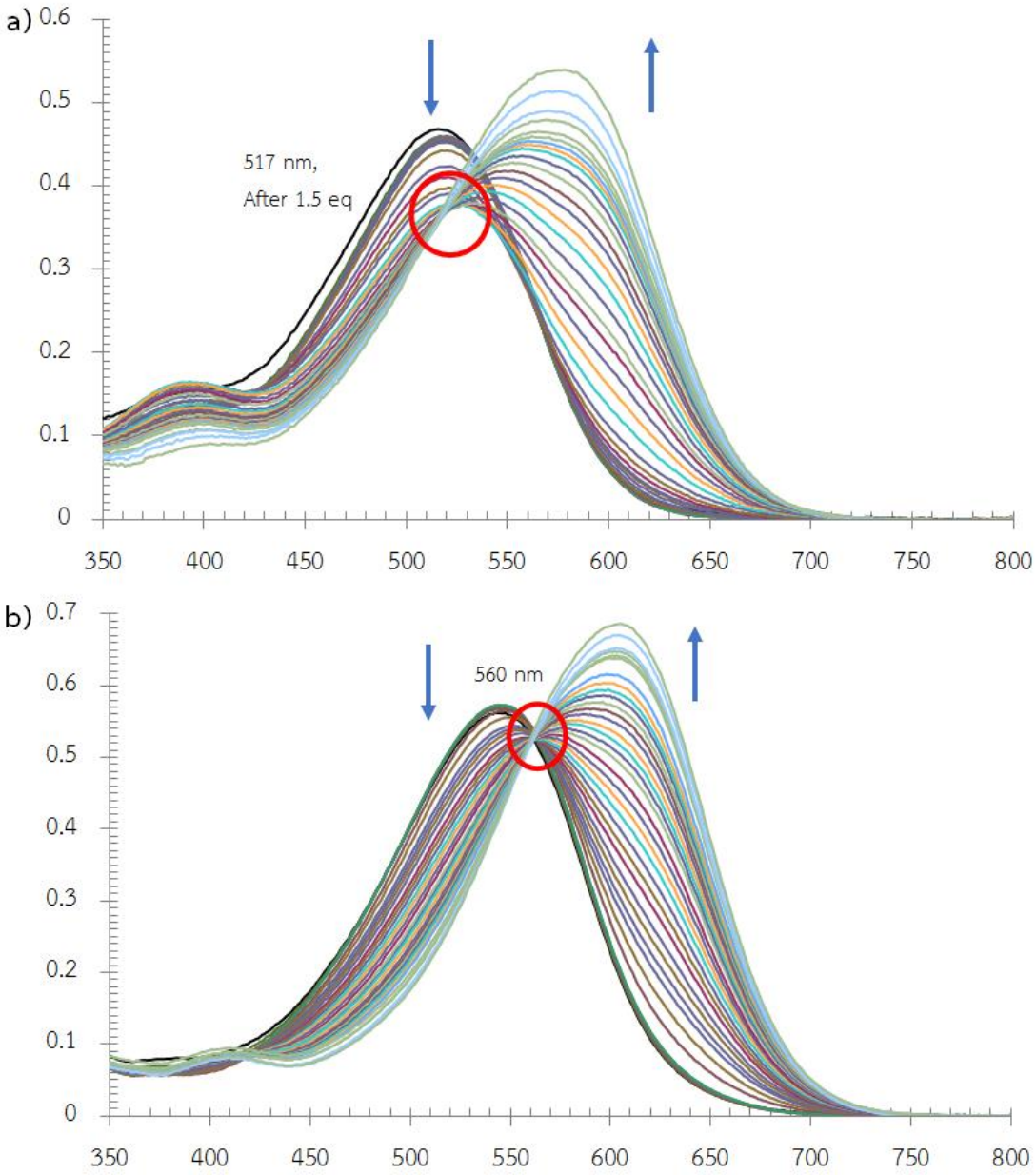

Figure 3.28 UV-Visible spectrophotometric titration UV-Visible of **N2** (2×10^{-5} M) with (a) 0-10 eq of F^- in MeCN, (b) 0-10 eq of F^- in DMSO

In the case of $H_2PO_4^-$ in MeCN, only one complex formation is evident because on the single isobestic point at 435 nm thoughout the titration. However, the titration of **N2** with $H_2PO_4^-$ in DMSO was much more complicate, i.e., when A:L ratio was 0-6, the absorbance at 400 nm increased, along with color change from purple to light yellow. When A:L ratio was more than 5 , the absorbance at 400 nm decreased and a new band at 610 nm was observed with a color change to blue. These results suggest

a formation of more than one complex. The interaction in the first complex at low A:L ratio should occur via hydrogen bonding between $H_2PO_4^-$ and ligand as mentioned earlier. The second complex at higher A:L ratio where the absorption shifted back to quinone-hydrazone form should happen as a result of deprotonation caused by the basic property of $H_2PO_4^-$.

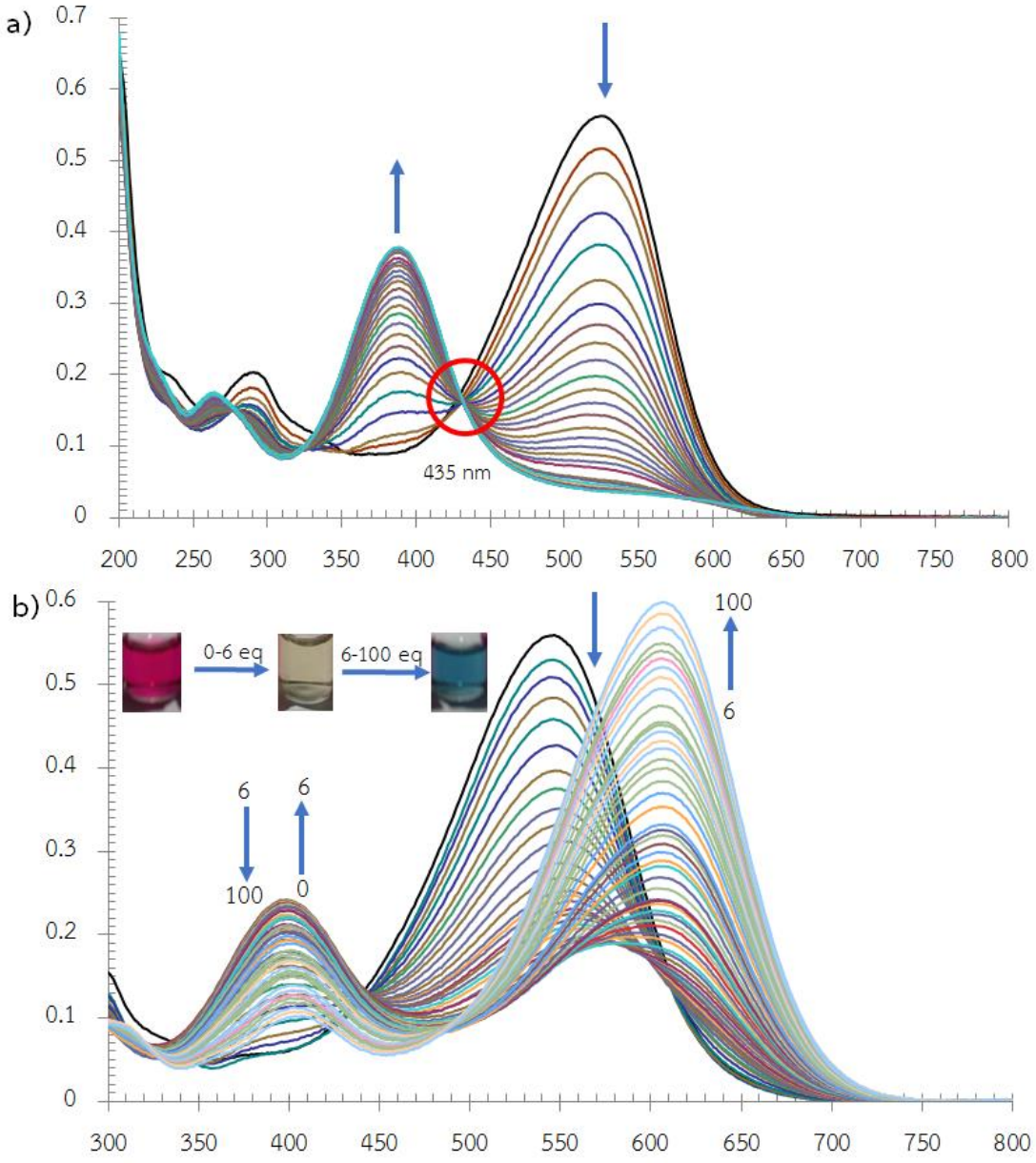

Figure 3.29 UV-Visible spectrophotometric titration UV-Visible of **N2** (2×10^{-5} M) with (a) 0-10 eq of $H_2PO_4^-$ in MeCN, (b) 0-100 eq of $H_2PO_4^-$ in DMSO

`

CHAPTER VI
CONCLUSION

4.1 Conclusion

The synthesis and characterization of six azo-diaza-18-crown-6 ether derivatives, five of which novel, were presented. The three ester derivatives **E1**, **E2** and **EE2** did not show any special sensing property towards metal ions of any type possibly due to the steric effect from ester substituents on azobenzene. Solvatochromic effects were observed in the cases of acid and nitro derivatives. The acid derivative **A2** showed sensing properties dependent on solvents: aqueous solution of **A2** changed from yellow to colorless upon the addition of Cr^{3+} and Hg^{2+} while its DMSO solution changed from orange to yellow or green tone. Unfortunately, this observation was not suitable for optical sensor because it could not be separated by human eye.

The nitro derivatives **N1** and **N2** also showed dependent sensing properties on solvent types. The addition of Cr^{3+} into **N1** or **N2** in MeCN induced a color change from pink to colorless along with a large hypsochromic shift (125 nm for **N1** and 165 nm for **N2**) in UV-Visible spectra. Metal ion Cr^{3+} possibly interacts with these sensors through oxygen atom in hydroxyl group. A titration of Cr^{3+} into **N2** suggests two complex formation of ML_2 and ML but their stability constants are too high to be accurately refined. The detection limits for Cr^{3+} in MeCN that rendered the colorless solution seen with the naked eye are 0.09 ppm and 0.27 ppm for **N1** and **N2**, respectively. These low detection limits for Cr^{3+} could be used to monitor Cr^{3+} that bring acute toxic to aquatic life ($\geq$ 0.57 ppm). Similar large blue shift of 160 nm and color change from purple to light yellow were also observed when Hg^{2+} was added to **N1** and **N2** solutions in DMSO. The detection limits of **N1** and **N2** for Hg^{2+} in DMSO are 0.90 ppm and 1.40 ppm, respectively. The apparent stability constant in logarithmic units of **N2** with Hg^{2+} (ML) complex is equal to 5.97.

The sensing properties toward anions are most prominent with nitro derivatives **N1** and **N2**. In MeCN and DMSO: F^- induced a red shift and $H_2PO_4^-$ a blue shift. In the case of F^-, the interaction probably occurs via hydrogen bonding which promote the

formation of hydrazone resulting in color changes from pink to purple in MeCN and purple to blue in DMSO. The large blue shift around 130-160 nm and color change from pink to colorless and purple to colorless of both **N1** and **N2** was observed in MeCN and DMSO, respectively. with $H_2PO_4^-$ which is possibly induced by hydrogen bonding of this anion with OH in hydroxyl group.

4.2 Future works

Future studies for this research will include refining the stability constants of both metal ion and anion complexes. Also sensing property of **N1** towards Ca^{2+} in MeCN is also interesting as it gives a distinct color change.

REFERENCES

[1] Lehn, J.-M. Supramolecular chemistry comcepts and perspective. Weinheim:Wiley-VCH, 1995.

[2] Lehn, J.-M. Supramolecular Chemistry—Scope and Perspectives Molecules, Supermolecules, and Molecular Devices (Nobel Lecture). Angewandte Chemie International Edition in English 27(1) (1988): 89-112.

[3] Lehn, J.-M. Perspectives in Supramolecular Chemistry—From Molecular Recognition towards Molecular Information Processing and Self-Organization. Angewandte Chemie International Edition in English 29(11) (1990): 1304-1319.

[4] Arabahmadi, R., Orojloo, M., and Amani, S. Azo Schiff bases as colorimetric and fluorescent sensors for recognition of F-, Cd2+ and Hg2+ ions. Analytical Methods 6(18) (2014): 7384-7393.

[5] Chereddy, N.R., Nagaraju, P., Niladri Raju, M.V., Saranraj, K., Thennarasu, S., and Rao, V.J. A two fluorophore embedded probe for collective and ratiometric detection of Hg2+ and F− ions. Dyes and Pigments 112 (2015): 201-209.

[6] Hama, H., Morozumi, T., and Nakamura, H. Novel Mg2+-responsive fluorescent chemosensor based on benzo-15-crown-5 possessing 1-naphthaleneacetamide moiety. Tetrahedron Letters 48(10) (2007): 1859-1861.

[7] Li, P., Zhang, Y.-M., Lin, Q., Li, J.-Q., and Wei, T.-B. A novel colorimetric HSO4− sensor in aqueous media. Spectrochimica Acta Part A: Molecular and Biomolecular Spectroscopy 90 (2012): 152-157.

[8] Luboch, E., Wagner-Wysiecka, E., and Biernat, J.F. Chromogenic azocrown ethers with peripheral alkyl, alkoxy, hydroxy or dimethylamino group. Journal of Supramolecular Chemistry 2(1–3) (2002): 279-291.

[9] Luboch, E., Wagner-Wysiecka, E., Poleska-Muchlado, Z., and Kravtsov, V.C. Synthesis and properties of azobenzocrown ethers with **π**-electron donor, or **π**-electron donor and **π**-electron acceptor group(s) on benzene ring(s). Tetrahedron 61(45) (2005): 10738-10747.

[10] Yuan, X.-J., et al. New Pb(II)-selective membrane electrode based on a new Schiff base complex. Inorganic Chemistry Communications 15 (2012): 29-32.

[11] Zahran, E.M., Hua, Y., Li, Y., Flood, A.H., and Bachas, L.G. Triazolophanes: A New Class of Halide-Selective Ionophores for Potentiometric Sensors. Analytical Chemistry 82(1) (2010): 368-375.

[12] Sahoo, S.K., Kim, G.-D., and Choi, H.-J. Optical sensing of anions using C3v-symmetric tripodal receptors. Journal of Photochemistry and Photobiology C: Photochemistry Reviews 27 (2016): 30-53.

[13] Carter, K.P., Young, A.M., and Palmer, A.E. Fluorescent Sensors for Measuring Metal Ions in Living Systems. Chemical Reviews 114(8) (2014): 4564-4601.

[14] Kaur, N. and Kumar, S. Colorimetric metal ion sensors. Tetrahedron 67(48) (2011): 9233-9264.

[15] Quang, D.T. and Kim, J.S. Fluoro- and Chromogenic Chemodosimeters for Heavy Metal Ion Detection in Solution and Biospecimens. Chemical Reviews 110(10) (2010): 6280-6301.

[16] Cheng, Y., Zhang, M., Yang, H., Li, F., Yi, T., and Huang, C. Azo dyes based on 8-hydroxyquinoline benzoates: Synthesis and application as colorimetric Hg2+-selective chemosensors. Dyes and Pigments 76(3) (2008): 775-783.

[17] Kumar, A., Kumar, V., and Upadhyay, K.K. A ninhydrin based colorimetric molecular switch for Hg2+ and CH3COO−/F−. Tetrahedron Letters 52(50) (2011): 6809-6813.

[18] Liu, J., et al. A BODIPY derivative for colorimetric and fluorometric sensing of fluoride ion and its logic gates behavior. Sensors and Actuators B: Chemical 208 (2015): 538-545.

[19] Na, S.-Y. and Kim, H.-J. Azo dye-based colorimetric chemodosimeter for the rapid and selective sensing of cyanide in aqueous solvent. Tetrahedron Letters 56(3) (2015): 493-495.

[20] Bühlmann, P., Pretsch, E., and Bakker, E. Carrier-Based Ion-Selective Electrodes and Bulk Optodes. 2. Ionophores for Potentiometric and Optical Sensors. Chemical Reviews 98(4) (1998): 1593-1688.

[21] Pedersen, C.J. Cyclic polyethers and their complexes with metal salts. Journal of the American Chemical Society 89(26) (1967): 7017-7036.

[22] Abe, A.M.M., Helaja, J., and Koskinen, A.M.P. Novel Crown Ether and Salen Metal Chelation Driven Molecular Pincers. Organic Letters 8(20) (2006): 4537-4540.

[23] Ding, L., Wu, M., Li, Y., Chen, Y., and Su, J. New fluoro- and chromogenic chemosensors for the dual-channel detection of Hg2+ and F−. Tetrahedron Letters 55(34) (2014): 4711-4715.

[24] Ho, I.T., Lee, G.-H., and Chung, W.-S. Synthesis of Upper-Rim Allyl- and p-Methoxyphenylazocalix[4]arenes and Their Efficiencies in Chromogenic Sensing of Hg2+ Ion. The Journal of Organic Chemistry 72(7) (2007): 2434-2442.

[25] Kim, T.H., Kim, S.H., Van Tan, L., Dong, Y., Kim, H., and Kim, J.S. Diazo-coupled calix[4]arenes for qualitative analytical screening of metal ions. Talanta 74(5) (2008): 1654-1658.

[26] Liu, H., Wan, X., Liu, T., Li, Y., and Yao, Y. Cascade sensitive and selective fluorescence OFF–ON–OFF sensor for Cr3+ cation and F− anion. Sensors and Actuators B: Chemical 200 (2014): 191-197.

[27] Aldrey, A., et al. Colorimetric macrocyclic anion probes bearing nitrophenylurea and nitrophenylthiourea binding groups. Tetrahedron 69(23) (2013): 4578-4585.

[28] Kumar, M., Babu, J.N., and Bhalla, V. Azophenol appended (thia)calix[4]arenes for colorimetric sensing of anions: A complexation induced extended conjugation. Talanta 81(1–2) (2010): 9-14.

[29] Luboch, E., Wagner-Wysiecka, E., and Rzymowski, T. 4-Hexylresorcinol-derived hydroxyazobenzocrown ethers as chromoionophores. Tetrahedron 65(51) (2009): 10671-10678.

[30] Shao, J., Lin, H., and Lin, H. A novel chromo- and fluorogenic dual responding H2PO4− receptor based on an azo derivative. Dyes and Pigments 80(2) (2009): 259-263.

[31] Kim, T.H., et al. Transition metal ion selective ortho-ester diazophenylcalix[4]arene. Talanta 71(3) (2007): 1294-1297.

[32] Barbour, L.J., De Wall, S.L., Meadows, E.S., and Gokel, G.W. Experimental Evidence for Alkali-Metal Ion Cation–**π** Interactions Using Bibracchial Lariat Ether Complexes. Industrial & Engineering Chemistry Research 39(10) (2000): 3436-3441.

[33] Berdnikova, D.V., Fedorov, Y.V., and Fedorova, O.A. Azadithiacrown ether based ditopic receptors capable of simultaneous multi-ionic recognition of Ag+ and Hg2+. Dyes and Pigments 96(1) (2013): 287-295.

[34] Bronson, R.T., et al. Efficient Immobilization of a Cadmium Chemosensor in a Thin Film: Generation of a Cadmium Sensor Prototype. Organic Letters 7(6) (2005): 1105-1108.

[35] Capel-Cuevas, S., de Orbe-Payá, I., Santoyo-González, F., and Capitán-Vallvey, L.F. Double-armed crown ethers for calcium optical sensors. Talanta 78(4–5) (2009): 1484-1488.

[36] Carreira-Barral, I., et al. A merged experimental and theoretical conformational study on alkaline-earth complexes with lariat ethers derived from 4,13-diaza-18-crown-6. Inorganica Chimica Acta 370(1) (2011): 270-278.

[37] Kubo, K., Ishige, R., and Sakurai, T. Complexation and fluorescence behavior of diazacrown ether carrying two anthryl pendants. Talanta 49(2) (1999): 339-344.

[38] Li, H., Li, L., and Yin, B. Highly selective fluorescent chemosensor for Fe3 + detection based on diaza-18-crown-6 ether appended with dual coumarins. Inorganic Chemistry Communications 42 (2014): 1-4.

[39] Ma, S.-L., et al. Synthesis and crystal structure of copper complex of bis(p-chlorophenol)-containing diaza-18-crown-6 ligand. Journal of Molecular Structure 703(1–3) (2004): 25-29.

[40] Kursunlu, A.N., Deveci, P., and Guler, E. Synthesis and spectroscopic–electrochemical properties of novel ratiometric Hg (II) chemosensor containing Bodipy and the N-phenylaza-15-crown-5 moiety. Journal of Luminescence 136 (2013): 430-436.

[41] Khedr, A.M., Gaber, M., Issa, R.M., and Erten, H. Synthesis and spectral studies of 5-[3-(1,2,4-triazolyl-azo]-2,4-dihydroxybenzaldehyde (TA) and its Schiff bases with 1,3-diaminopropane (TAAP) and 1,6-diaminohexane (TAAH). Their analytical application for spectrophotometric microdetermination of cobalt(II). Application in some radiochemical studies. Dyes and Pigments 67(2) (2005): 117-126.

[42] Mahmoud, M.R., Ibrahim, S.A., and Hamed, M.A. Low excitation energy band of 4-hydroxyazobenzene derivatives. Spectrochimica Acta Part A: Molecular Spectroscopy 39(8) (1983): 729-733.

[43] Rezaeian, K. and Khanmohammadi, H. Naked-eye detection of biologically important anions by a new chromogenic azo-azomethine sensor. Spectrochimica Acta Part A: Molecular and Biomolecular Spectroscopy 133 (2014): 31-37.

[44] Matazo, D.R.C., Ando, R.A., Borin, A.C., and Santos, P.S. Azo–Hydrazone Tautomerism in Protonated Aminoazobenzenes: Resonance Raman Spectroscopy and Quantum-Chemical Calculations. The Journal of Physical Chemistry A 112(19) (2008): 4437-4443.

[45] Kao, T.-L., et al. Upper Rim Allyl- and Arylazo-Coupled Calix[4]arenes as Highly Sensitive Chromogenic Sensors for Hg2+ Ion. The Journal of Organic Chemistry 70(8) (2005): 2912-2920.

[46] Rezaeian, K., Khanmohammadi, H., and Arab, V. Rational design of a novel azoimine appended maleonitrile-based Salen chemosensor for rapid naked-eye detection of copper(II) ion in aqueous media. Spectrochimica Acta Part A: Molecular and Biomolecular Spectroscopy 151 (2015): 848-853.

[47] Radchatawedchakoon, W., Sangsuwan, W., Kruanetr, S., and Sakee, U. Synthesis and evaluation of simple naked-eye colorimetric chemosensors for anions based on azo dye-thiosemicarbazones. Spectrochimica Acta Part A: Molecular and Biomolecular Spectroscopy 121 (2014): 306-312.

[48] Kaur, N., Dhaka, G., and Singh, J. Simple naked-eye ratiometric and colorimetric receptor for anions based on azo dye featuring with benzimidazole unit. Tetrahedron Letters 56(9) (2015): 1162-1165.

[49] Khanmohammadi, H., Rezaeian, K., and Abdollahi, A. Colorimetric detection of anions in aqueous media using N-monosubstituted diaminomaleonitrile-based azo-azomethine receptors: Real-life applications. Spectrochimica Acta Part A: Molecular and Biomolecular Spectroscopy 139 (2015): 405-412.

[50] Su, N., et al. Syntheses and aggregate study of bisphenol-containing diaza-18-crown-6 ligands. Tetrahedron 55(32) (1999): 9737-9742.

[51] Woods, M. and Sherry, A.D. Synthesis and Luminescence Studies of Aryl Substituted Tetraamide Complexes of Europium(III): A New Approach to pH Responsive Luminescent Europium Probes. Inorganic Chemistry 42(14) (2003): 4401-4408.

[52] Vetrogon, V.I., Lukyanenko, N.G., Schwing-Weill, M.J., and Arnaud-Neu, F. A PC compatible computer program for the calculation of equilibrium constants by the simultaneous processing of different sets of experimental results. Talanta 41(12) (1994): 2105-2112.

[53] Gunnlaugsson, T., Leonard, J.P., and Murray, N.S. Highly Selective Colorimetric Naked-Eye Cu(II) Detection Using an Azobenzene Chemosensor. Organic Letters 6(10) (2004): 1557-1560.

[54] Udhayakumari, D., Velmathi, S., and Boobalan, M.S. Novel chemosensor for multiple target anions: The detection of F− and CN− ion via different approach. Journal of Fluorine Chemistry 175 (2015): 180-184.

[55] Arabahmadi, R. and Amani, S. A new fluoride ion colorimetric sensor based on azo–azomethine receptors. Supramolecular Chemistry 26(5-6) (2014): 321-328.

[56] Debnath, D., Roy, S., Li, B.-H., Lin, C.-H., and Misra, T.K. Synthesis, structure and study of azo-hydrazone tautomeric equilibrium of 1,3-dimethyl-5-(arylazo)-6-amino-uracil derivatives. Spectrochimica Acta Part A: Molecular and Biomolecular Spectroscopy 140 (2015): 185-197.

[57] Liu, G. and Shao, J. Fluorescence anion sensors based on combination of conformational restriction and photo-induced electron transfer. Journal of Luminescence 135 (2013): 312-317.

[58] Sheng, R., Wang, P., Liu, W., Wu, X., and Wu, S. A new colorimetric chemosensor for Hg2+ based on coumarin azine derivative. Sensors and Actuators B: Chemical 128(2) (2008): 507-511.

[59] Shu, J., Wang, Z., Huang, Y., Huang, N., Ren, C., and Zhang, W. Adsorption removal of Congo red from aqueous solution by polyhedral Cu2O nanoparticles: Kinetics, isotherms, thermodynamics and mechanism analysis. Journal of Alloys and Compounds 633 (2015): 338-346.

[60] Su, N., Bradshaw, J.S., Zhang, X.X., Savage, P.B., Krakowiak, K.E., and Izatt, R.M. Syntheses of diaza-18-crown-6 ligands containing two units each of 4-hydroxyazobenzene, benzimidazole, uracil, anthraquinone, or ferrocene groups. Journal of Heterocyclic Chemistry 36(3) (1999): 771-775.

[61] Su, N., et al. Syntheses and Metal Ion Complexation of Novel 8-Hydroxyquinoline-Containing Diaza-18-Crown-6 Ligands and Analogues. The Journal of Organic Chemistry 64(24) (1999): 8855-8861.

[62] Thiampanya, P., Muangsin, N., and Pulpoka, B. Azocalix[4]arene Strapped Calix[4]pyrrole: A Confirmable Fluoride Sensor. Organic Letters 14(16) (2012): 4050-4053.

[63] Wachtveitl, J., et al. Ultrafast Conformational Dynamics in Cyclic Azobenzene Peptides of Increased Flexibility. Biophysical Journal 86(4) (2004): 2350-2362.

APPENDIX

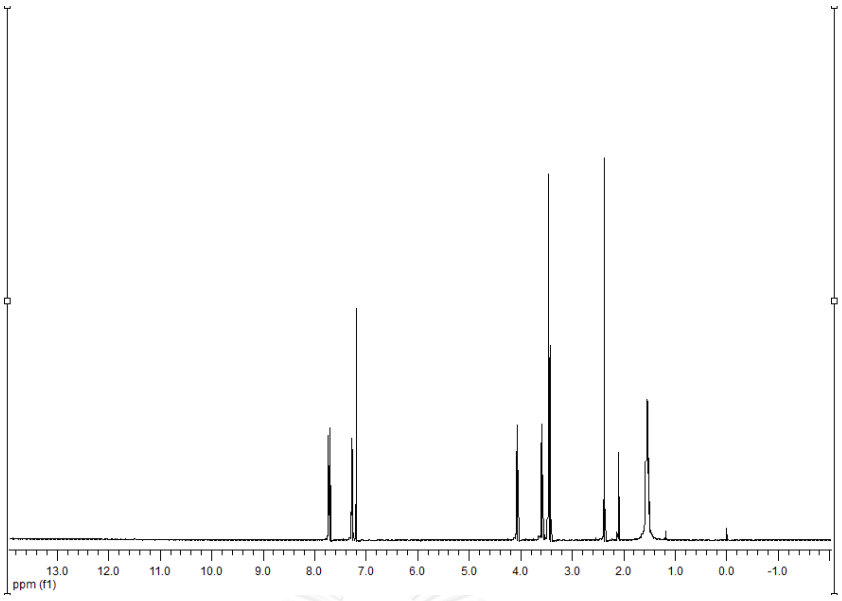

Figure A1 ^{1}H-NMR spectrum of triethyleneditosylate **1** in $CDCl_3$ at 400 MHz

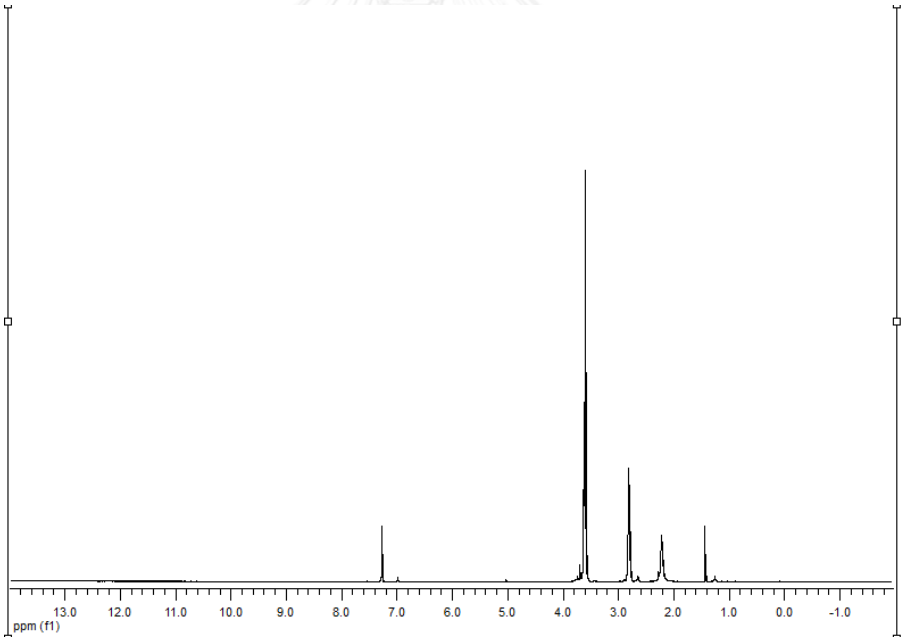

Figure A2 ^{1}H-NMR spectrum of diazacrown ether **2** in $CDCl_3$ at 400 MHz

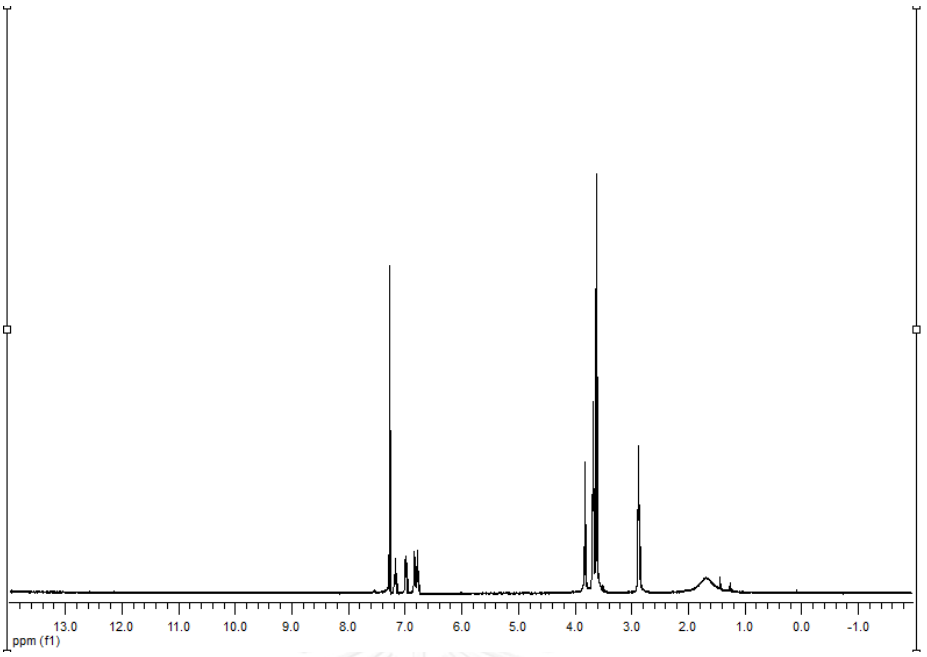

Figure A3 ^{1}H-NMR spectrum of phenol methyl diazacrown ether **3** in $CDCl_3$ at 400 MHz

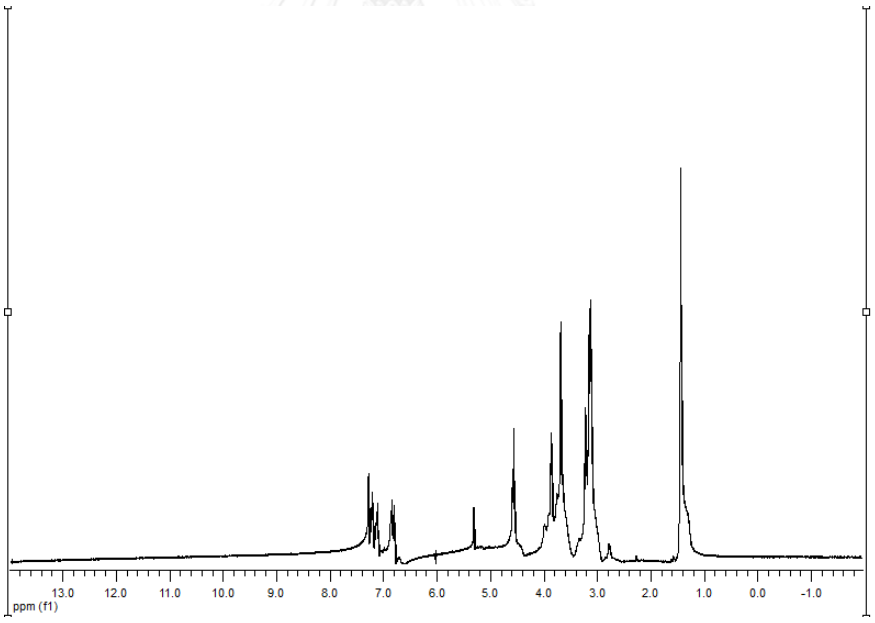

Figure A4 ^{1}H-NMR spectrum of phenol ethyl diazacrown ether **5** in $CDCl_3$ at 400 MHz

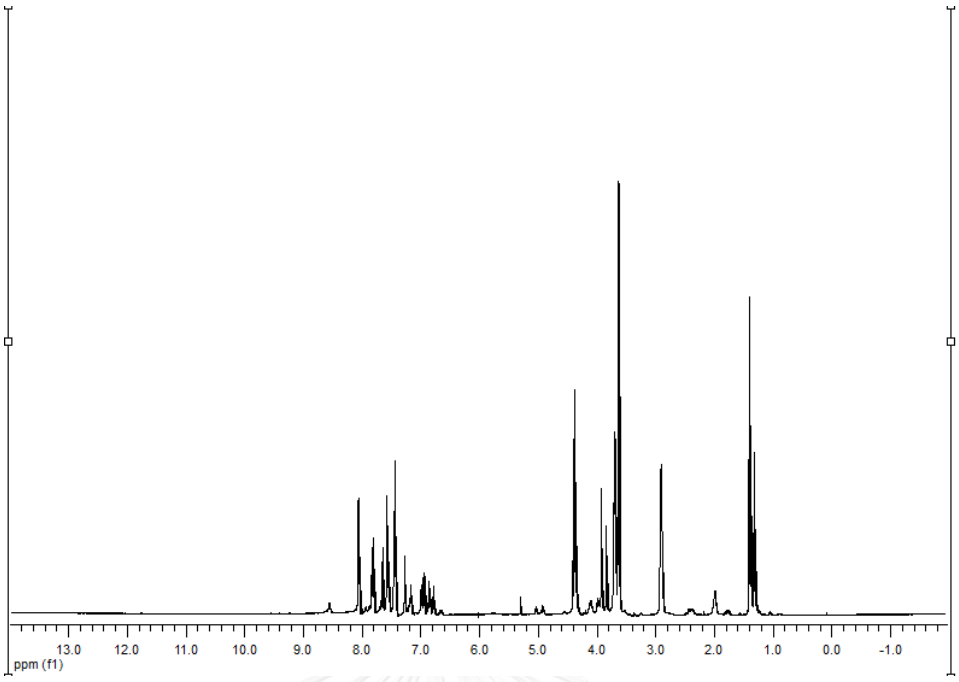

Figure A5 ^{1}H-NMR spectrum of **E1** in $CDCl_3$ at 400 MHz

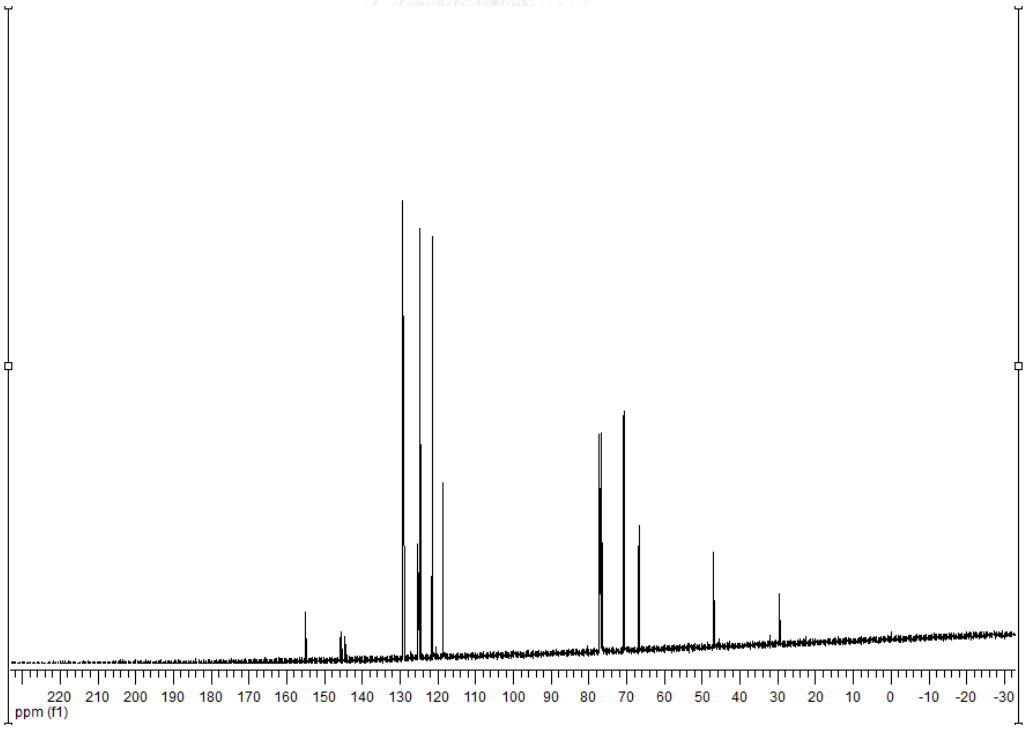

Figure A6 ^{13}C-NMR spectrum of **E1** in $CDCl_3$ at 400 MHz

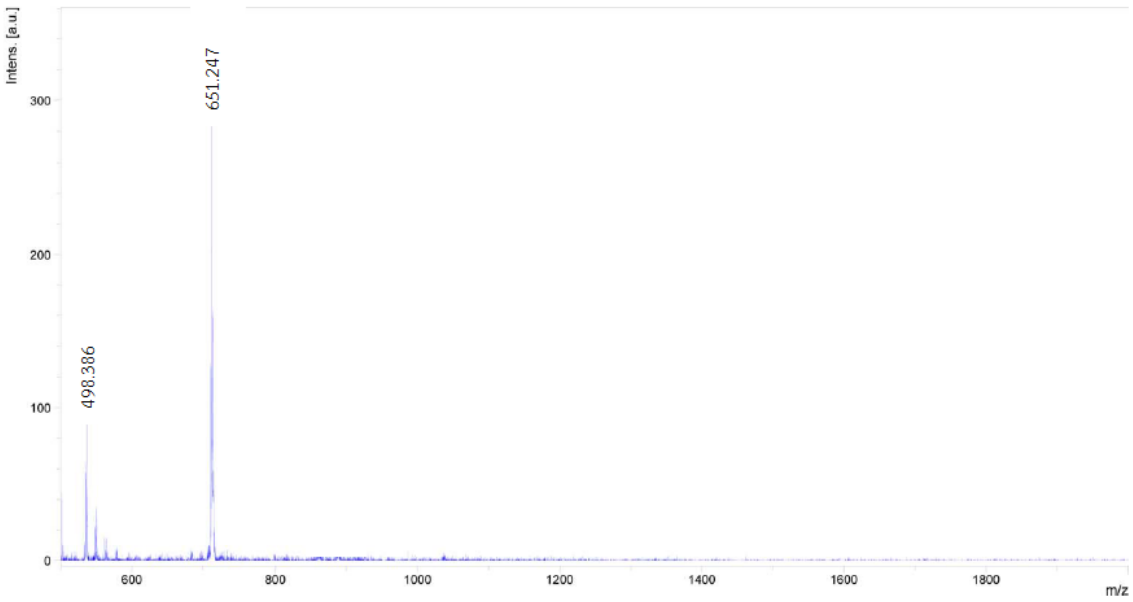

Figure A7 MALDI-TOF mass spectrum of **E1** at 651.247 m/z

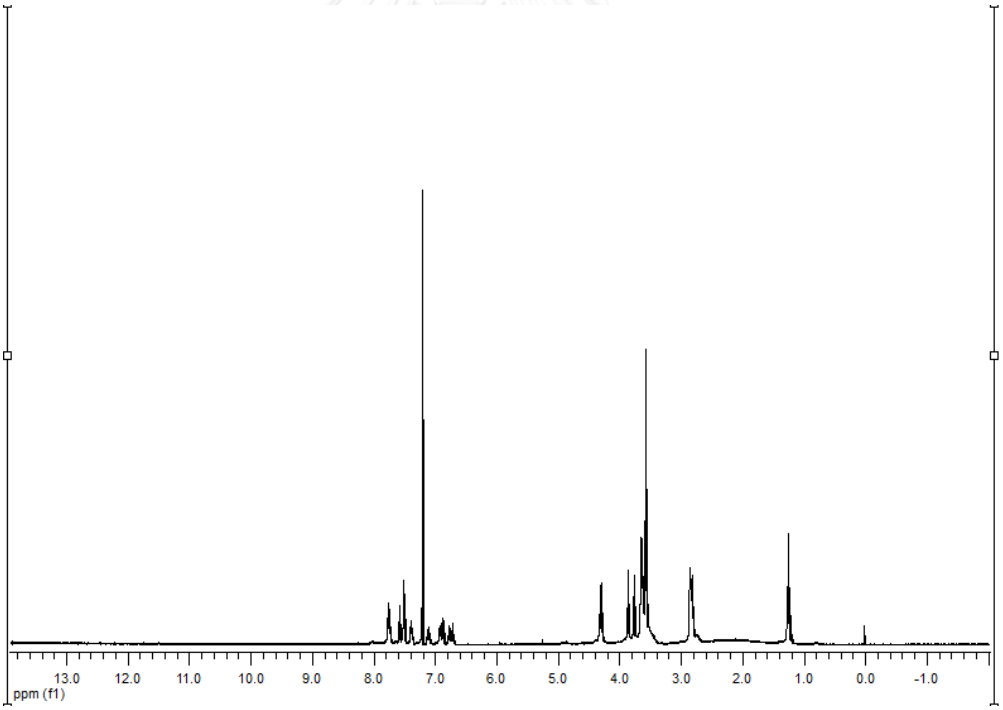

Figure A8 ^{1}H-NMR spectrum of **E2** in $CDCl_3$ at 400 MHz

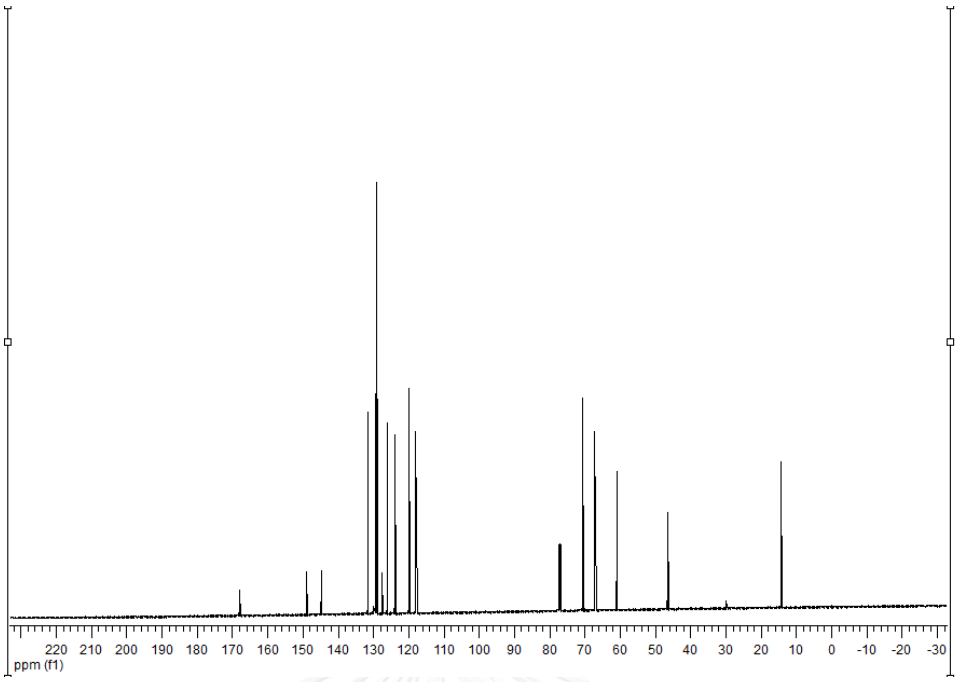

Figure A9 ^{13}C-NMR spectrum of **E2** in $CDCl_3$ at 400 MHz

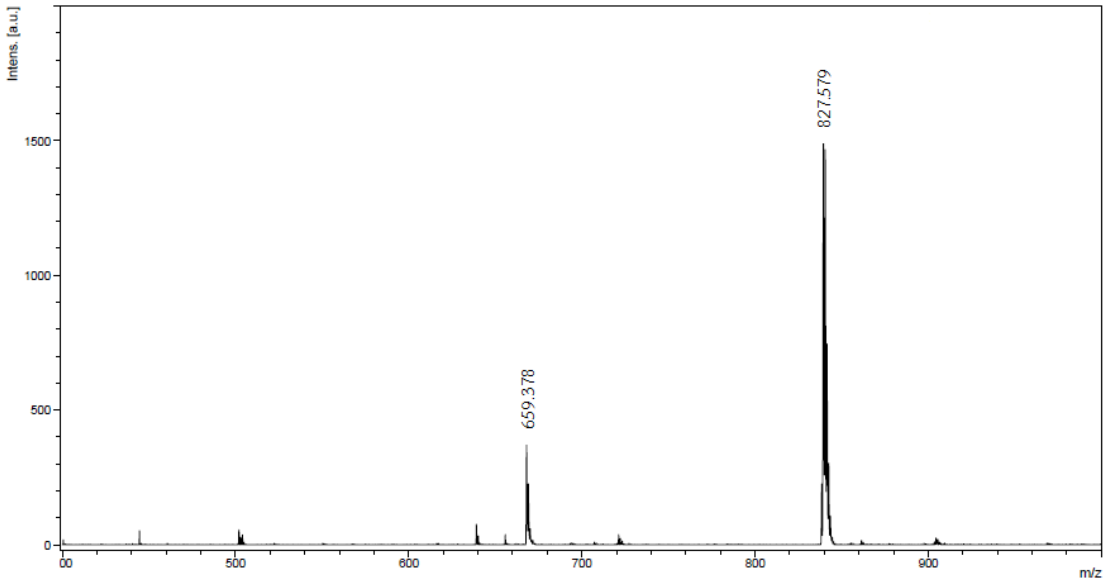

Figure A10 MALDI-TOF mass spectrum of **E2** at 827.579 m/z

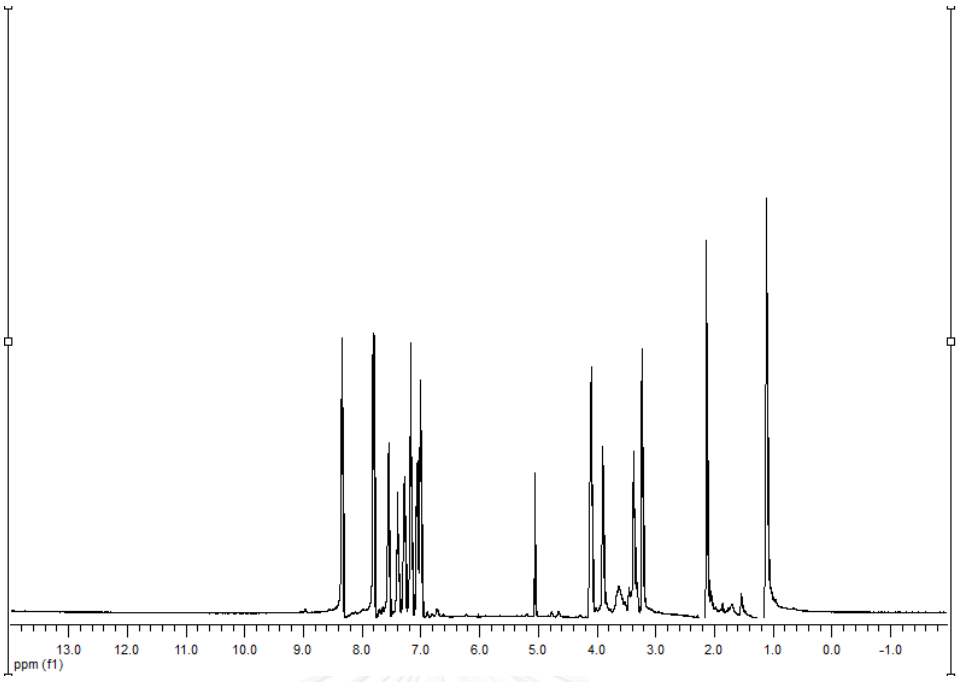

Figure A11 ^{1}H-NMR spectrum of **EE2** in $CDCl_3$ at 400 MHz

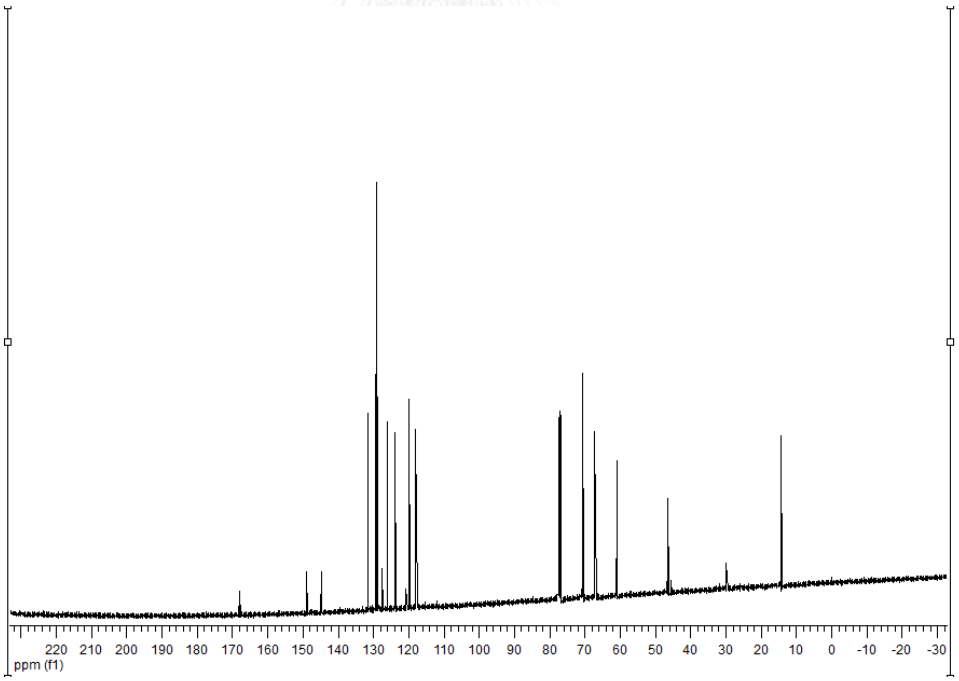

Figure A12 ^{13}C-NMR spectrum of **EE2** in $CDCl_3$ at 400 MHz

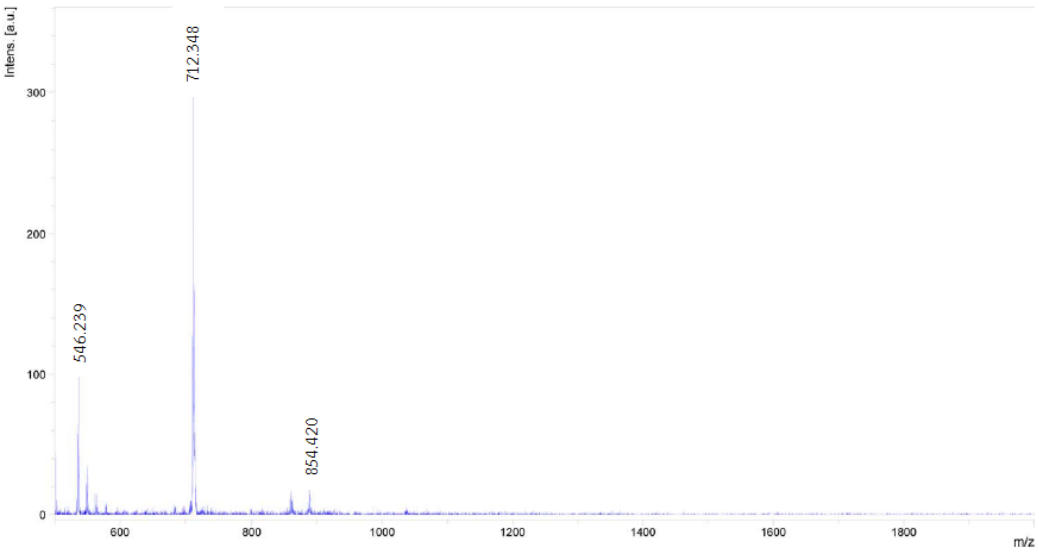

Figure A13 MALDI-TOF mass spectrum of **EE2** at 854.420 m/z

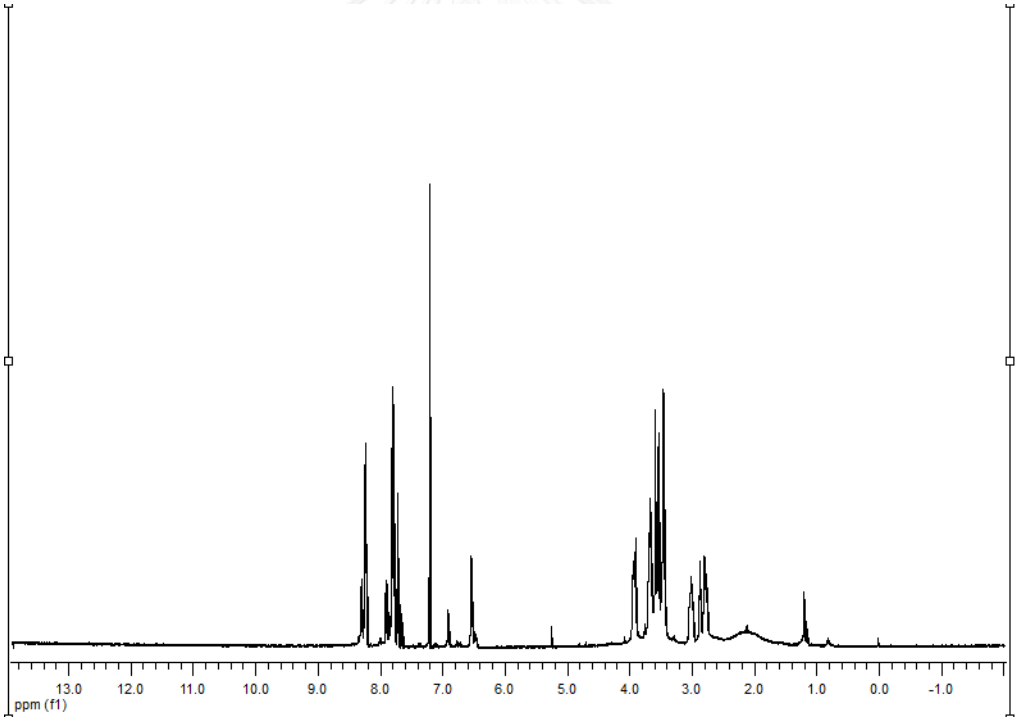

Figure A14 ^{1}H-NMR spectrum of **A2** in $CDCl_3$ at 400 MHz

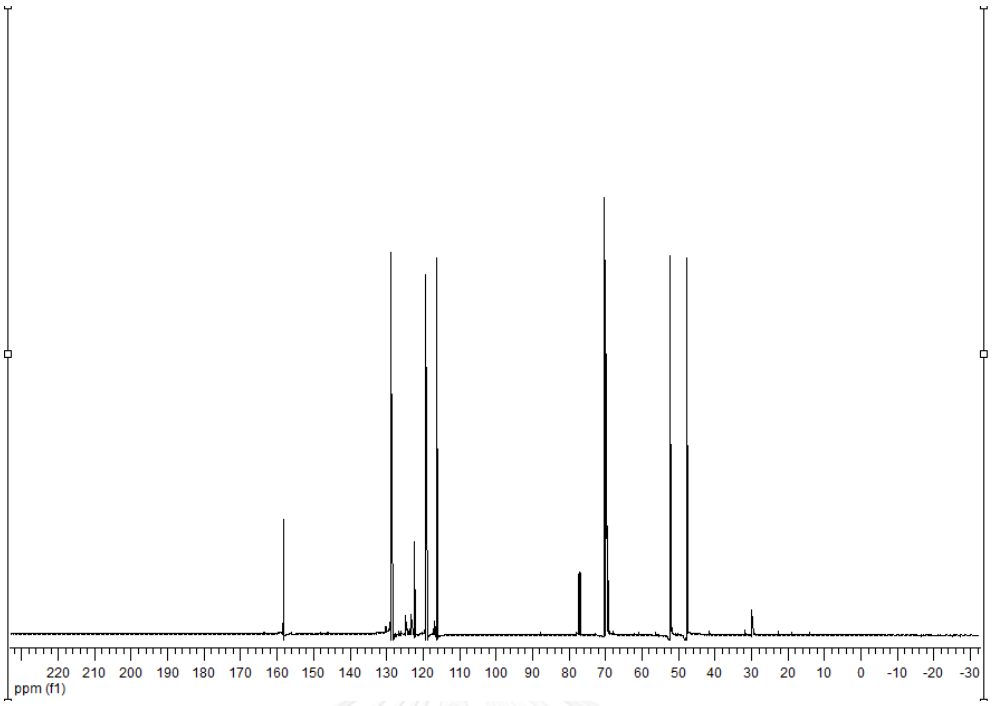

Figure A15 ^{13}C-NMR spectrum of **A2** in $CDCl_3$ at 400 MHz

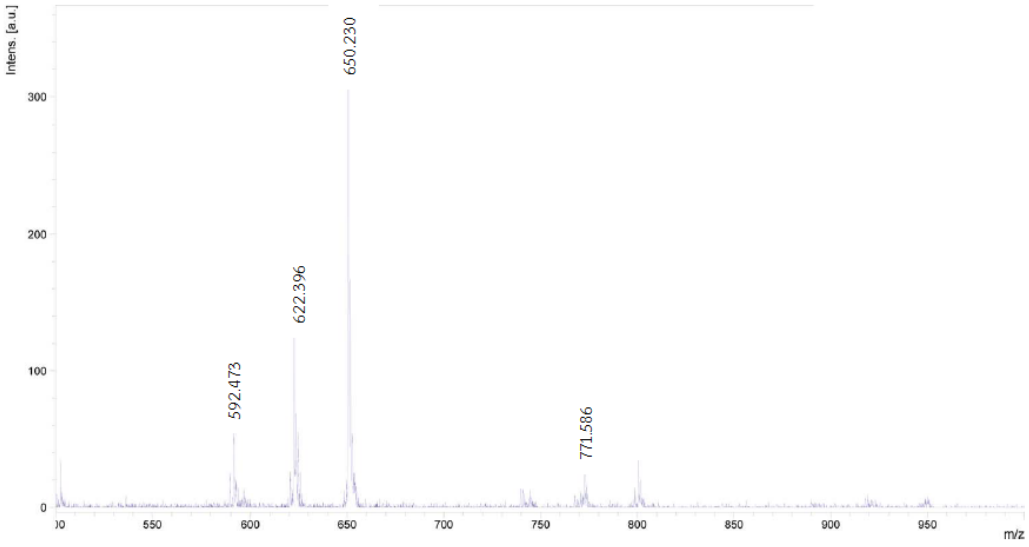

Figure A16 MALDI-TOF mass spectrum of **A2** at 771.586m/z

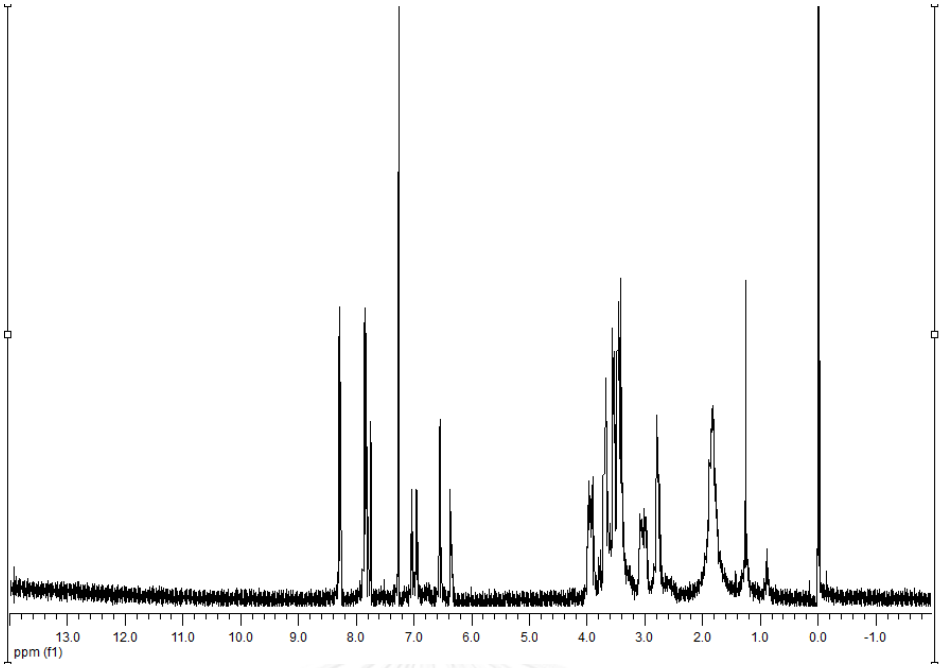

Figure A 17 ^{1}H-NMR spectrum of **N1** in $CDCl_3$ at 400 MHz

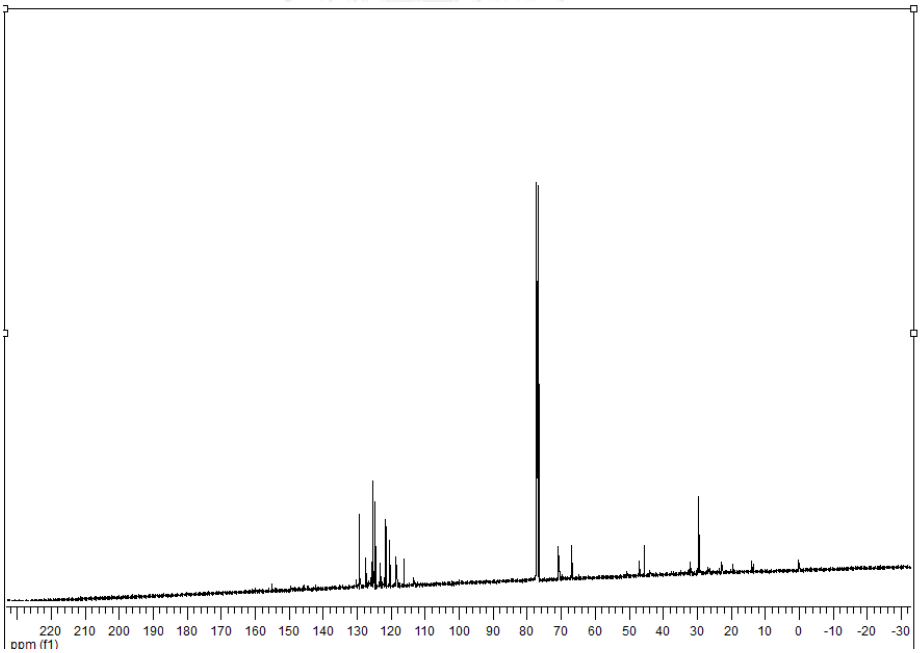

Figure A18 ^{13}C-NMR spectrum of **N1** in $CDCl_3$ at 400 MHz

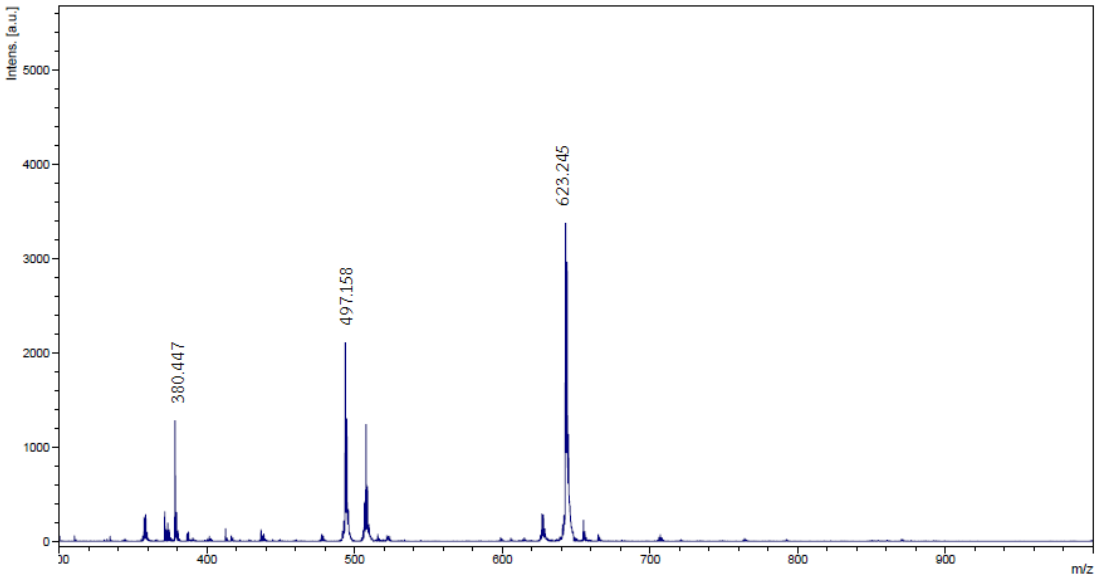

Figure A19 MALDI-TOF mass spectrum of **N1** at 623.245 m/z

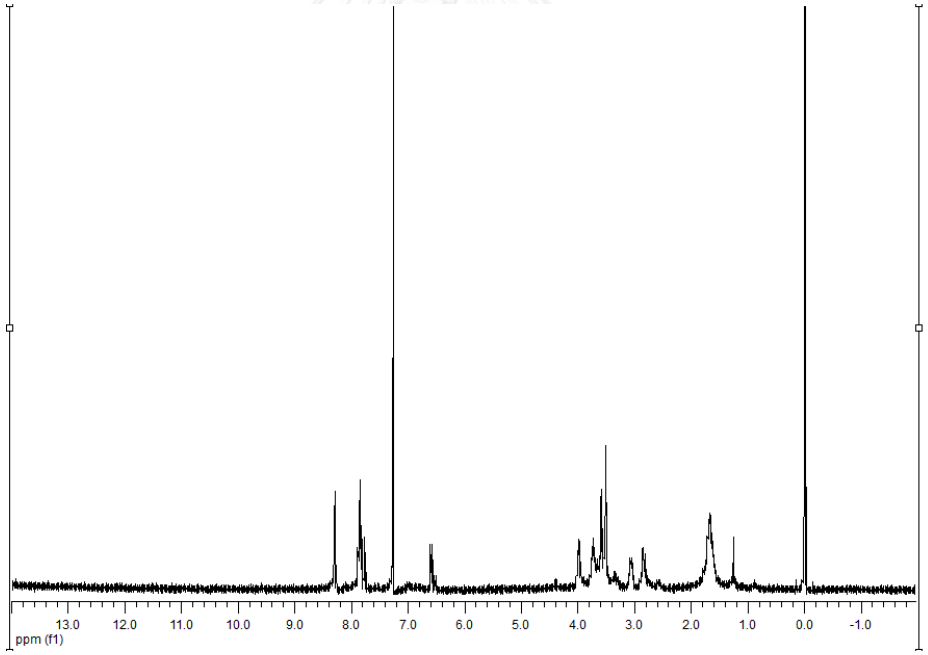

Figure A20 ^{1}H-NMR spectrum of **N2** in $CDCl_3$ at 400 MHz

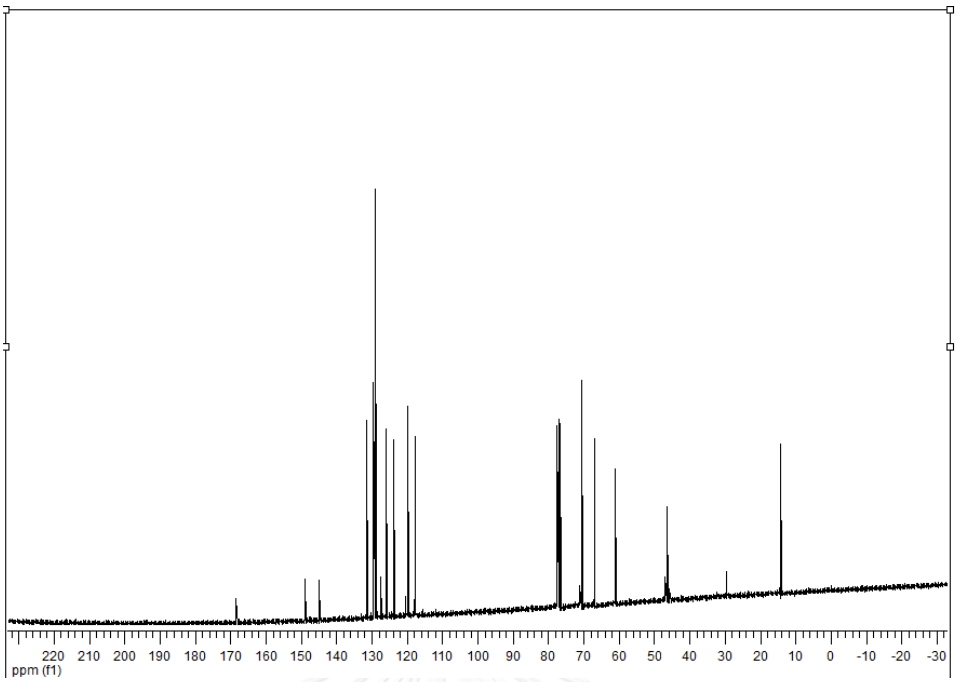

Figure A21 ^{13}C-NMR spectrum of **N2** in $CDCl_3$ at 400 MHz

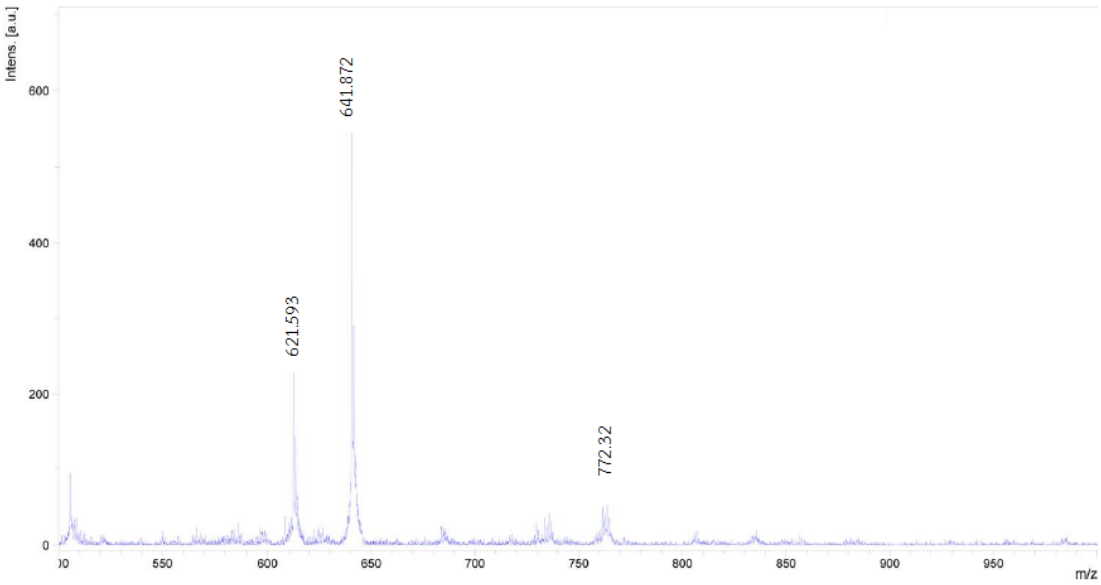

Figure A22 MALDI-TOF mass spectrum of **N2** at 772.32m/z

VITA

Genalral Biographical Information

Mister Narongsak Koonrugsa was born on 29th December 1986 in Nakhonphathom, Thailand, He has graduated with a high school, Mathematics and Science Program, from Nakprasith School, Nakhonphathom in 2004. Then, he has graduated with the Bachelor's degree from department of Chemistry, faculty of Science, Chulalongkorn University in 2008. Afterwards, He was a Doctoral degree student of Inorganic Chemistry in Supramolecular Chemistry Research Unit (SCRU) at Chulalongkorn University under supervision of Assistant Professor Dr. Saowarux Fuangswasdi

Scholarship

2004-2008 The Science Achievement Scholarship of Thailand (SAST)

2009-2012 Teaching Assistant Scholarship, Chulalongkorn University

Conference attendance

2011 Poste presentation at The Pure and Applied Chemistry International Conference 2011 (PACCON2011) 5-7 January 2011, Miracle Grand Hotel, Bangkok, Thailand